

# 8

---

## **Supplementary Materials**

# **Climate Models and Their Evaluation**

---

### **Coordinating Lead Authors:**

David A. Randall (USA), Richard A. Wood (UK)

### **Lead Authors:**

Sandrine Bony (France), Robert Colman (Australia), Thierry Fichefet (Belgium), John Fyfe (Canada), Vladimir Kattsov (Russian Federation), Andrew Pitman (Australia), Jagadish Shukla (USA), Jayaraman Srinivasan (India), Ronald J. Stouffer (USA), Akimasa Sumi (Japan), Karl E. Taylor (USA)

### **Contributing Authors:**

K. AchutaRao (USA), R. Allan (UK), A. Berger (Belgium), H. Blatter (Switzerland), C. Bonfils (USA, France), A. Boone (France, USA), C. Bretherton (USA), A. Broccoli (USA), V. Brovkin (Germany, Russian Federation), W. Cai (Australia), M. Claussen (Germany), P. Dirmeyer (USA), C. Doutriaux (USA, France), H. Drange (Norway), J.-L. Dufresne (France), S. Emori (Japan), P. Forster (UK), A. Frei (USA), A. Ganopolski (Germany), P. Gent (USA), P. Gleckler (USA), H. Goosse (Belgium), R. Graham (UK), J.M. Gregory (UK), R. Gudgel (USA), A. Hall (USA), S. Hallegatte (USA, France), H. Hasumi (Japan), A. Henderson-Sellers (Switzerland), H. Hendon (Australia), K. Hodges (UK), M. Holland (USA), A.A.M. Holtslag (Netherlands), E. Hunke (USA), P. Huybrechts (Belgium), W. Ingram (UK), F. Joos (Switzerland), B. Kirtman (USA), S. Klein (USA), R. Koster (USA), P. Kushner (Canada), J. Lanzante (USA), M. Latif (Germany), N.-C. Lau (USA), M. Meinshausen (Germany), A. Monahan (Canada), J.M. Murphy (UK), T. Osborn (UK), T. Pavlova (Russian Federation), V. Petoukhov (Germany), T. Phillips (USA), S. Power (Australia), S. Rahmstorf (Germany), S.C.B. Raper (UK), H. Renssen (Netherlands), D. Rind (USA), M. Roberts (UK), A. Rosati (USA), C. Schär (Switzerland), A. Schmittner (USA, Germany), J. Scinocca (Canada), D. Seidov (USA), A.G. Slater (USA, Australia), J. Slingo (UK), D. Smith (UK), B. Soden (USA), W. Stern (USA), D.A. Stone (UK), K. Sudo (Japan), T. Takemura (Japan), G. Tselioudis (USA, Greece), M. Webb (UK), M. Wild (Switzerland)

### **Review Editors:**

Elisa Manzini (Italy), Taroh Matsuno (Japan), Bryant McAvaney (Australia)

### **This chapter should be cited as:**

Randall, D.A., R.A. Wood, S. Bony, R. Colman, T. Fichefet, J. Fyfe, V. Kattsov, A. Pitman, J. Shukla, J. Srinivasan, R.J. Stouffer, A. Sumi and K.E. Taylor, 2007: Climate Models and Their Evaluation. In: *Climate Change 2007: The Physical Science Basis. Contribution of Working Group I to the Fourth Assessment Report of the Intergovernmental Panel on Climate Change* [Solomon, S., D. Qin, M. Manning, Z. Chen, M. Marquis, K.B. Averyt, M.Tignor and H.L. Miller (eds.)]. Cambridge University Press, Cambridge, United Kingdom and New York, NY, USA.

## Appendix 8.A: Supplementary Figures and Tables

### Supplementary Figures for Section 8.3

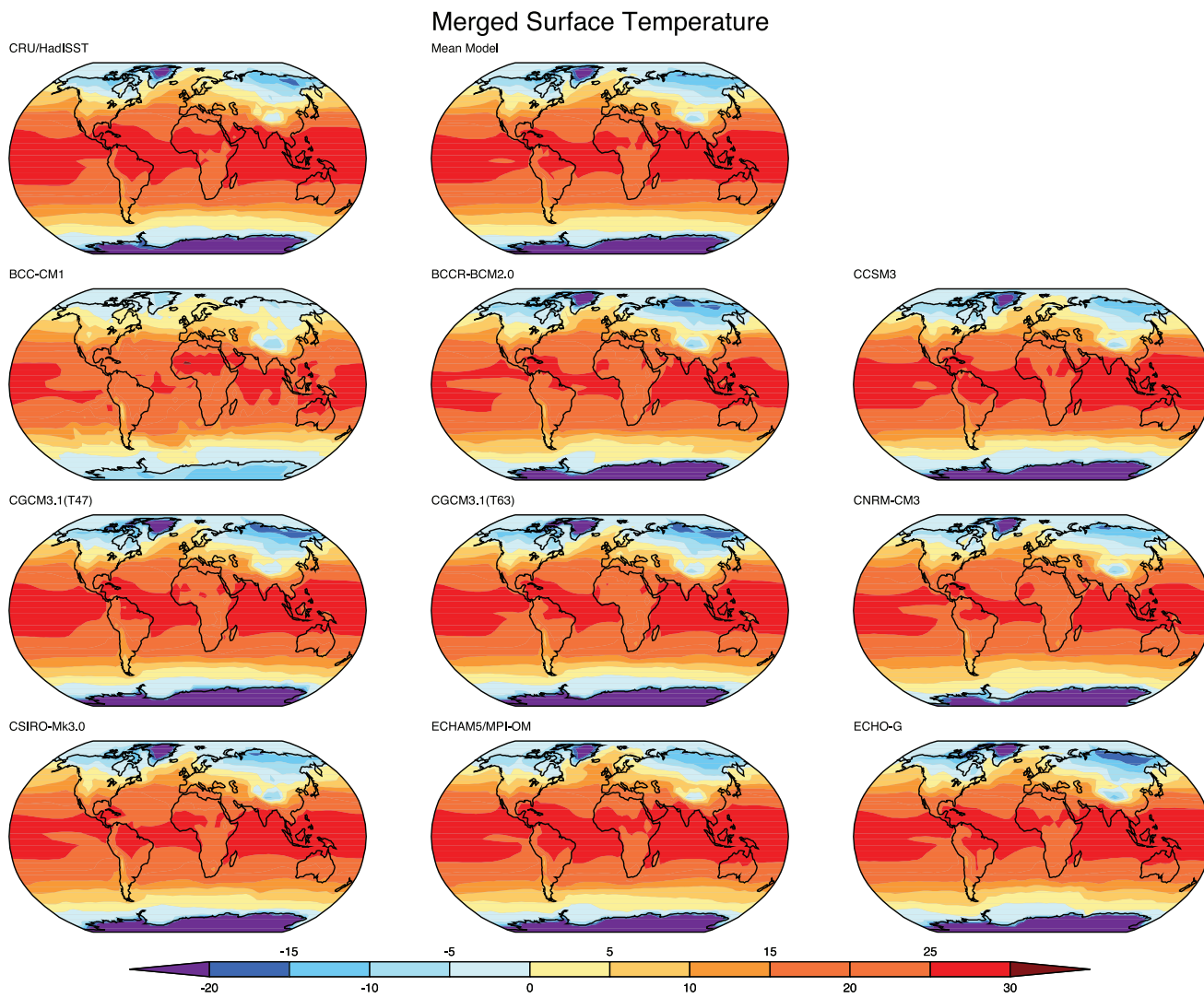
These figures are cited as supplementary material in Chapter 8, Section 3. They contain supportive analyses that, due to space limitations, could not be shown in the main report. There are a number of places in the text where the reader is encouraged to view these supplementary figures. The results presented here support the points made in the report. The figures present results from individual models, which are the basis for the construction of the multi-model averages and model spreads shown in section 8.3. References cited here are given at the end of the main chapter text.

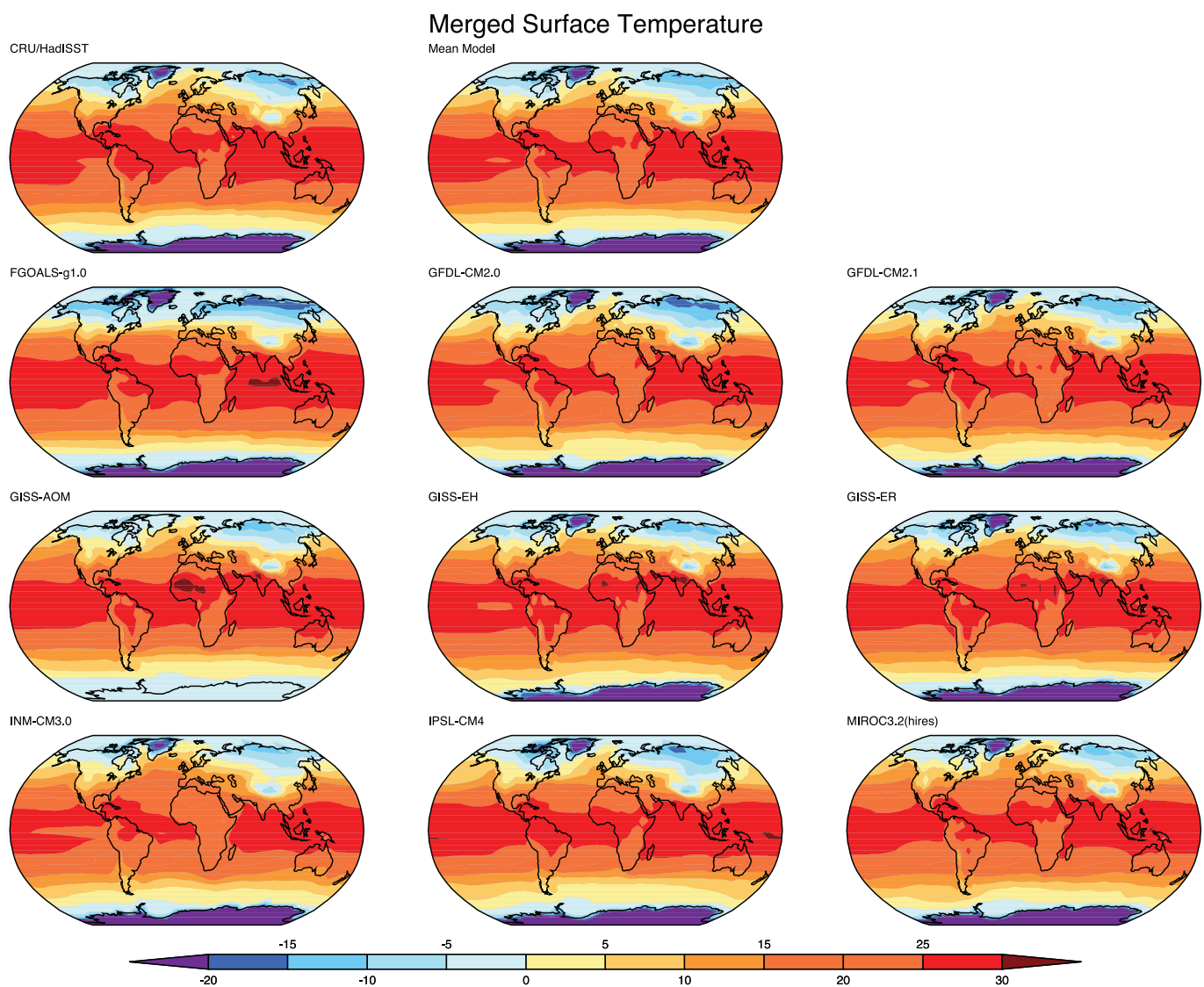
Note that results from some models have only recently become available and may not be included here.

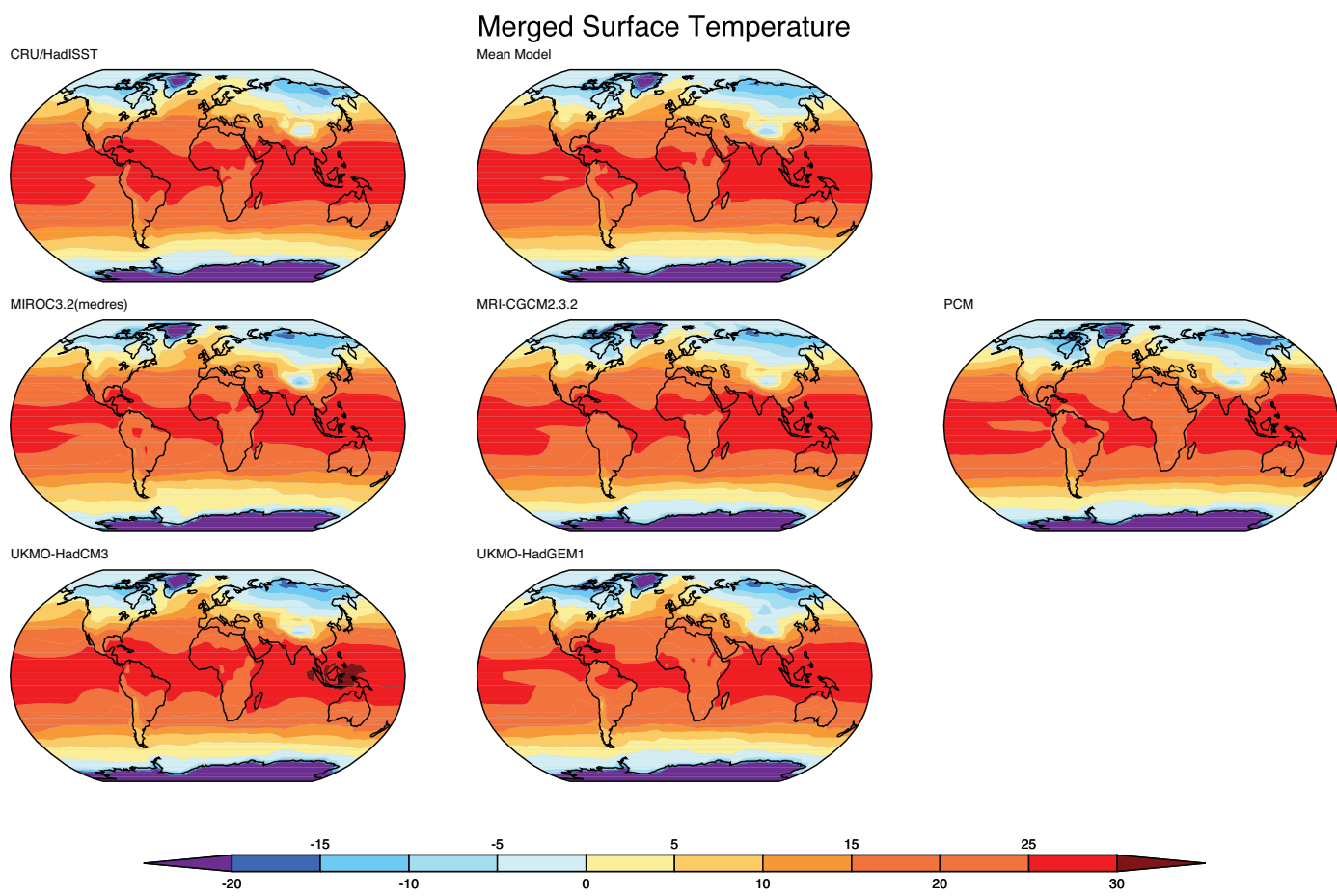
#### **Figure S8.1: Surface temperature:**

Each page of figure S8.1a shows:

- Upper left panel: Observed annual-mean sea surface temperature (SST) climatology and, over land, surface air temperature climatology ( $^{\circ}\text{C}$ ).
- Upper center panel: Corresponding field averaged over the multi-model ensemble ( $^{\circ}\text{C}$ ).
- All other panels: Corresponding individual model results ( $^{\circ}\text{C}$ ).



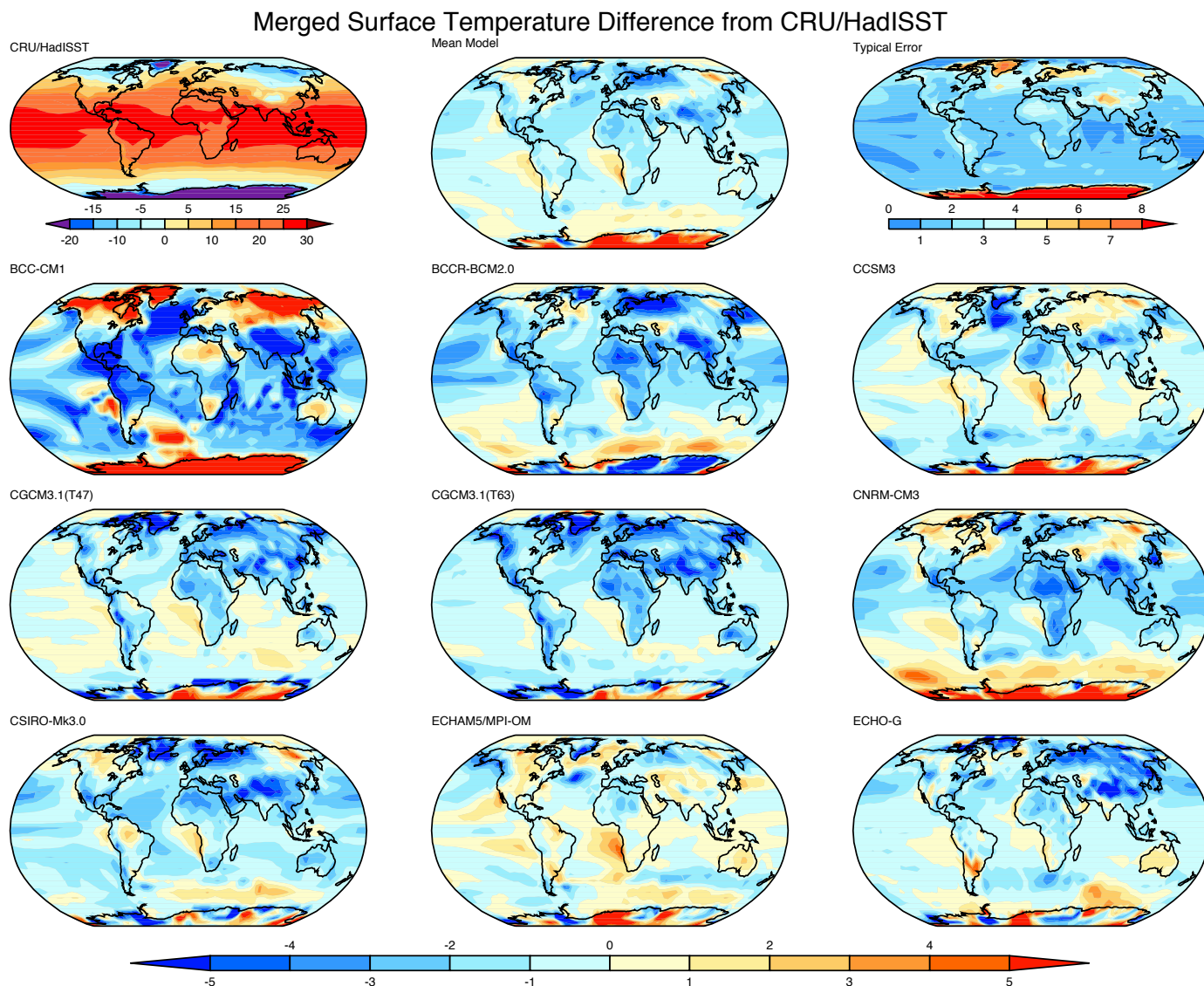


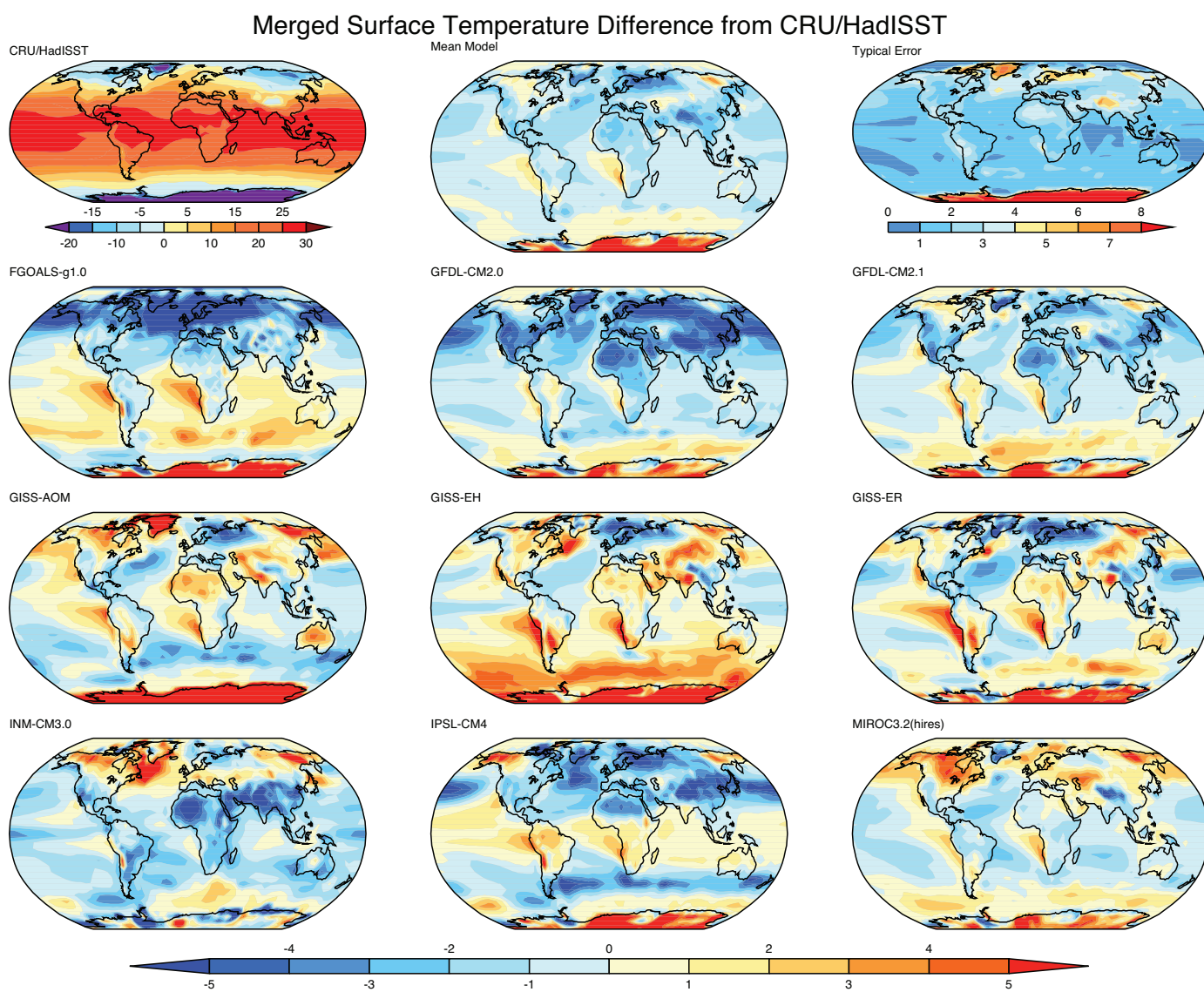


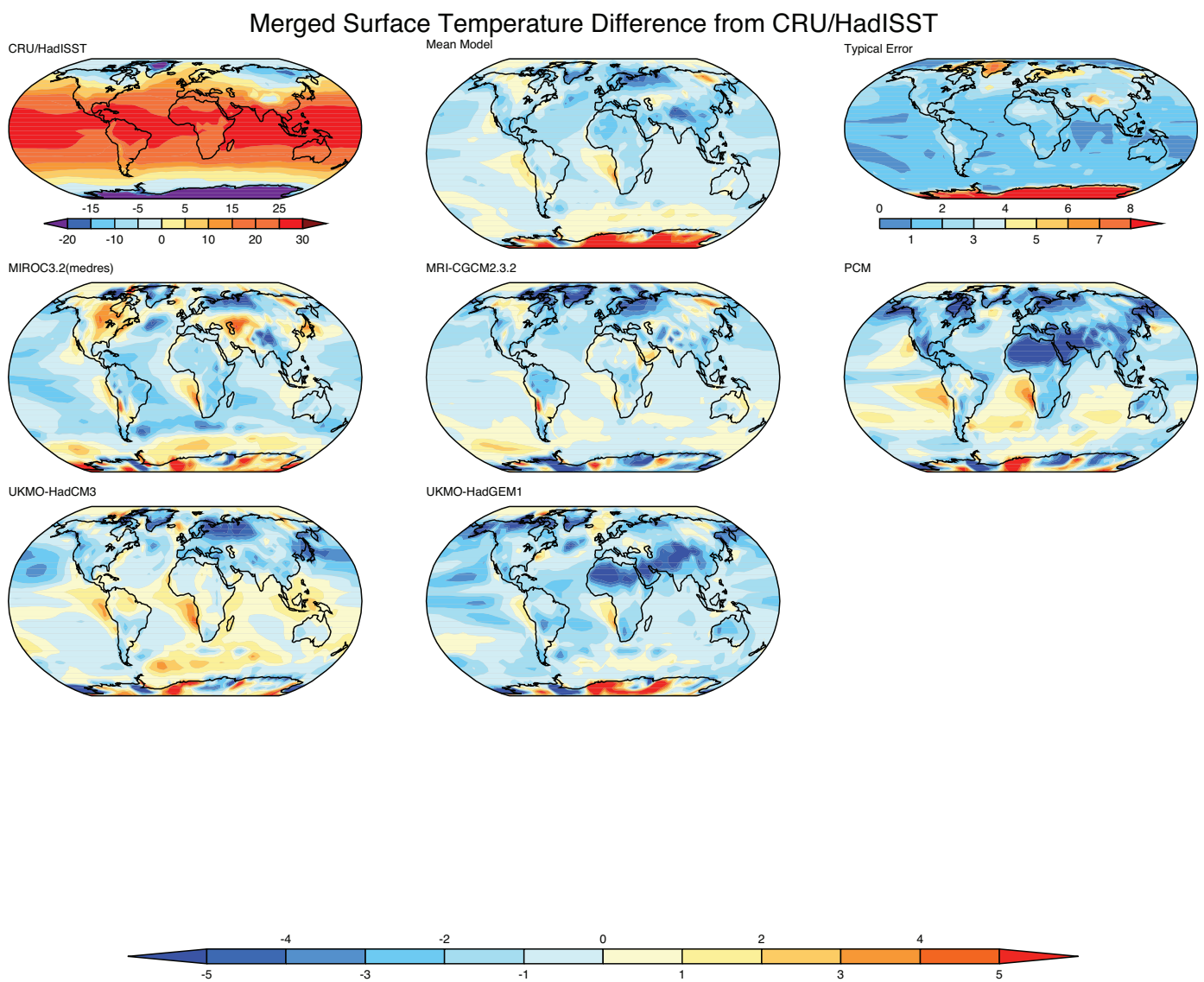
Each page of figure S8.1b shows:

- Upper left panel: Observed annual-mean sea surface temperature (SST) climatology and, over land, surface air temperature climatology ( $^{\circ}\text{C}$ ).
- Upper center panel: Multi-model mean error ( $^{\circ}\text{C}$ ), simulated minus observed.
- Upper right panel: Root-mean-square model error ( $^{\circ}\text{C}$ ), based on all available IPCC model simulations (i.e., square-root of the sum of the squares of individual model errors, divided by the number of models).
- All other panels: Individual model errors ( $^{\circ}\text{C}$ ), simulated minus observed.

The HadISST (Rayner et al., 2003) climatology of SST for 1980–1999 and the CRU (Jones et al., 1999) climatology of surface air temperature over land for 1961–1990 are shown here. The model results are for the same period of the CMIP3 20th Century simulations. In the presence of sea ice, the SST is assumed to be at the approximate freezing point of sea water ( $-1.8\text{ }^{\circ}\text{C}$ ).



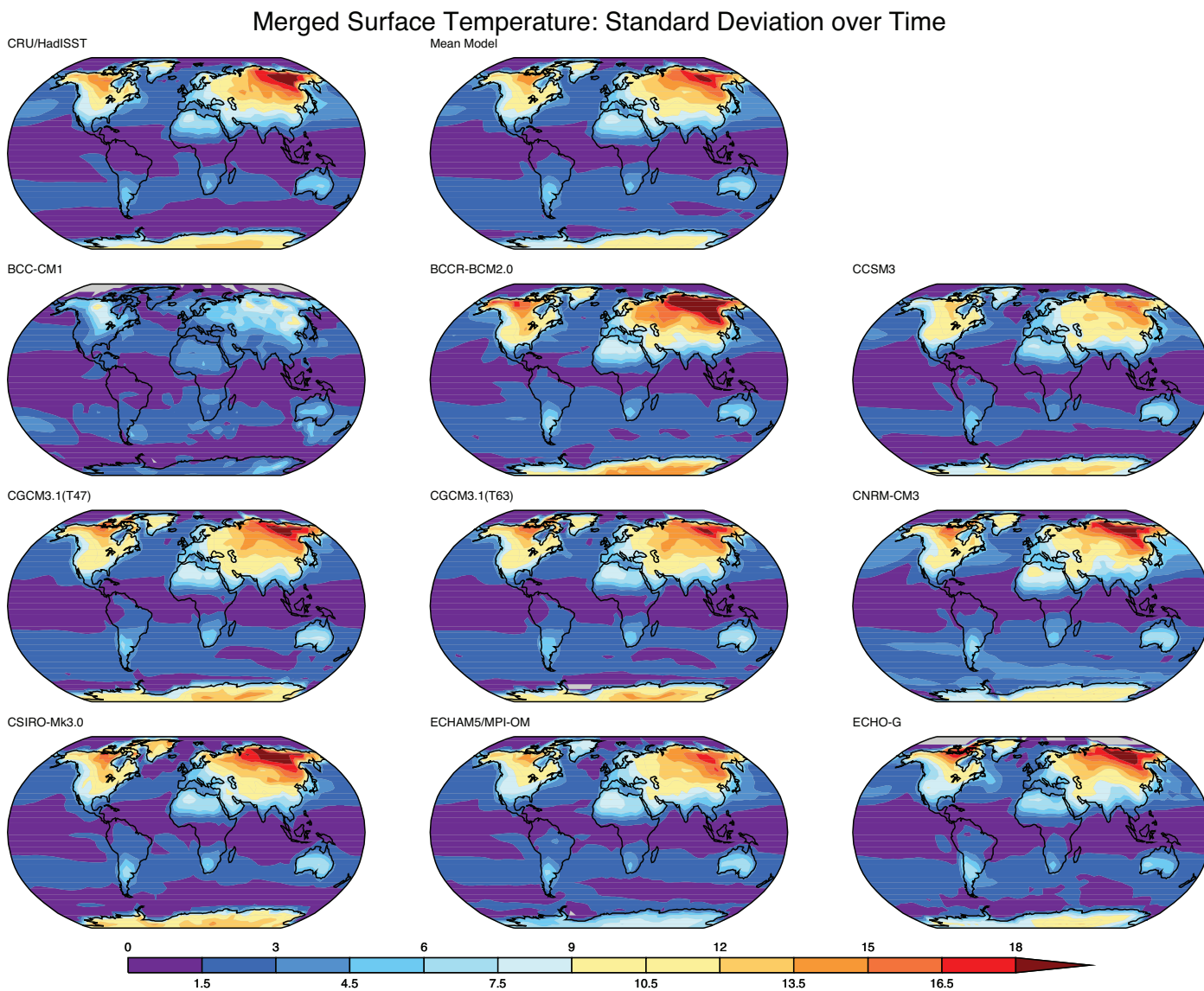


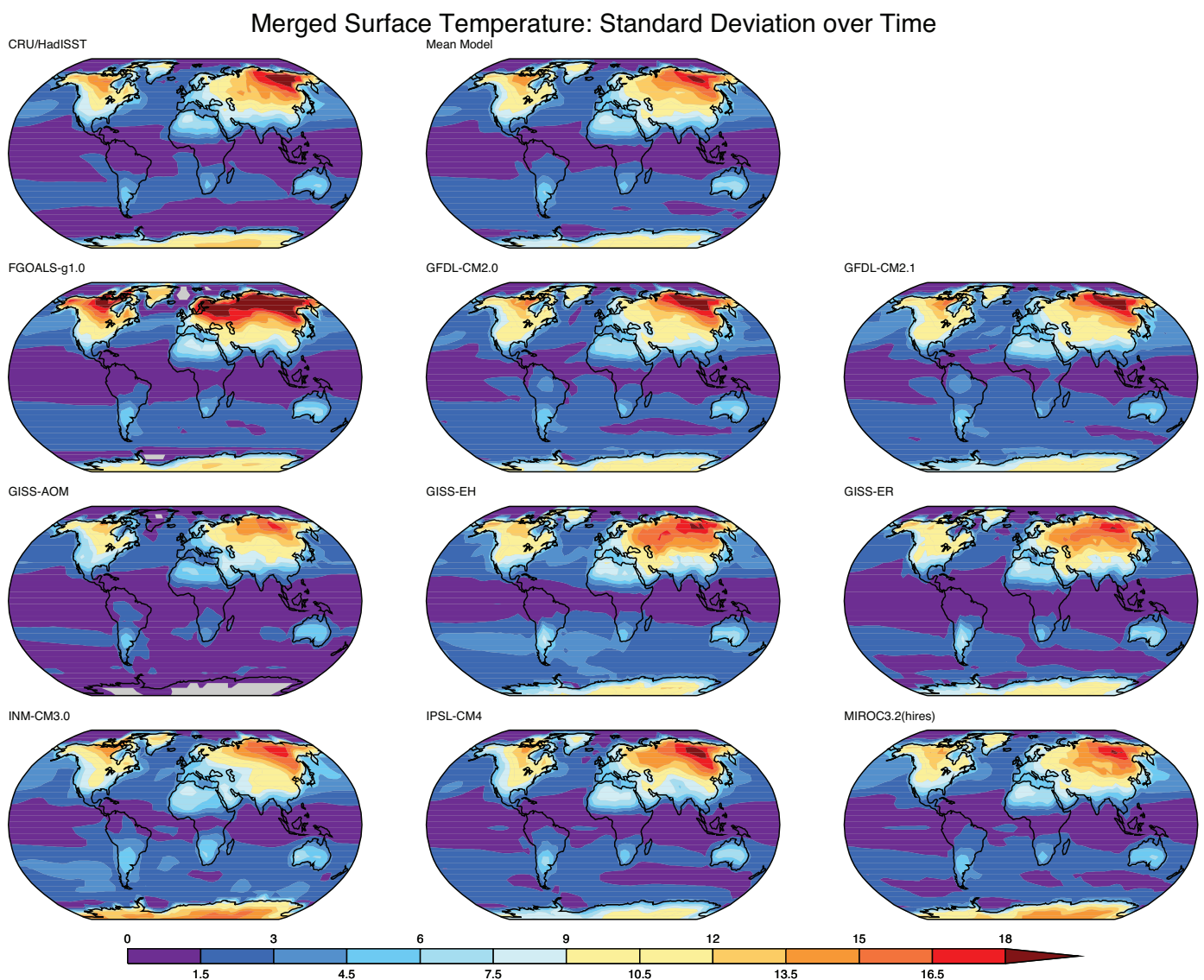


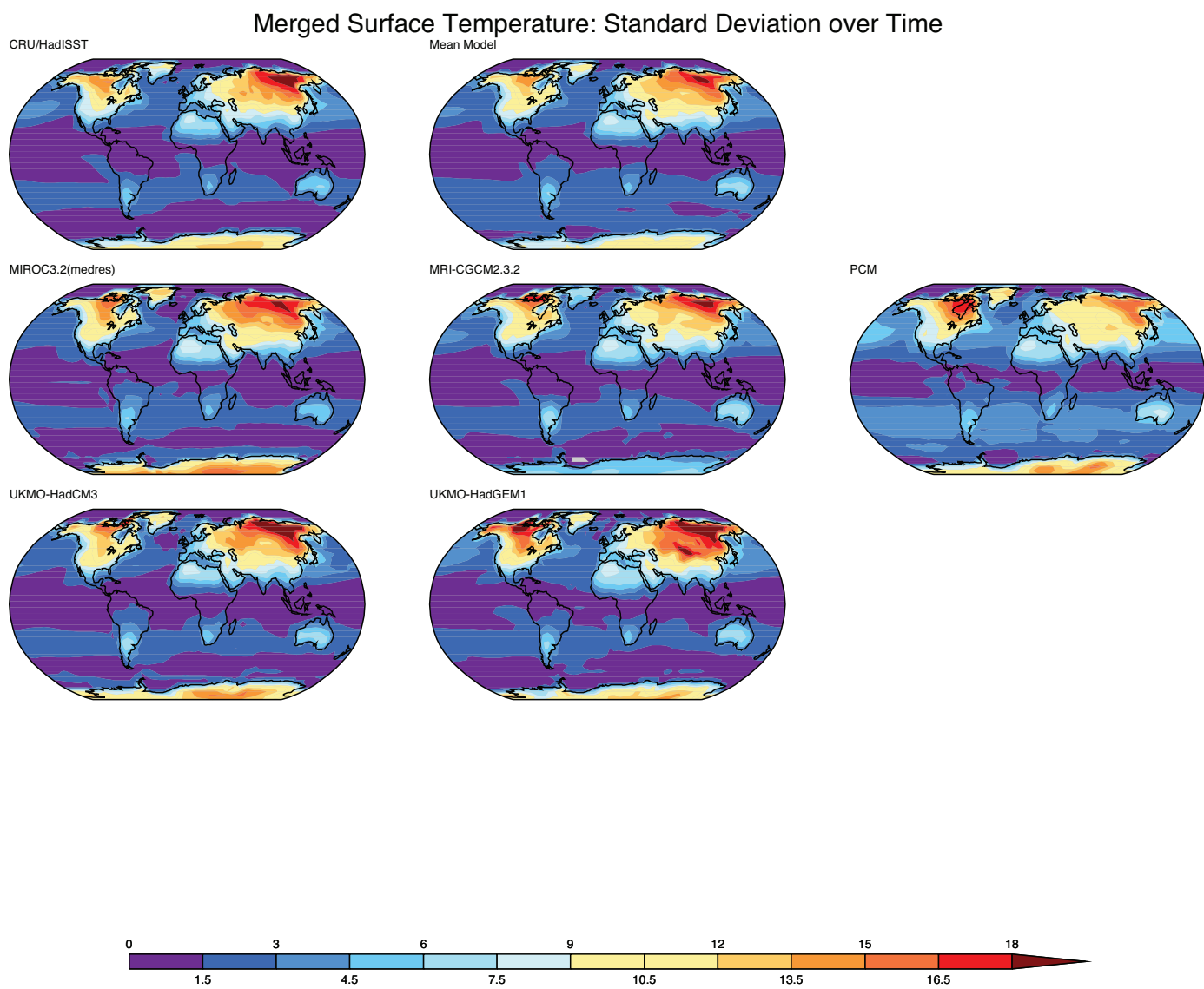
**Figure S8.2: Surface temperature standard deviation:**

Each page of figure S8.2a shows:

- Upper left panel: Observed standard deviation of sea surface temperature (SST) and, over land, surface air temperature ( $^{\circ}\text{C}$ ), computed over the climatological monthly mean annual cycle.
- Upper center panel: Corresponding field averaged over the multi-model ensemble ( $^{\circ}\text{C}$ ).
- All other panels: Corresponding individual model results ( $^{\circ}\text{C}$ ).



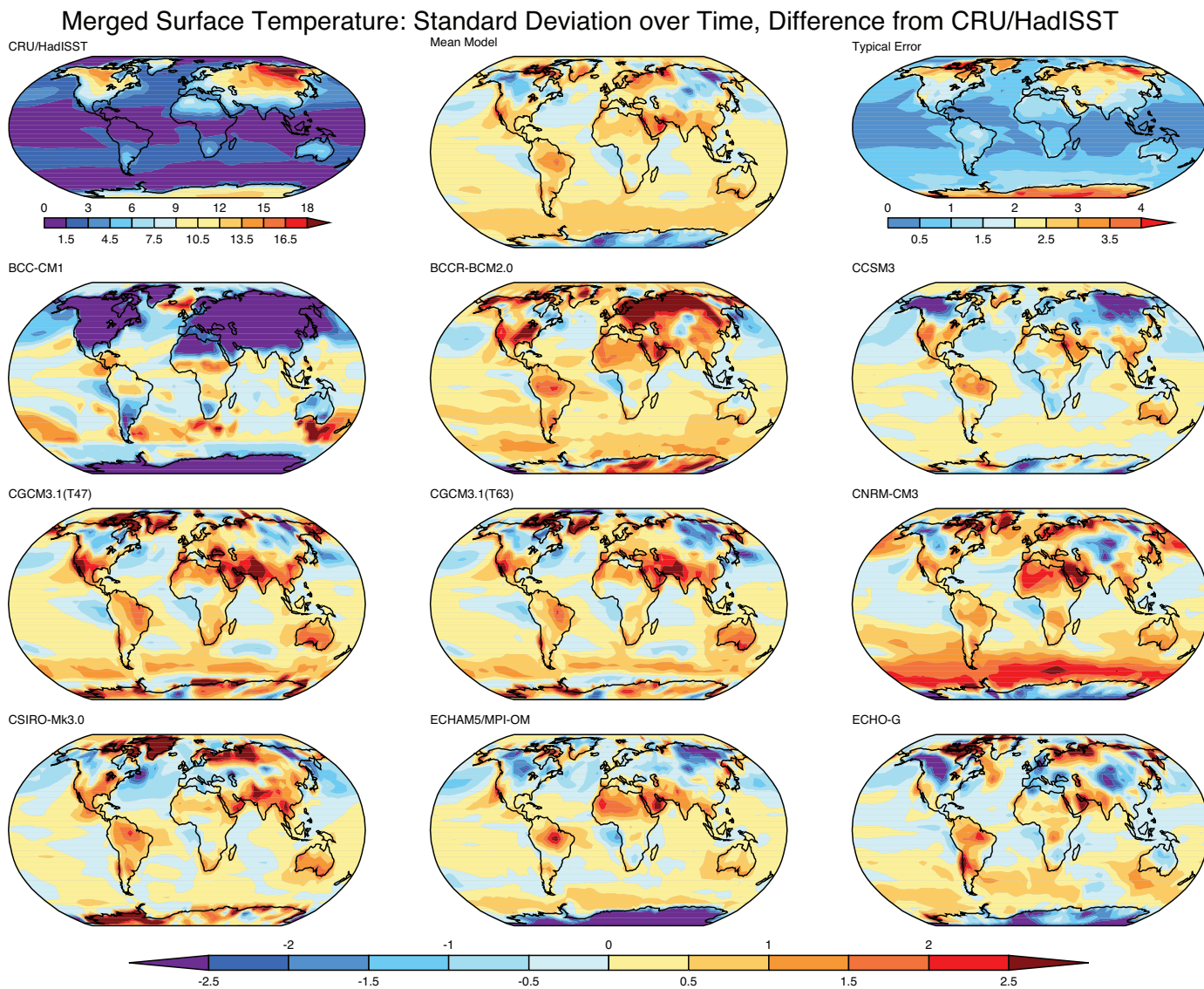


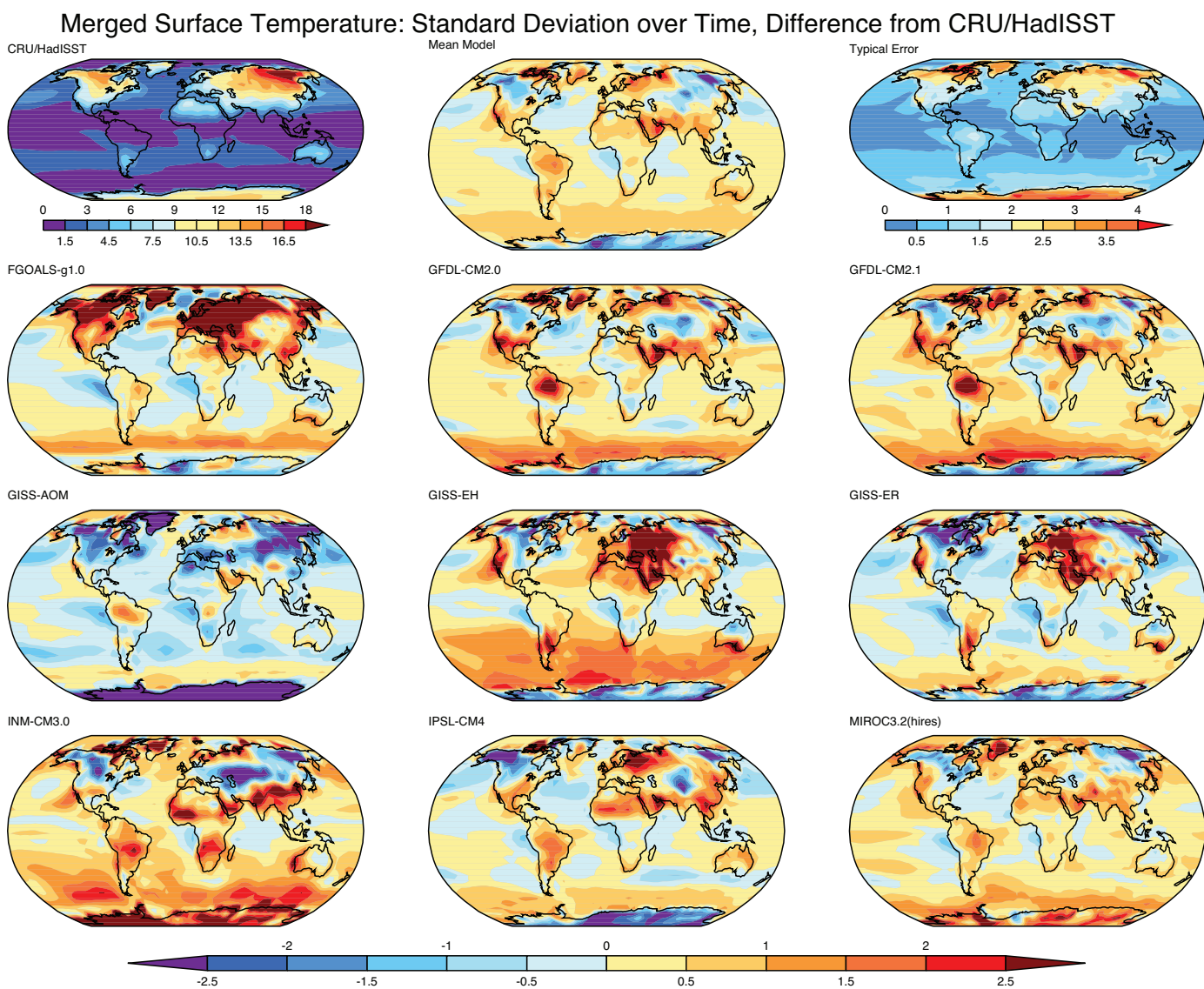


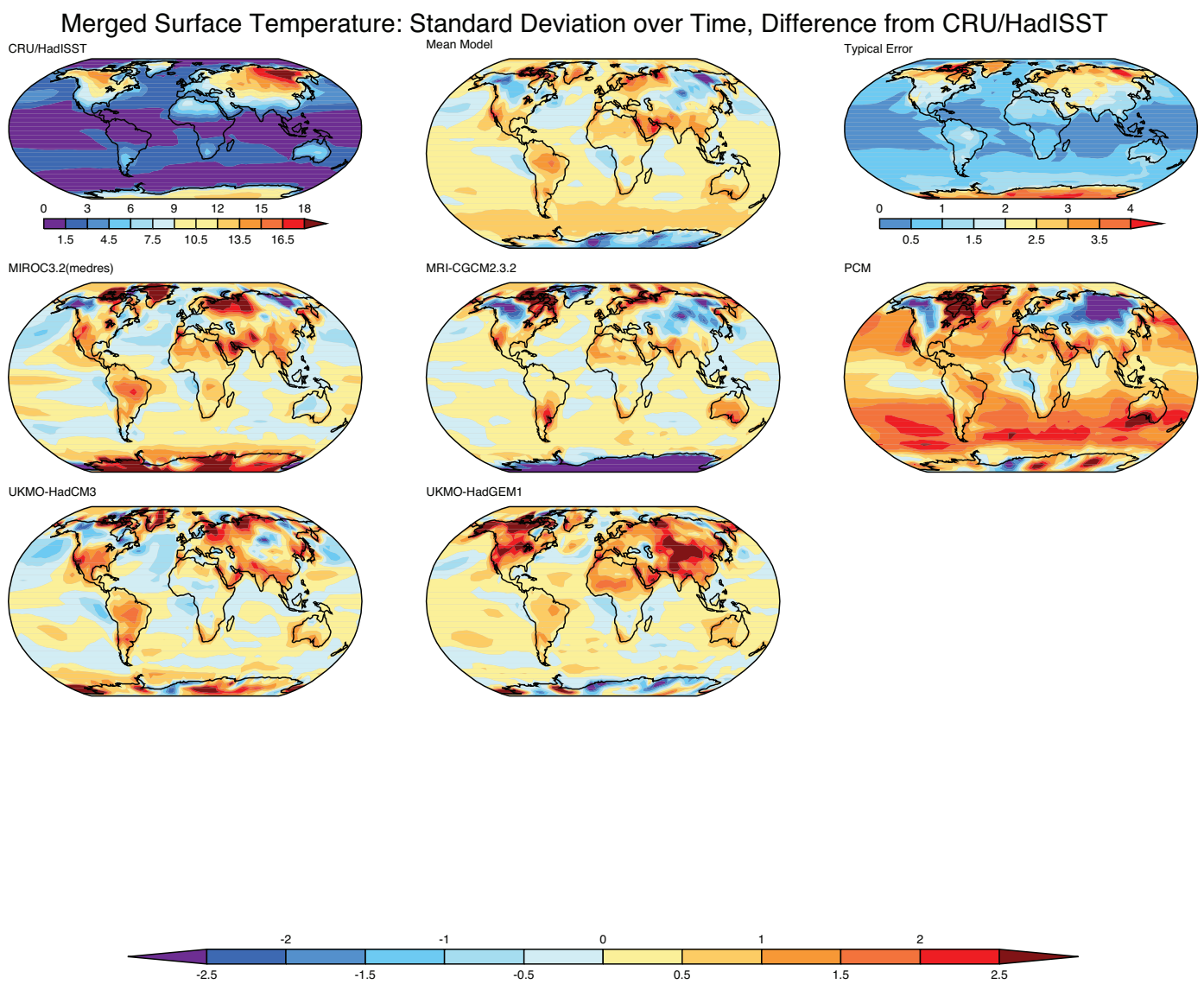
Each page of figure S8.2b shows:

- Upper left panel: Observed standard deviation of sea surface temperature (SST) and, over land, surface air temperature ( $^{\circ}\text{C}$ ), computed over the climatological monthly mean annual cycle.
- Upper center panel: Multi-model mean error ( $^{\circ}\text{C}$ ), simulated minus observed.
- Upper right panel: Root-mean-square model error ( $^{\circ}\text{C}$ ), based on all available IPCC model simulations (i.e., square-root of the sum of the squares of individual model errors, divided by the number of models).
- All other panels: Individual model errors ( $^{\circ}\text{C}$ ), simulated minus observed.

The HadISST (Rayner et al., 2003) climatology of SST for 1980–1999 and the CRU (Jones et al., 1999) climatology of surface air temperature over land for 1961–1990 are shown here. The model results are for the same period of the CMIP3 20th Century simulations. In the presence of sea ice, the SST is assumed to be at the approximate freezing point of sea water ( $-1.8\text{ }^{\circ}\text{C}$ ).



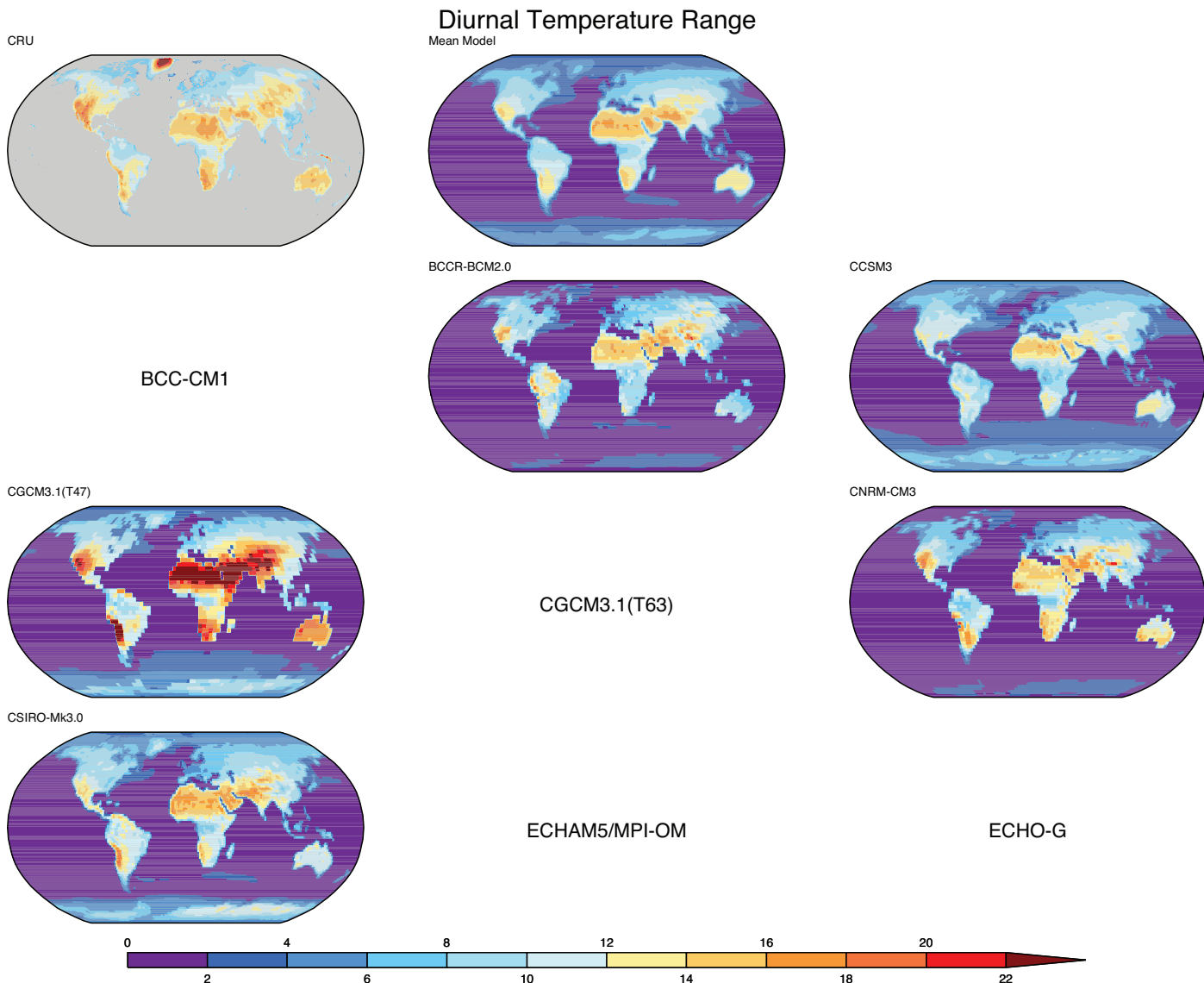


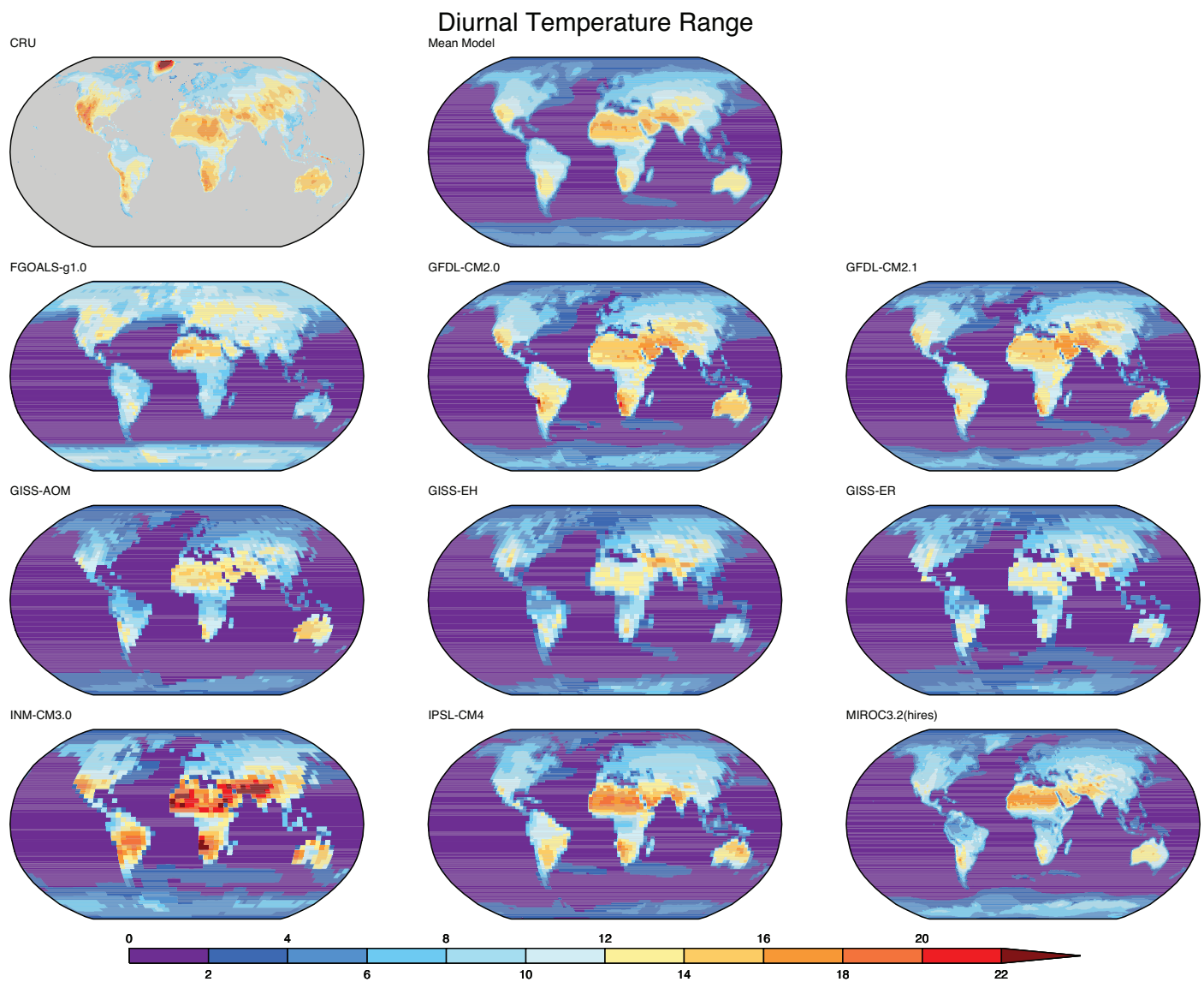


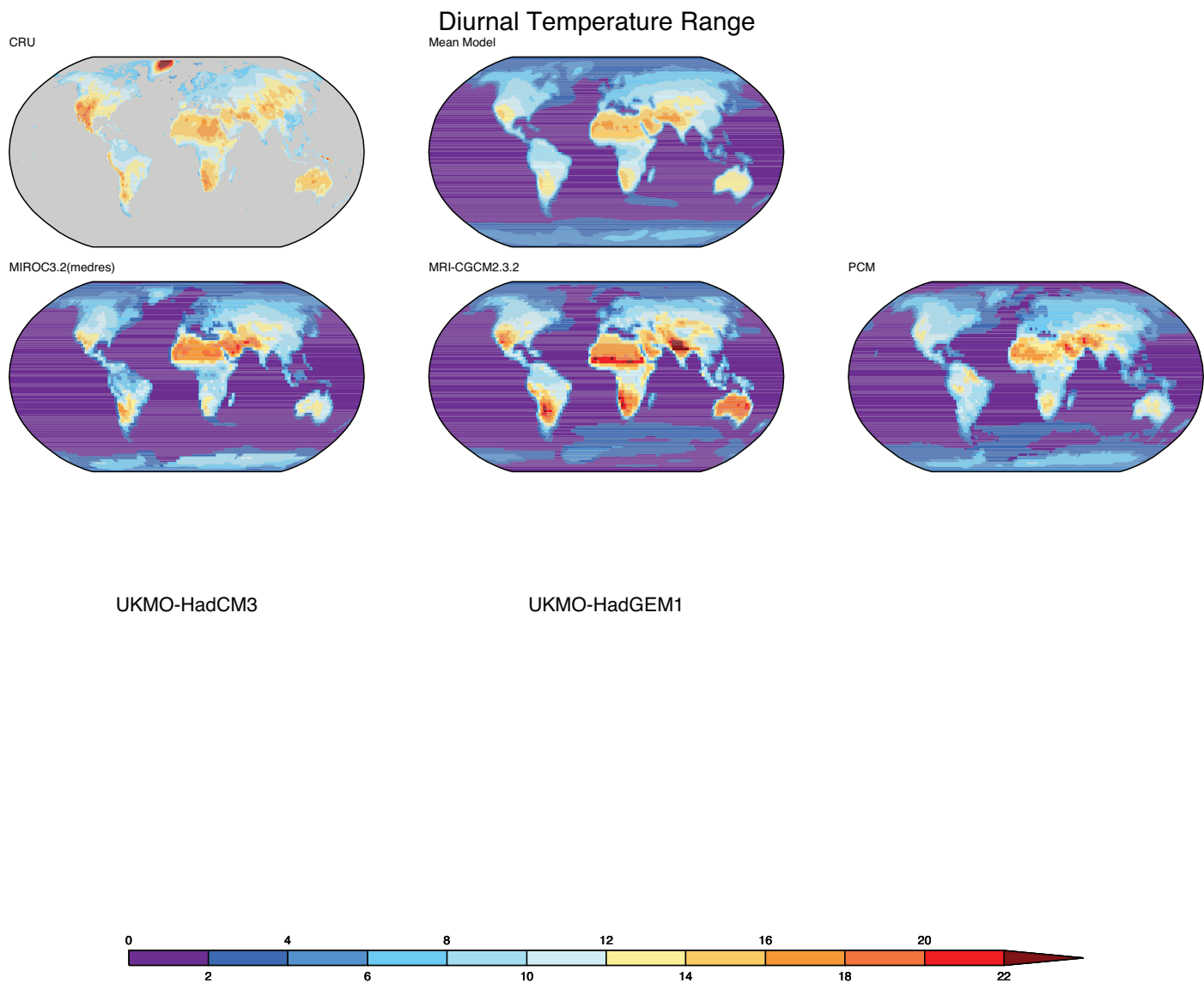
**Figure S8.3: Diurnal range of surface air temperature over land:**

Each page of figure S8.3a shows:

- Upper left panel: Observed diurnal range of surface air temperature over land, annual averaged ( $^{\circ}\text{C}$ ).
- Upper center panel: Corresponding field averaged over the multi-model ensemble ( $^{\circ}\text{C}$ ).
- All other panels: Corresponding individual model results ( $^{\circ}\text{C}$ ).

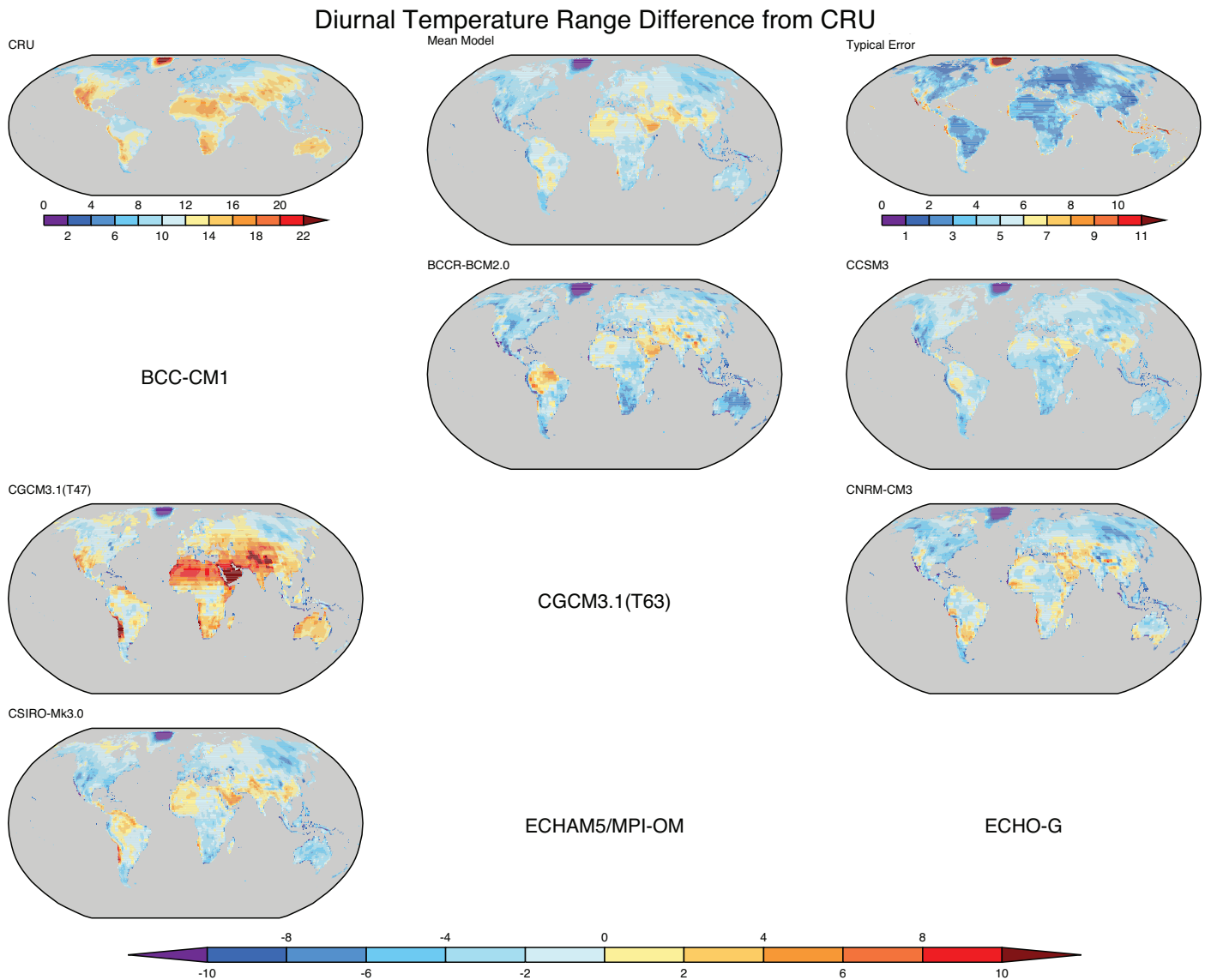


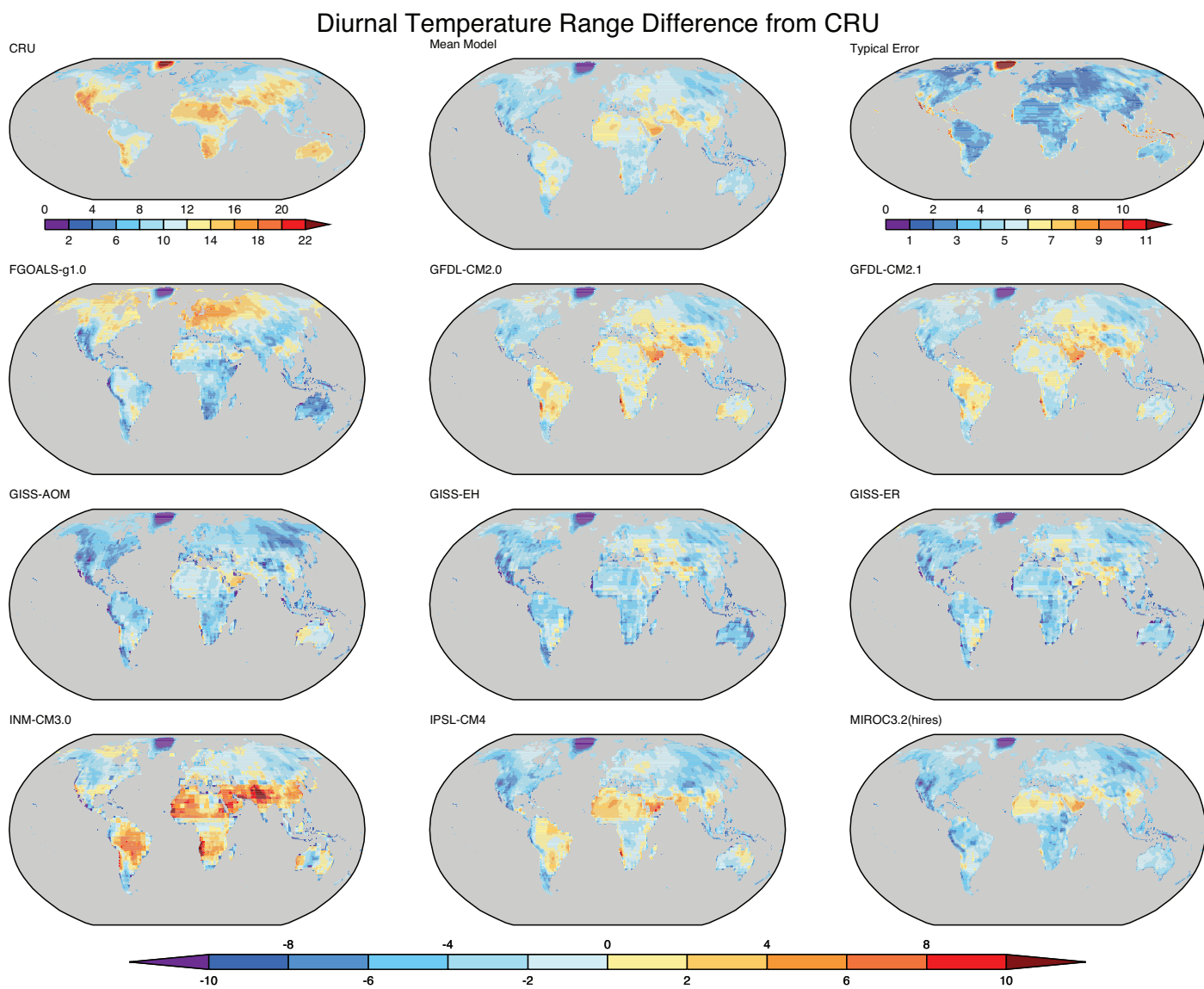




Each page of figure S8.3b shows:

- Upper left panel: Observed diurnal range of surface air temperature over land, annual averaged ( $^{\circ}\text{C}$ ).
- Upper center panel: Multi-model mean error ( $^{\circ}\text{C}$ ), simulated minus observed.
- Upper right panel: Root-mean-square model error ( $^{\circ}\text{C}$ ), based on all available IPCC model simulations (i.e., square-root of the sum of the squares of individual model errors, divided by the number of models).





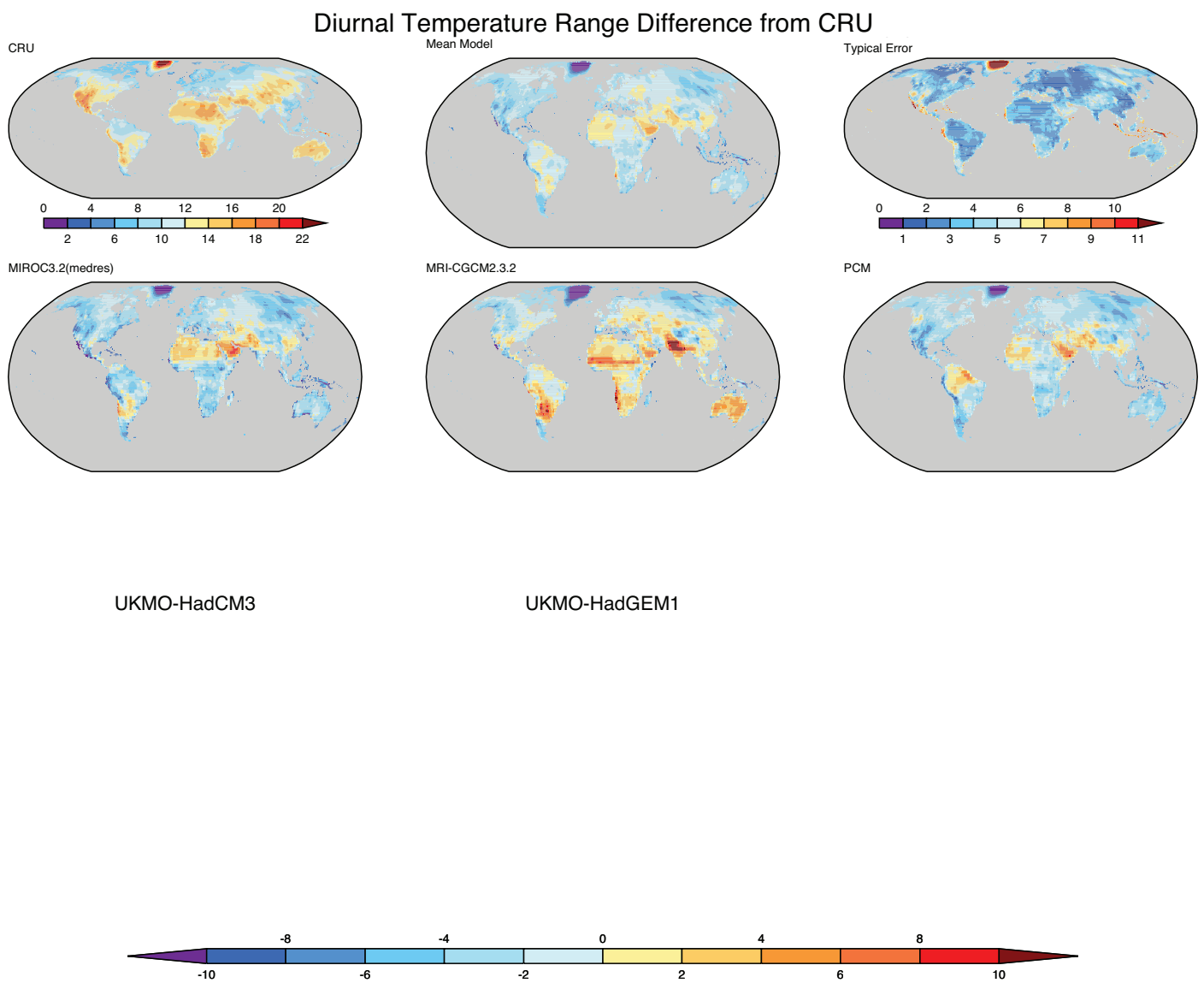
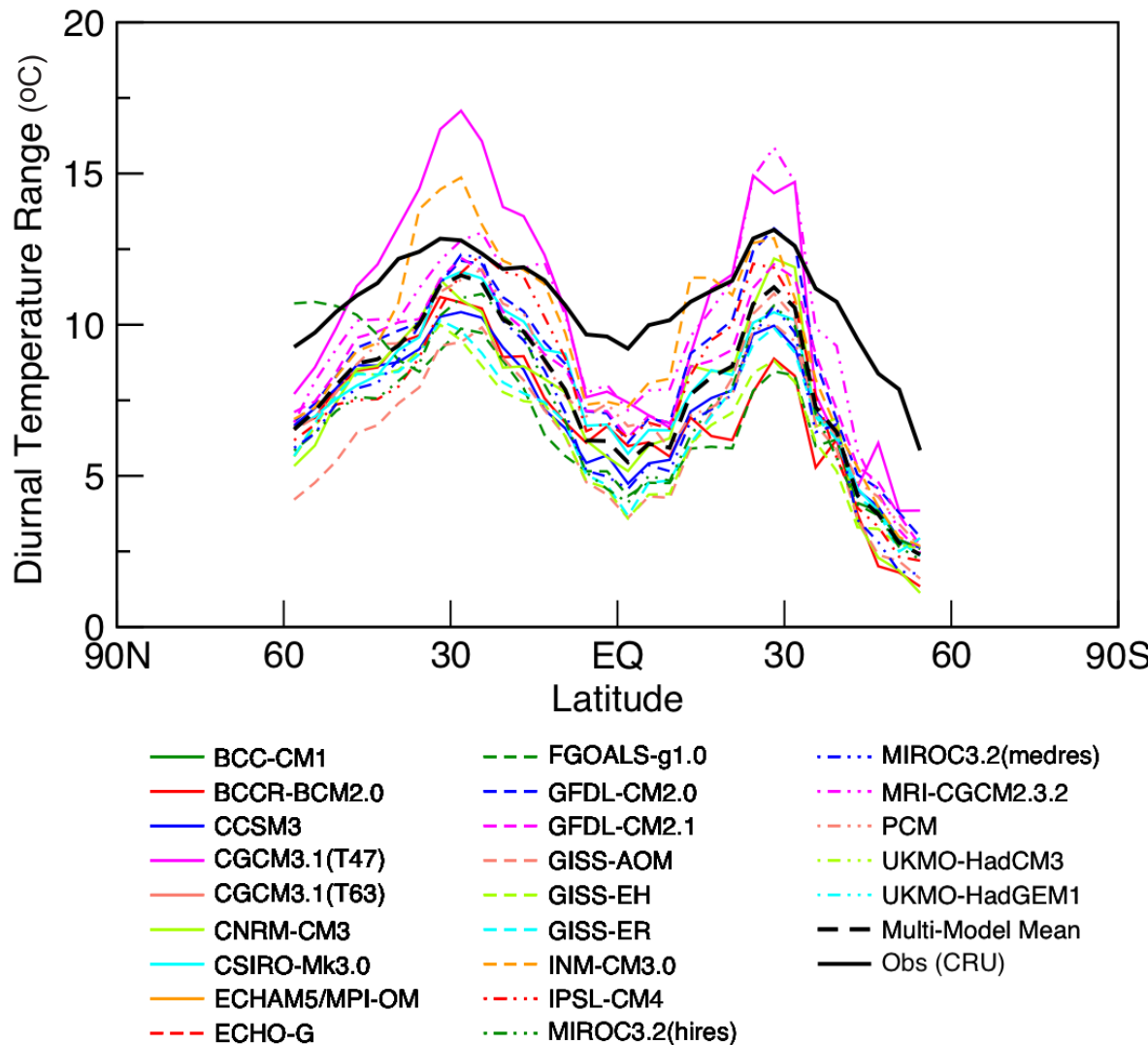


Figure S8.3c shows:

- Diurnal range of surface air temperature, averaged zonally over land areas and averaged annually.

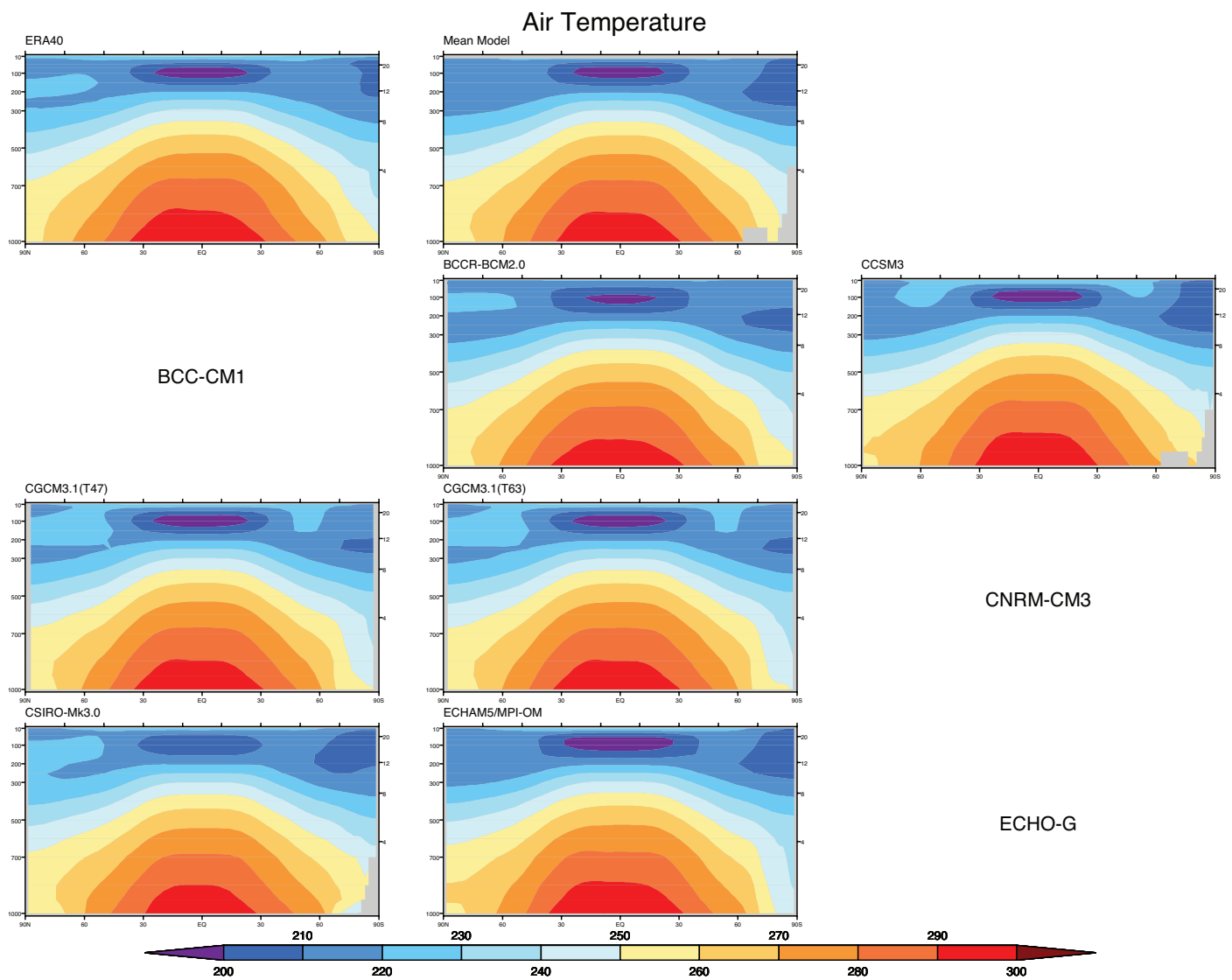
The observations are from the CRU surface air temperature dataset for the period 1961-1990 (Mitchell and Jones, 2005), and the model results are from years 1980-1999 of the CMIP3 20th Century simulations. Observations are unreliable over Greenland.

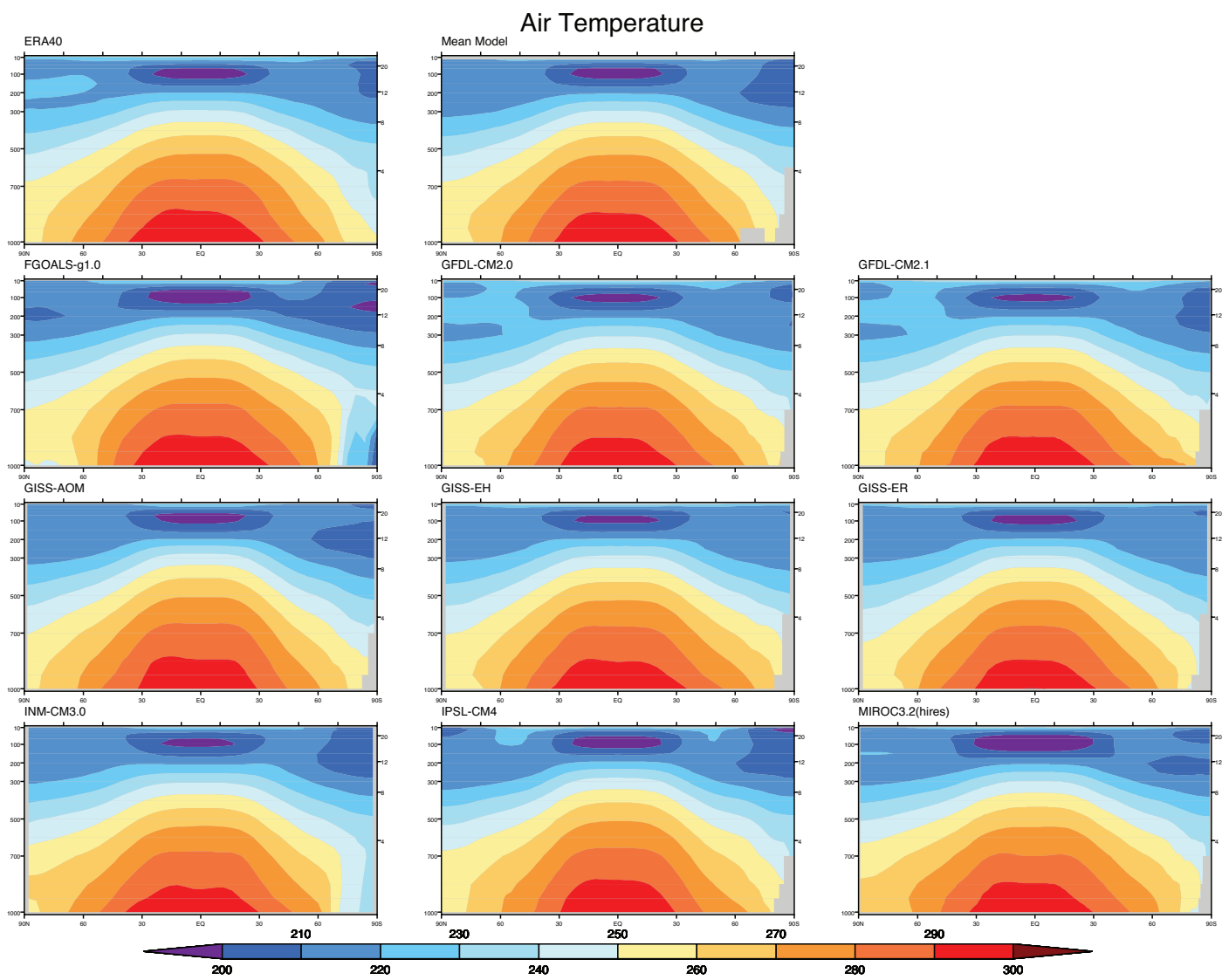


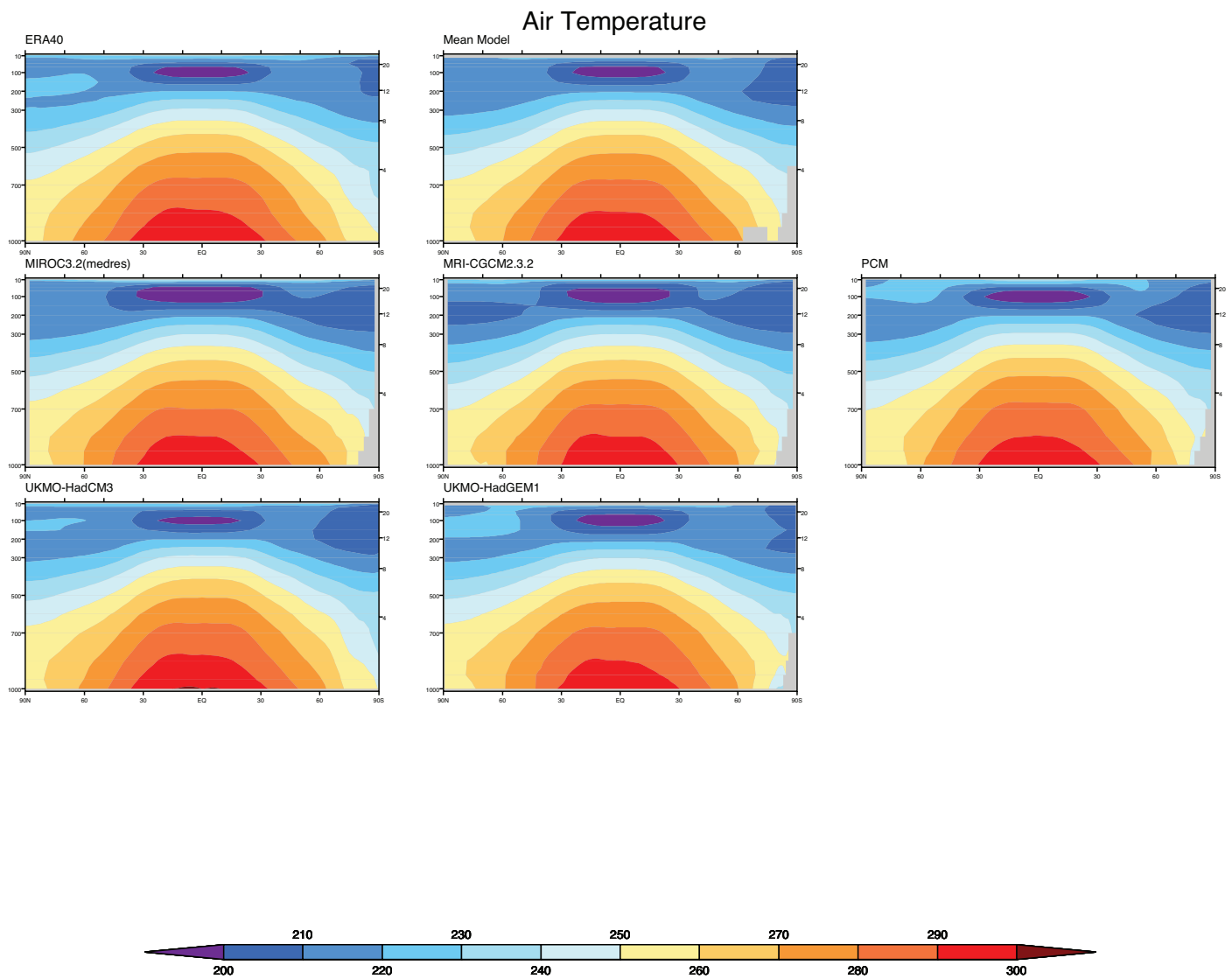
**Figure S8.4: Zonal mean air temperature cross-sections:**

Each page of figure S8.4a shows:

- Upper left panel: Observed annual-mean air temperature climatology ( $^{\circ}\text{C}$ ), averaged zonally.
- Upper center panel: Corresponding field averaged over the multi-model ensemble ( $^{\circ}\text{C}$ ).
- All other panels: Corresponding individual model results ( $^{\circ}\text{C}$ ).



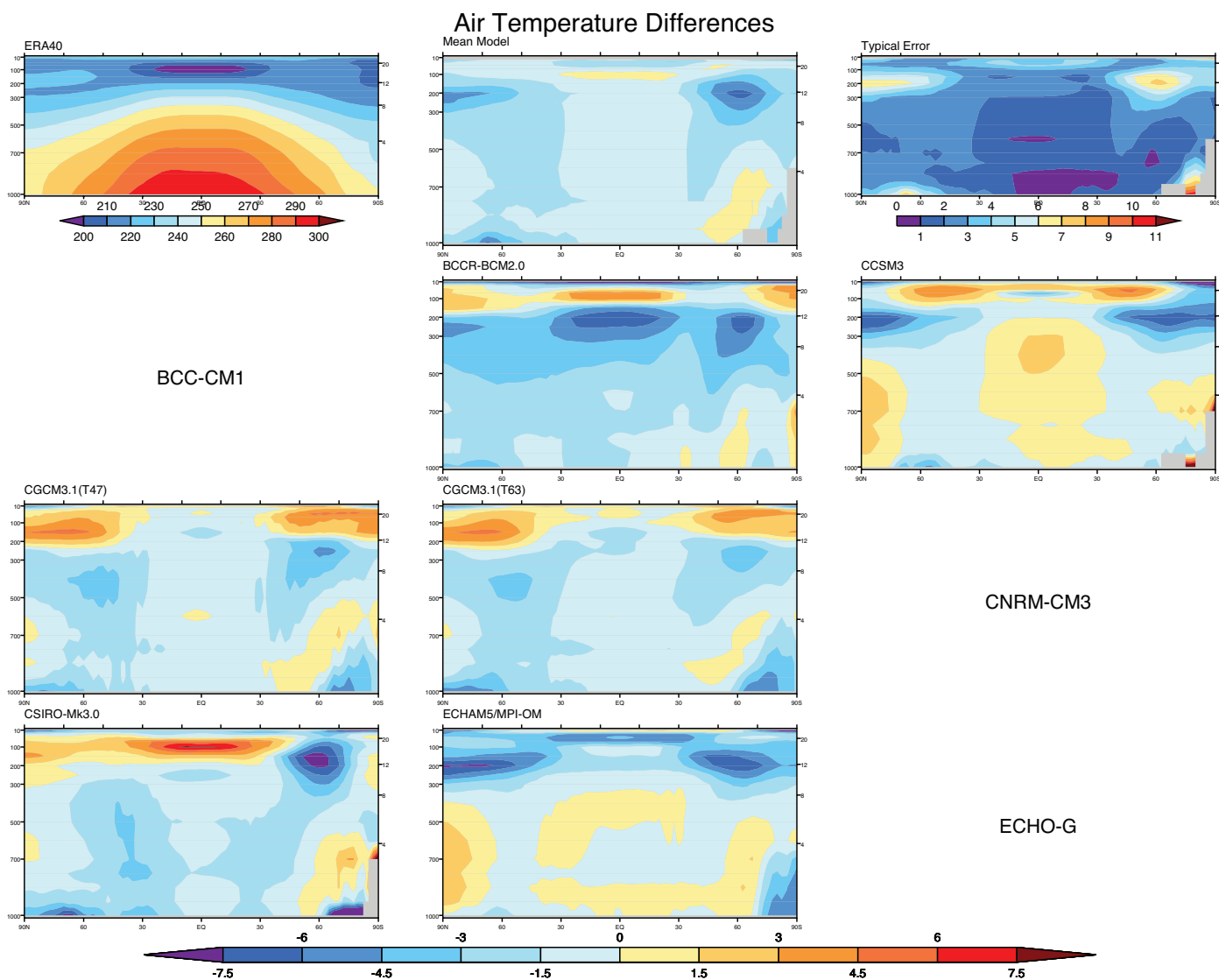


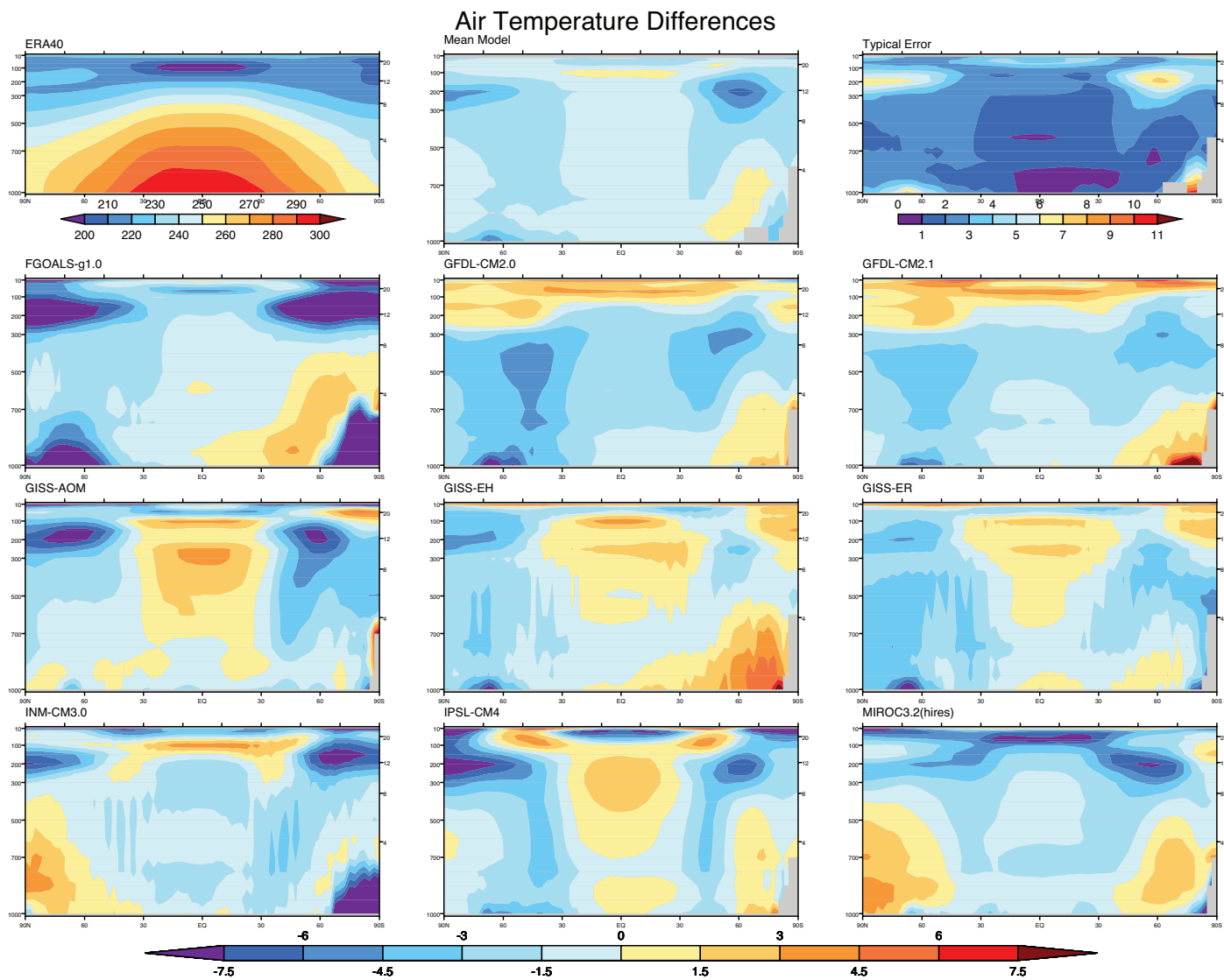


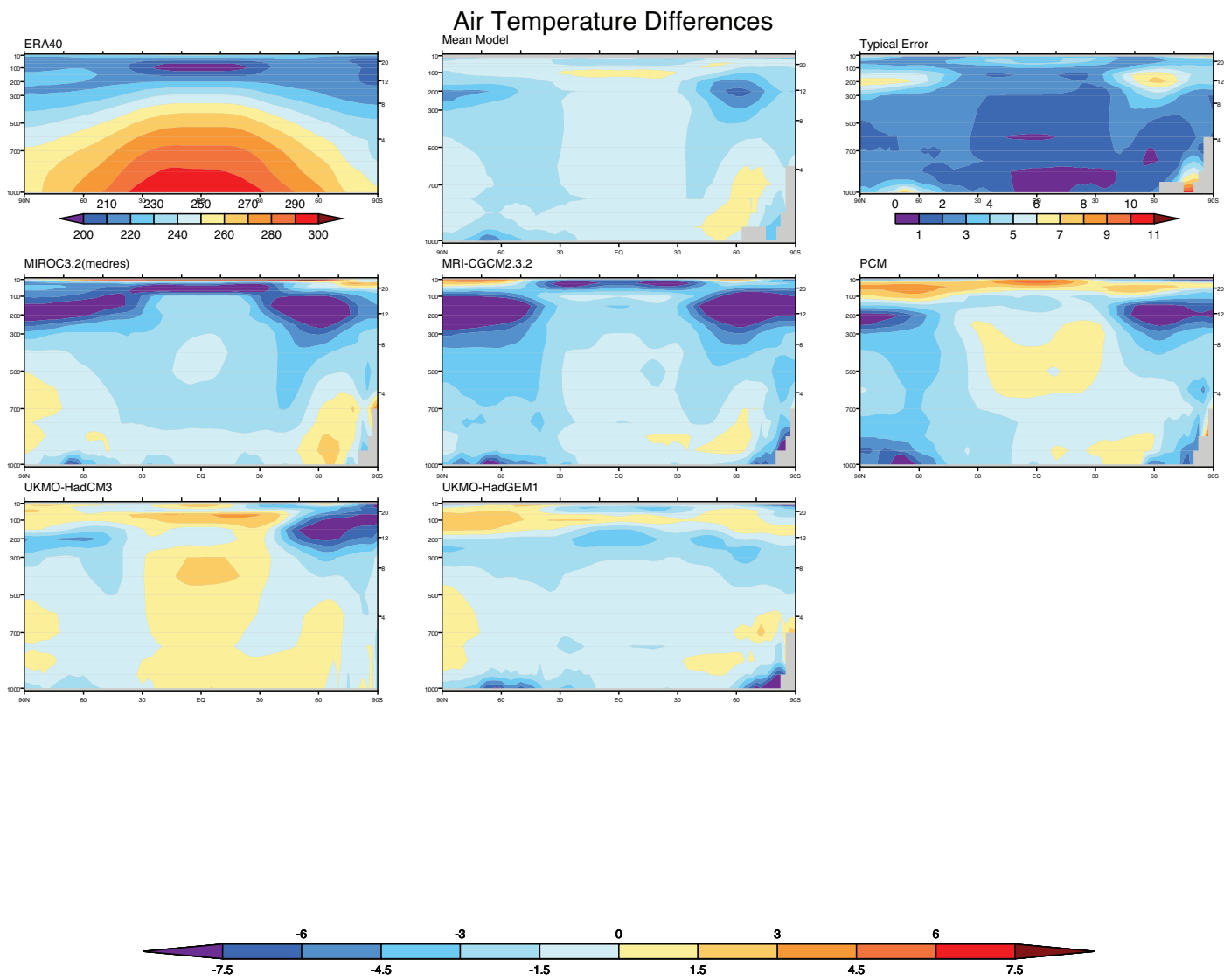
Each page of figure S8.4b shows:

- Upper left panel: Observed annual-mean air temperature climatology ( $^{\circ}\text{C}$ ), averaged zonally.
- Upper center panel: Multi-model mean error ( $^{\circ}\text{C}$ ), simulated minus observed.
- Upper right panel: Root-mean-square model error ( $^{\circ}\text{C}$ ), based on all available IPCC model simulations (i.e., square-root of the sum of the squares of individual model errors, divided by the number of models).
- All other panels: Individual model errors ( $^{\circ}\text{C}$ ), simulated minus observed.

The observational estimate is from years 1980-1999 of the ECMWF Reanalysis (ERA40, Uppala et al., 2005), and the model climatologies are calculated for the same period of the CMIP3 20th Century simulations.



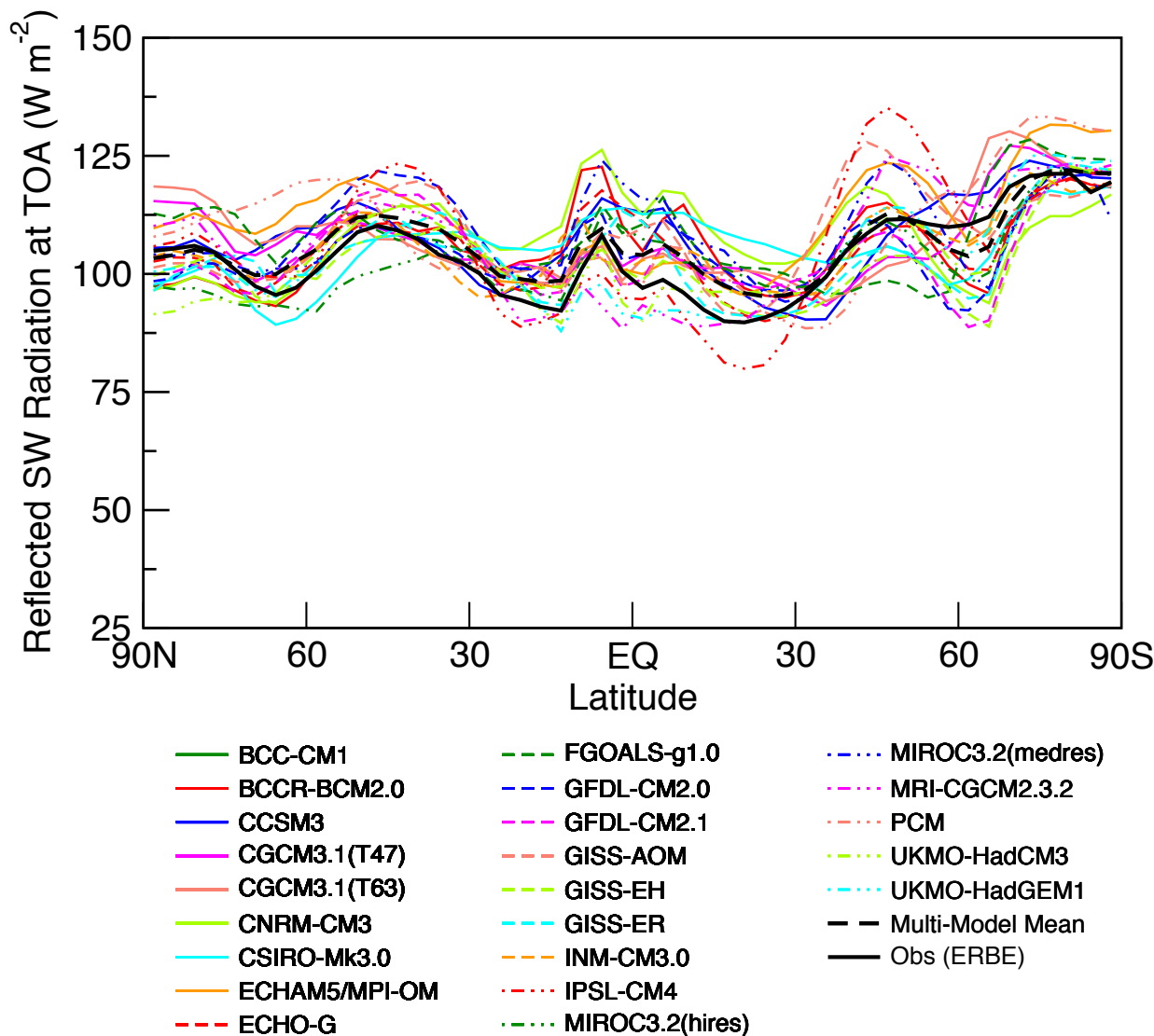




**Figures S8.5: Zonal mean shortwave radiation reflected to space:**

The first page of figure S8.5 shows:

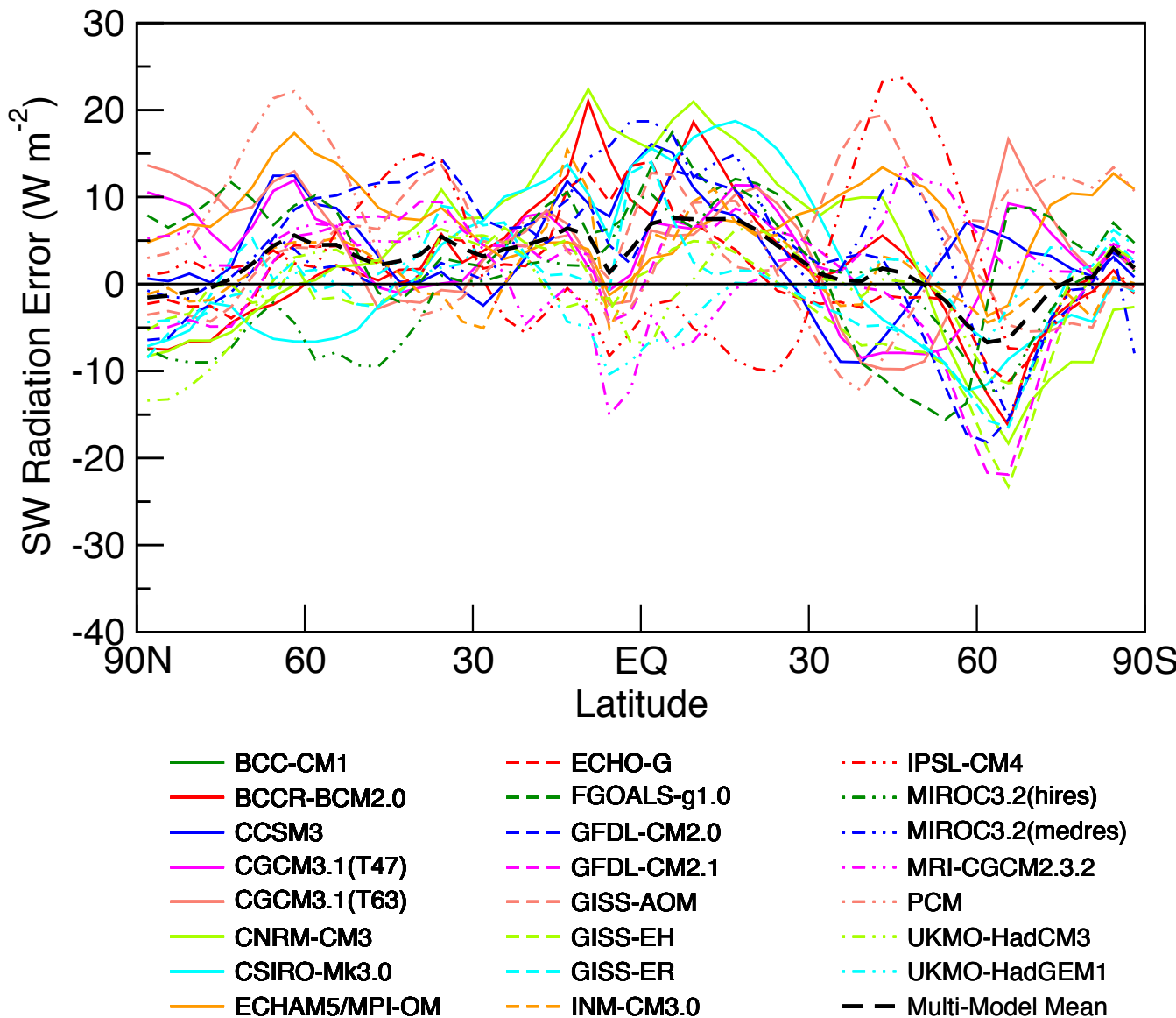
- Observed and simulated annual-mean, zonally-averaged shortwave radiation reflected to space.



The second page of figure S8.5 shows:

- Individual model errors in annual-mean zonally-averaged shortwave radiation reflected to space.

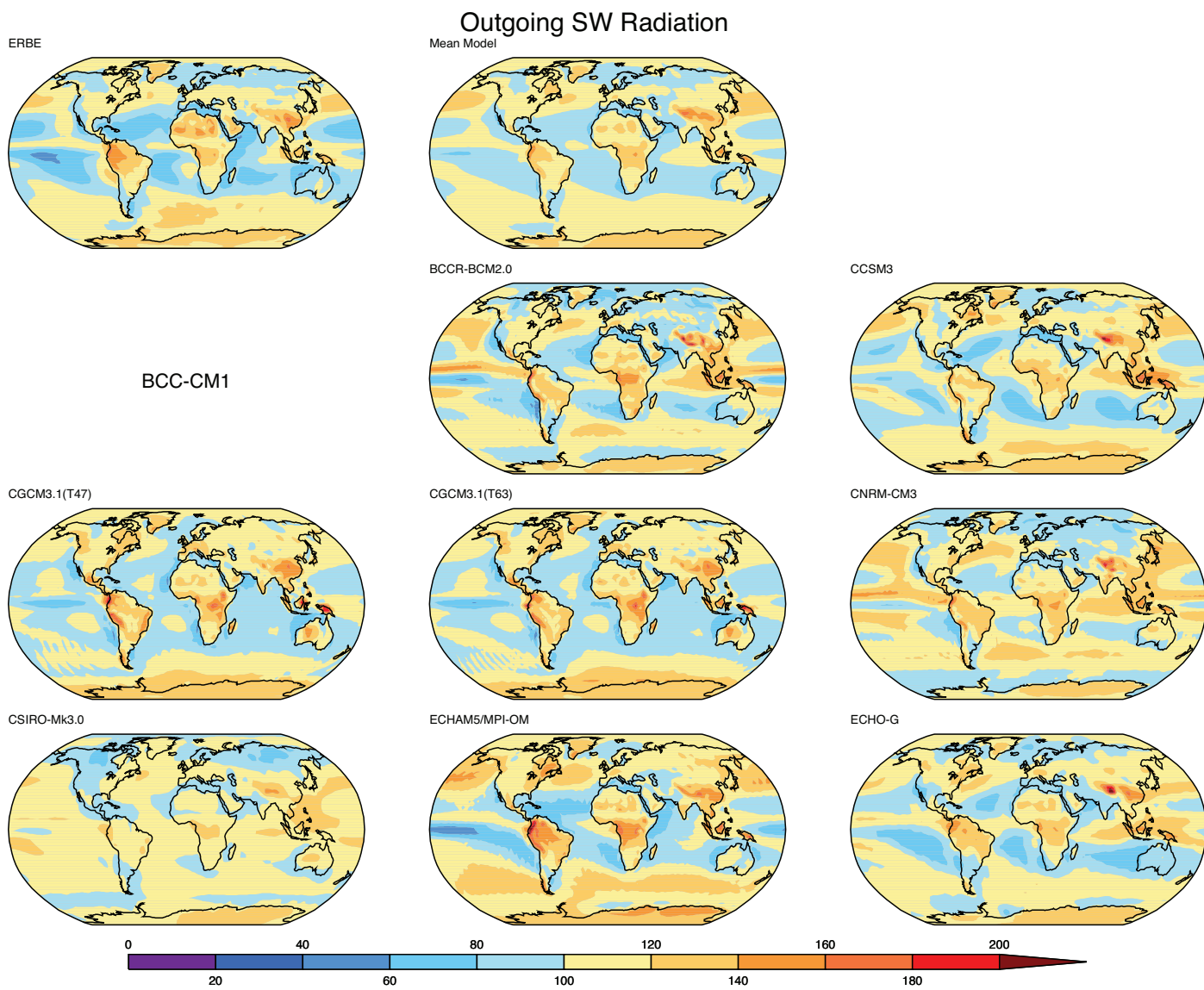
The ERBE (Barkstrom et al., 1989) observational estimates shown here are from 1985–1989 satellite-based radiometers, and the model results are for the same period of the CMIP3 20th Century simulations.

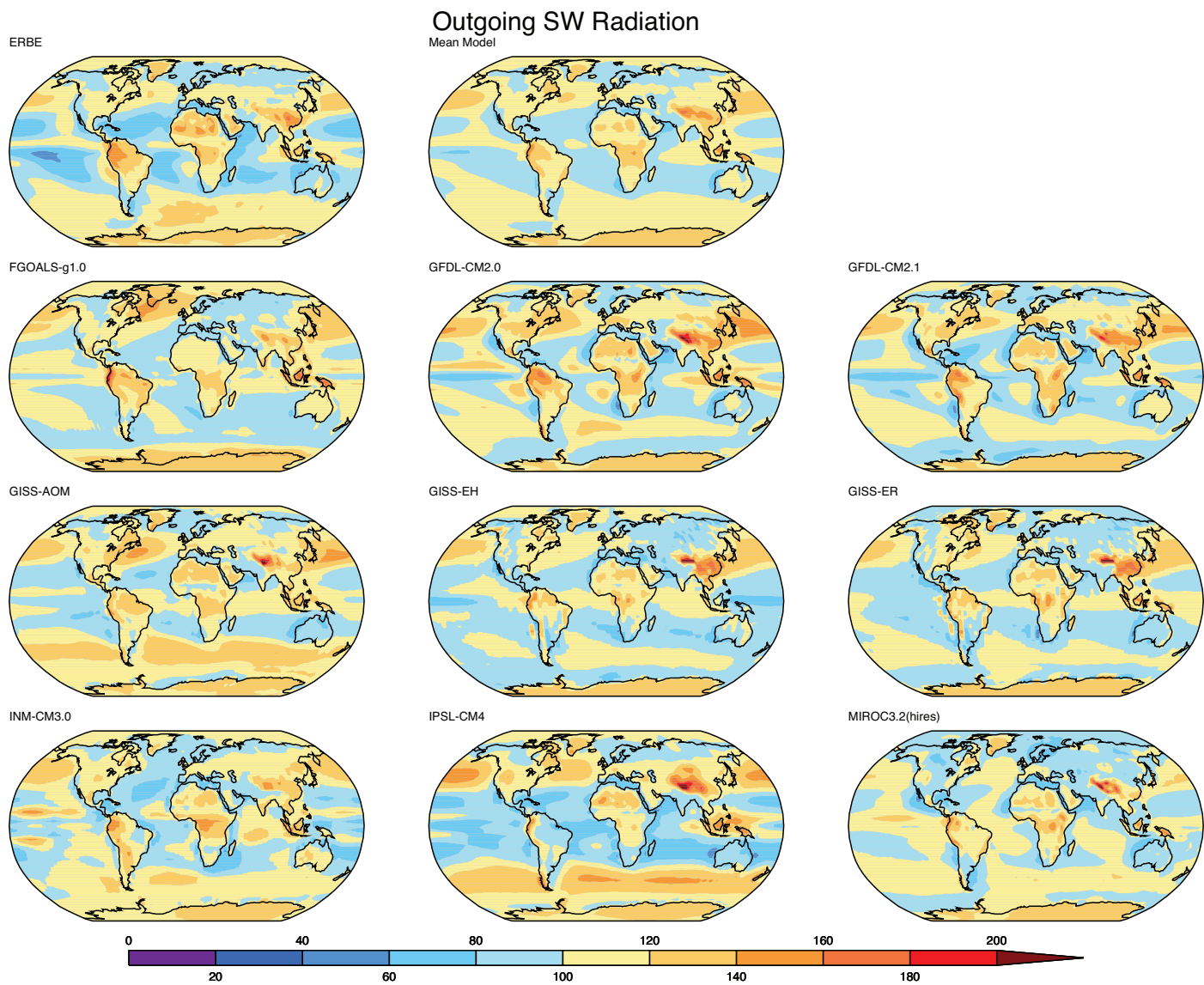


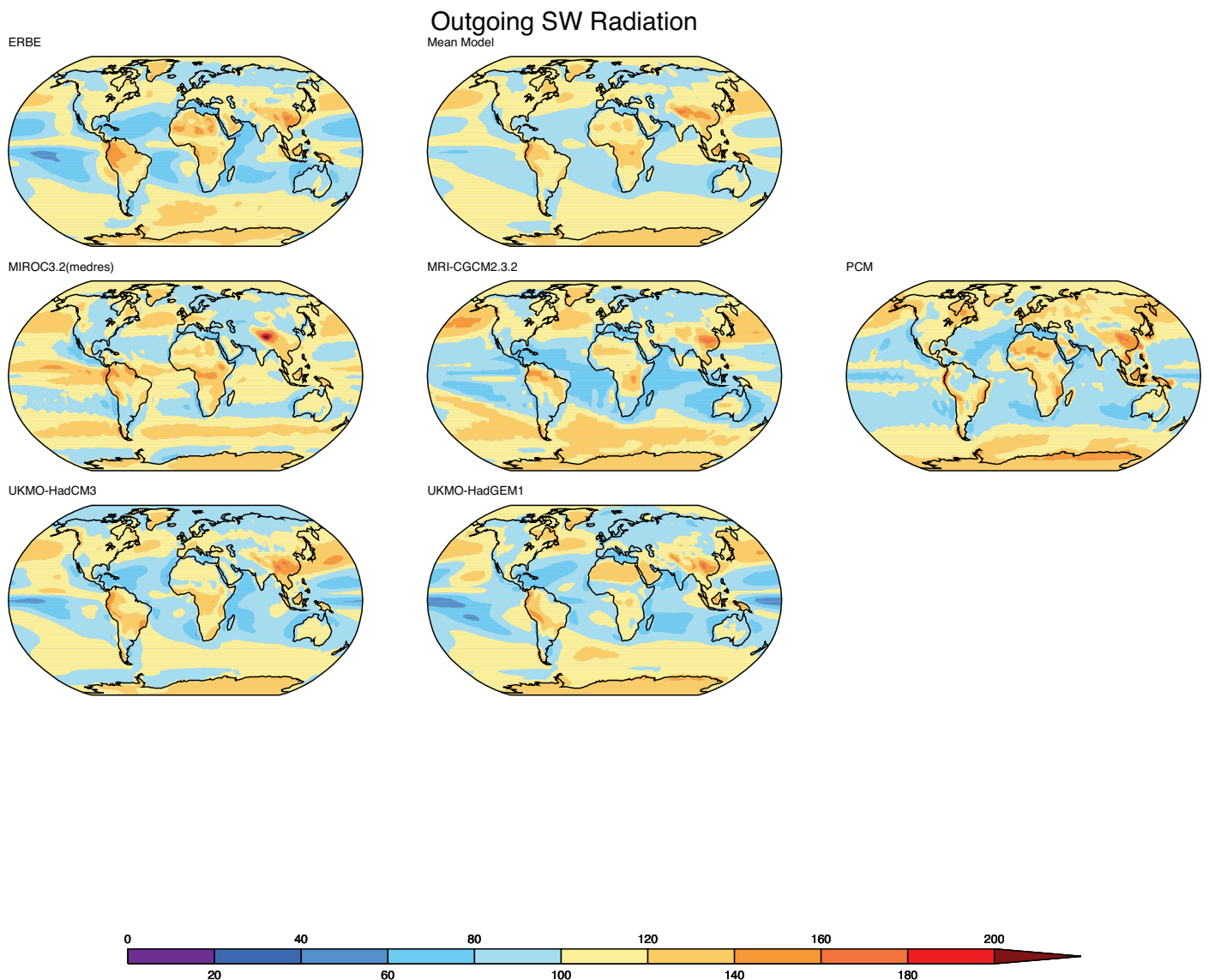
**Figure S8.6: Shortwave radiation reflected to space:**

Each page of figure S8.6a shows:

- Upper left panel: Observed shortwave radiation reflected to space ( $W m^{-2}$ ).
- Upper center panel: Corresponding field averaged over the multi-model ensemble ( $W m^{-2}$ ).
- All other panels: Corresponding individual model results ( $W m^{-2}$ ).



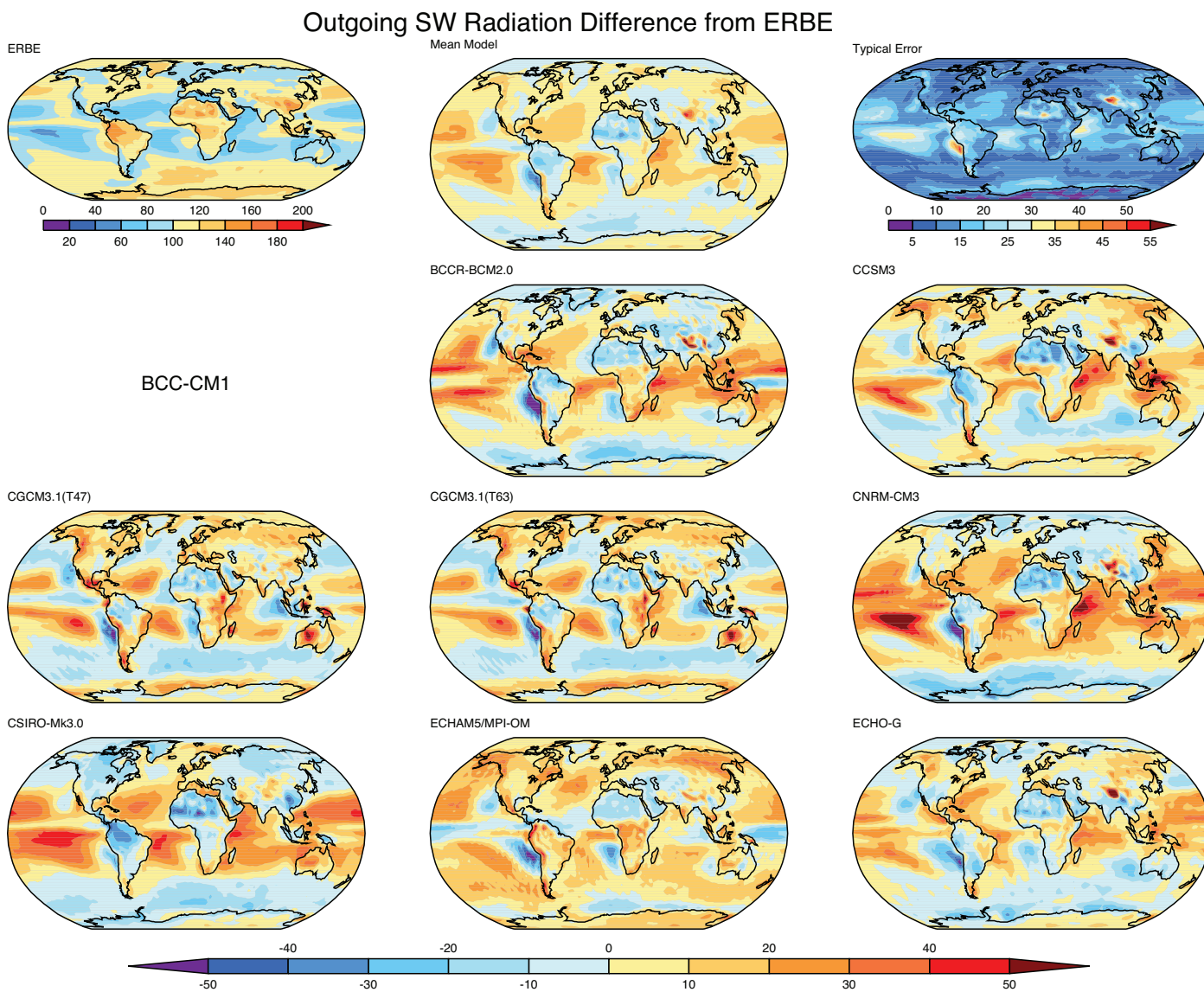


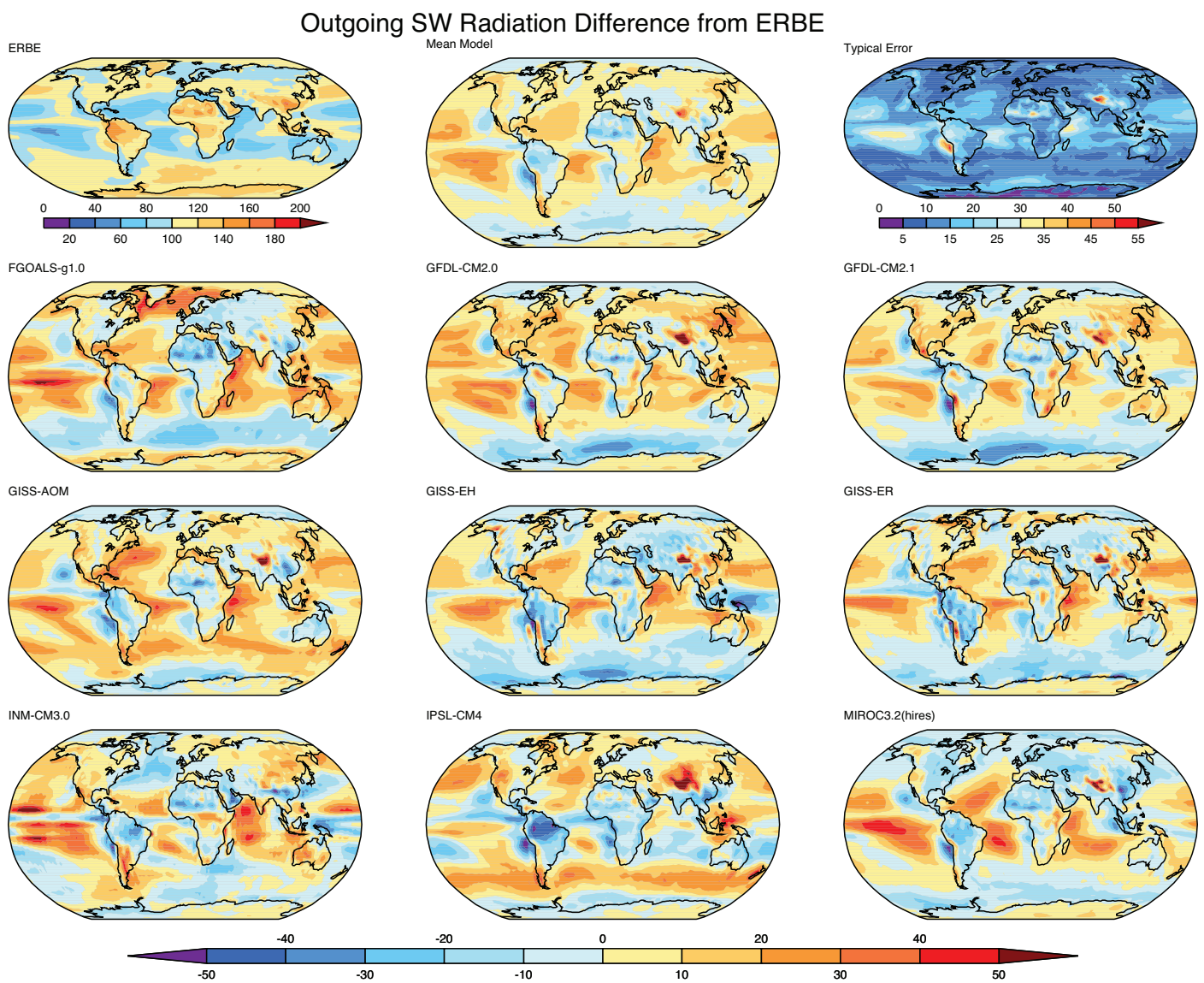


Each page of figure S8.6b shows:

- Upper left panel: Observed shortwave radiation reflected to space ( $W\ m^{-2}$ ).
- Upper center panel: Multi-model mean error ( $W\ m^{-2}$ ), simulated minus observed.
- Upper right panel: Root-mean-square model error ( $W\ m^{-2}$ ), based on all available IPCC model simulations (i.e., square-root of the sum of the squares of individual model errors, divided by the number of models).
- All other panels: Individual model errors ( $W\ m^{-2}$ ), simulated minus observed.

The ERBE (Barkstrom et al., 1989) observational estimates shown here are from 1985–1989 satellite-based radiometers, and the model results are for the same period of the CMIP3 20th Century simulations.





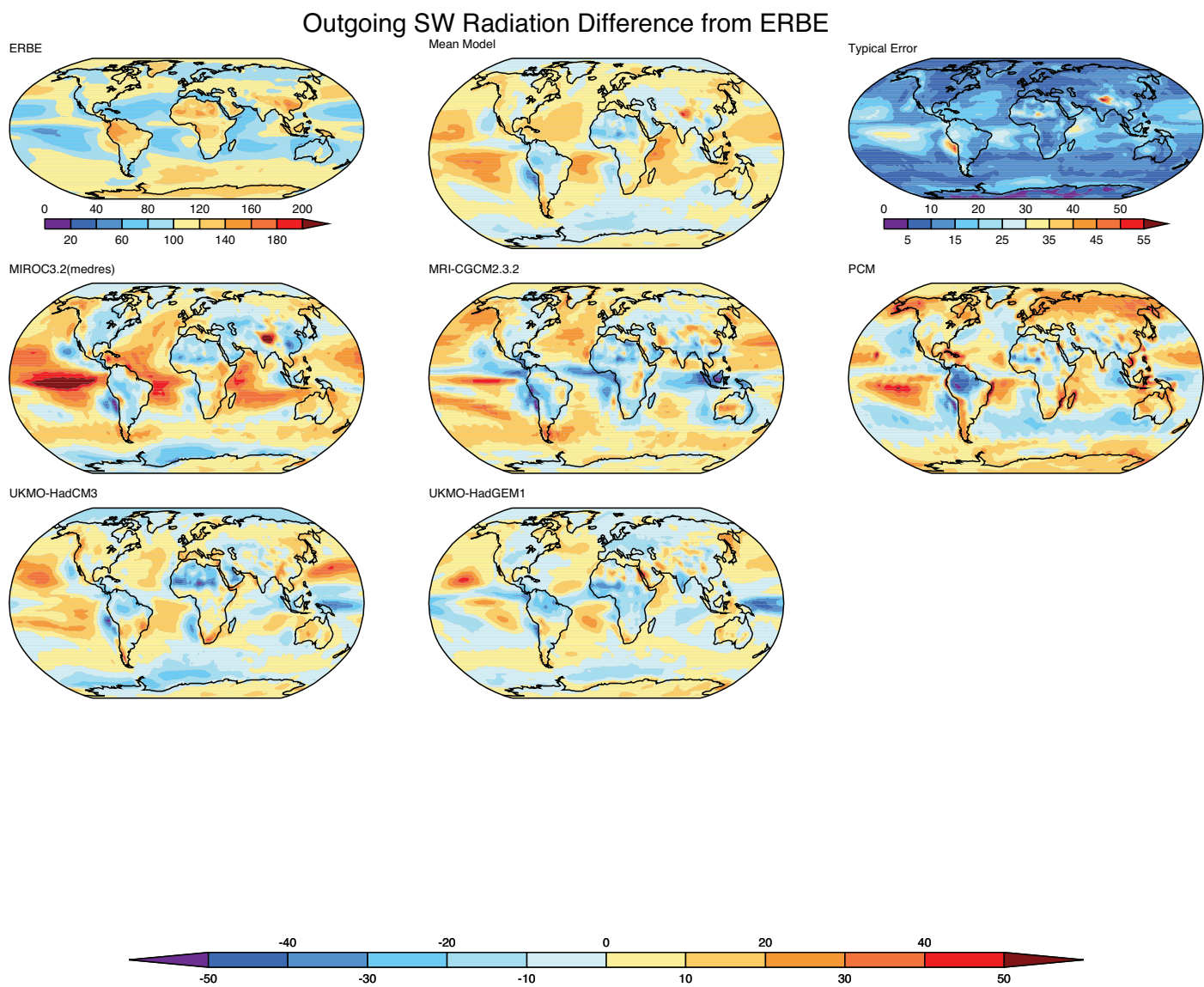
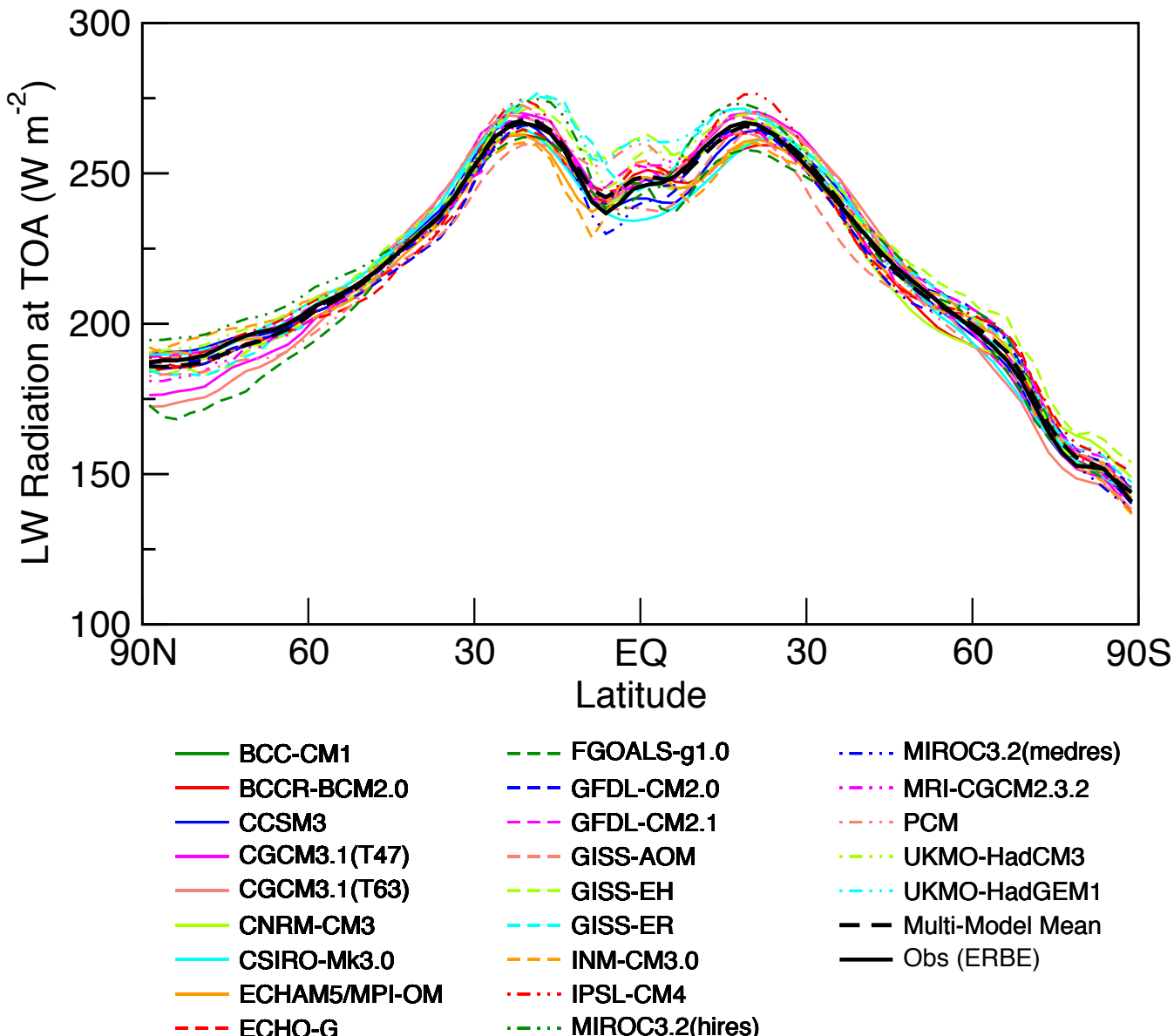


**Figure S8. 7: Zonal mean outgoing longwave radiation:**

The first page of figure S8.7 shows:

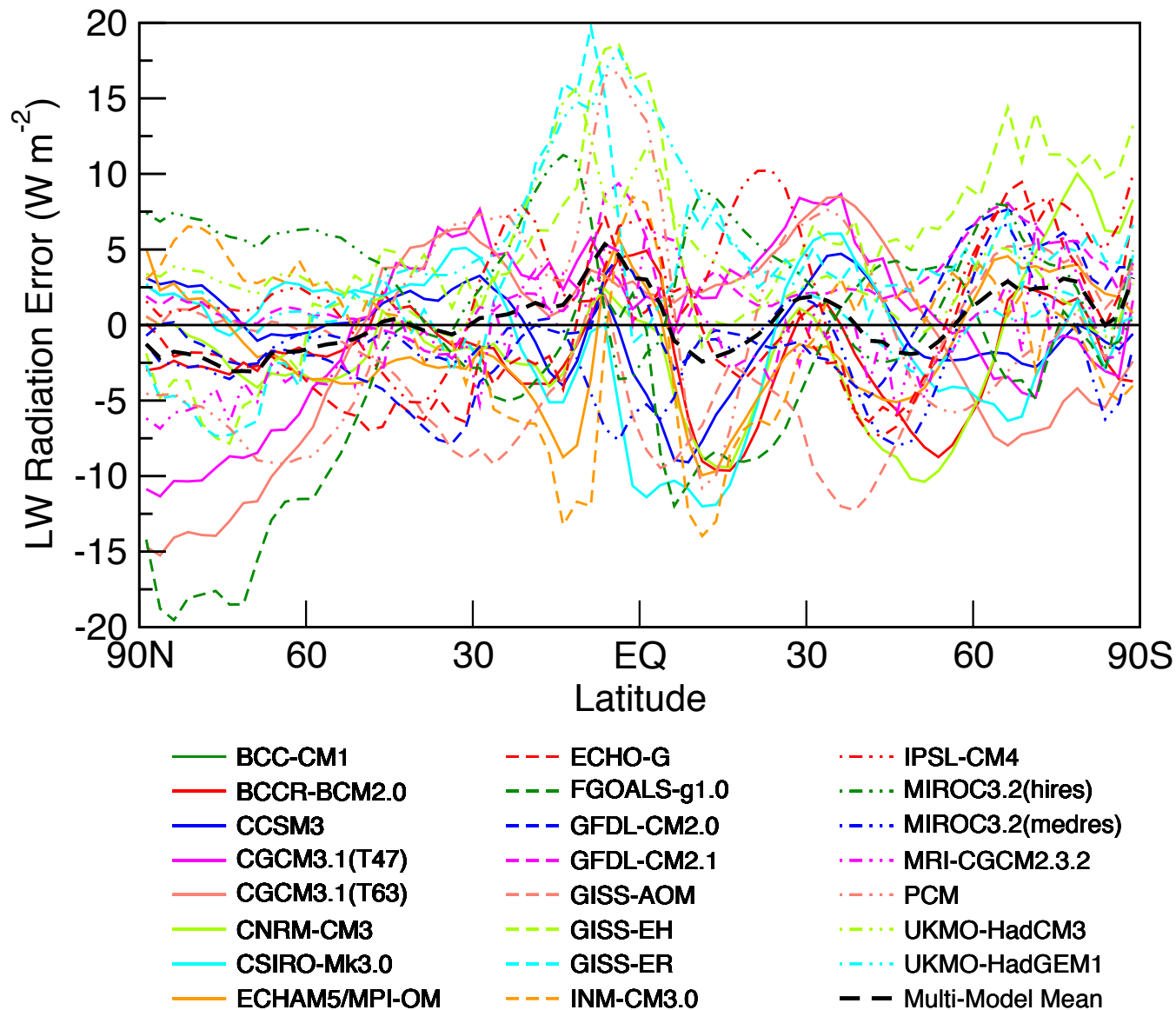
- Observed and simulated annual-mean, zonally-averaged outgoing longwave radiation.



The second page of figure S8.7 shows:

- Individual model errors in annual-mean zonally-averaged outgoing longwave radiation.

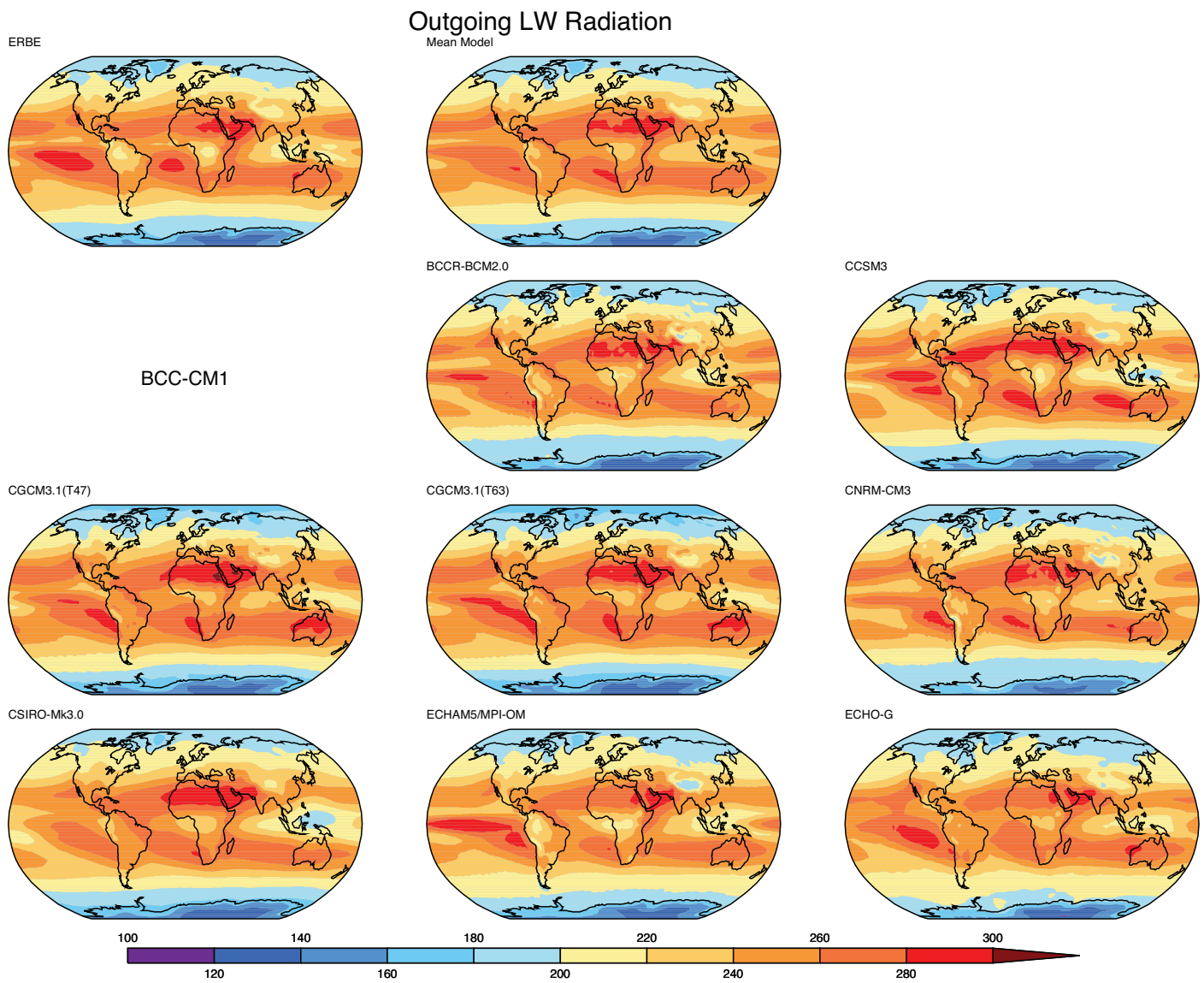
The ERBE (Barkstrom et al., 1989) observational estimates shown here are from 1985–1989 satellite-based radiometers, and the model results are for the same period of the CMIP3 20th Century simulations.

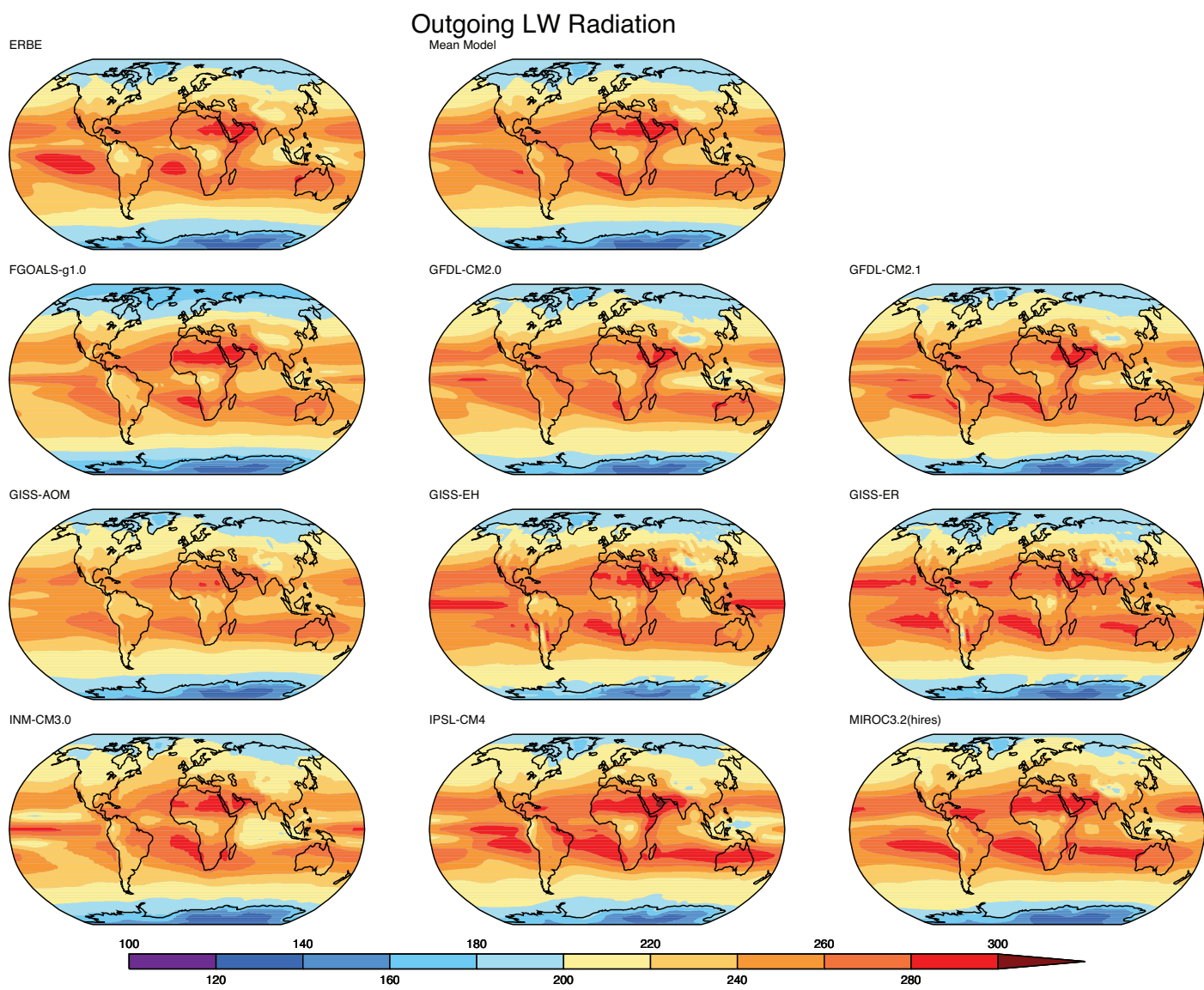


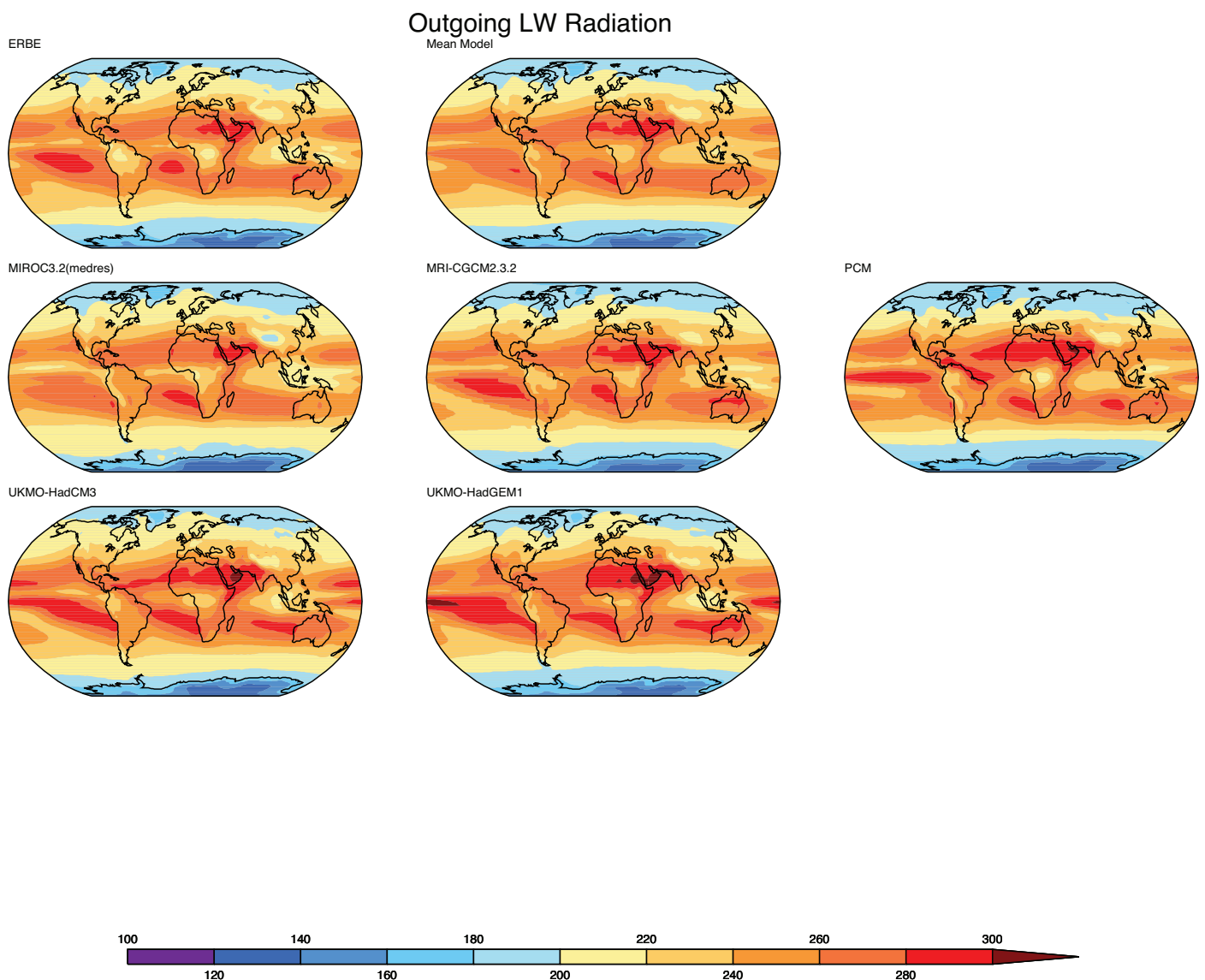
**Figure S8.8: Outgoing longwave radiation:**

Each page of figure S8.8a shows:

- Upper left panel: Observed outgoing longwave radiation ( $W\ m^{-2}$ ).
- Upper center panel: Corresponding field averaged over the multi-model ensemble ( $W\ m^{-2}$ ).
- All other panels: Corresponding individual model results ( $W\ m^{-2}$ ).



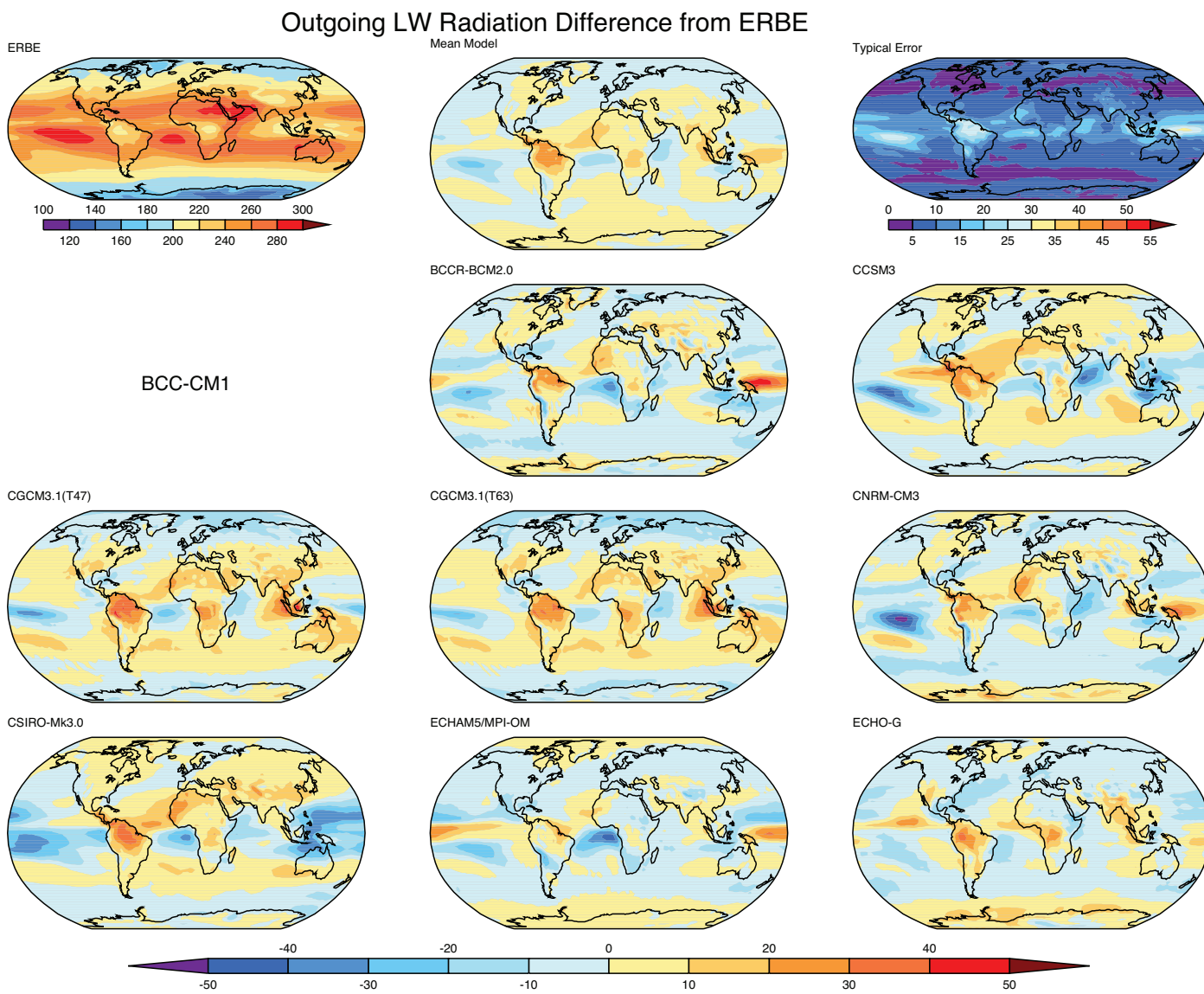


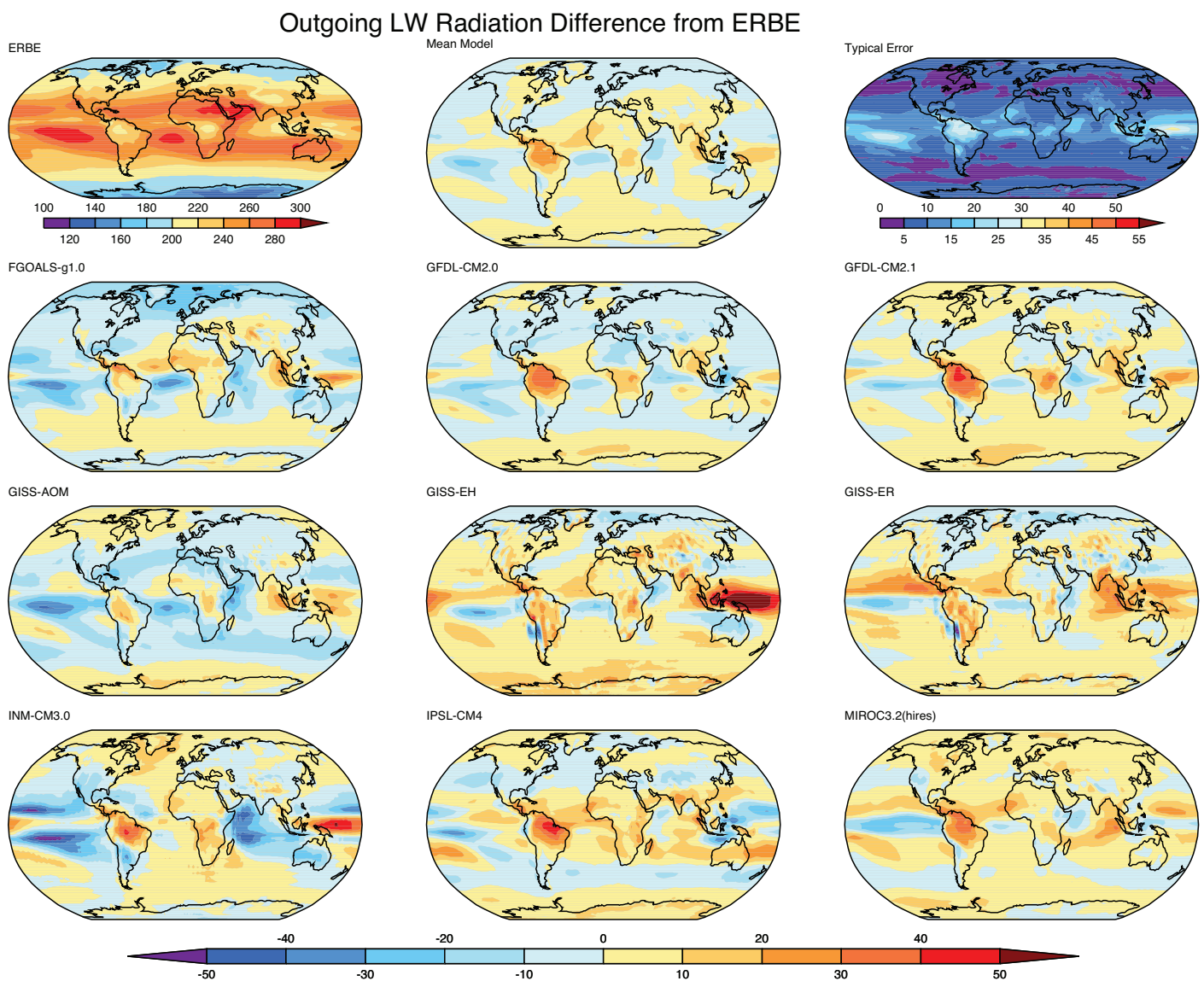


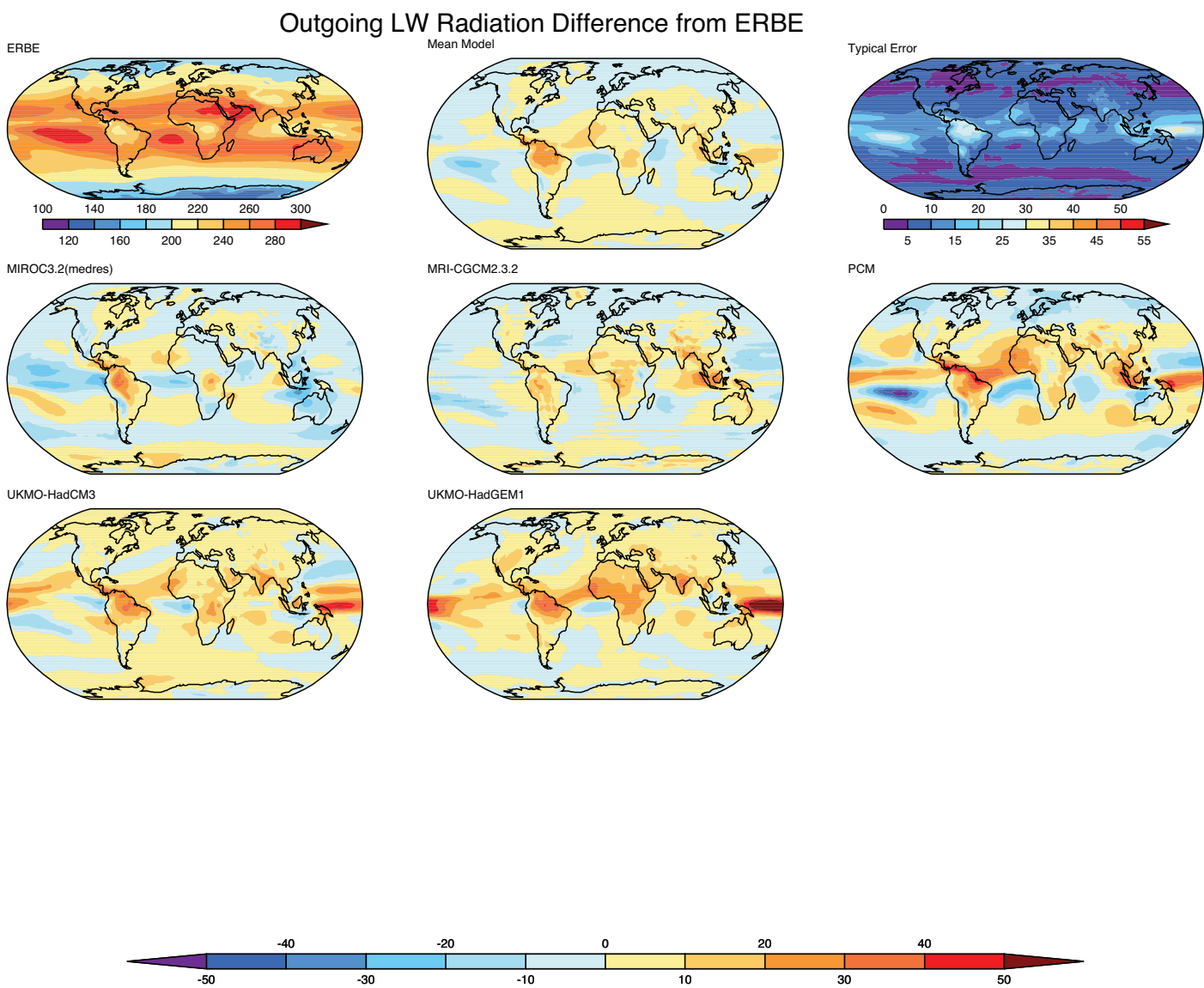
Each page of figure S8.8b shows:

- Upper left panel: Observed outgoing longwave radiation ( $W m^{-2}$ ).
- Upper center panel: Multi-model mean error ( $W m^{-2}$ ), simulated minus observed.
- Upper right panel: Root-mean-square model error ( $W m^{-2}$ ), based on all available IPCC model simulations (i.e., square-root of the sum of the squares of individual model errors, divided by the number of models).
- All other panels: Individual model errors ( $W m^{-2}$ ), simulated minus observed.

The ERBE (Barkstrom et al., 1989) observational estimates shown here are from 1985–1989 satellite-based radiometers, and the model results are for the same period of the CMIP3 20th Century simulations in the multi-model dataset at PCMDI.



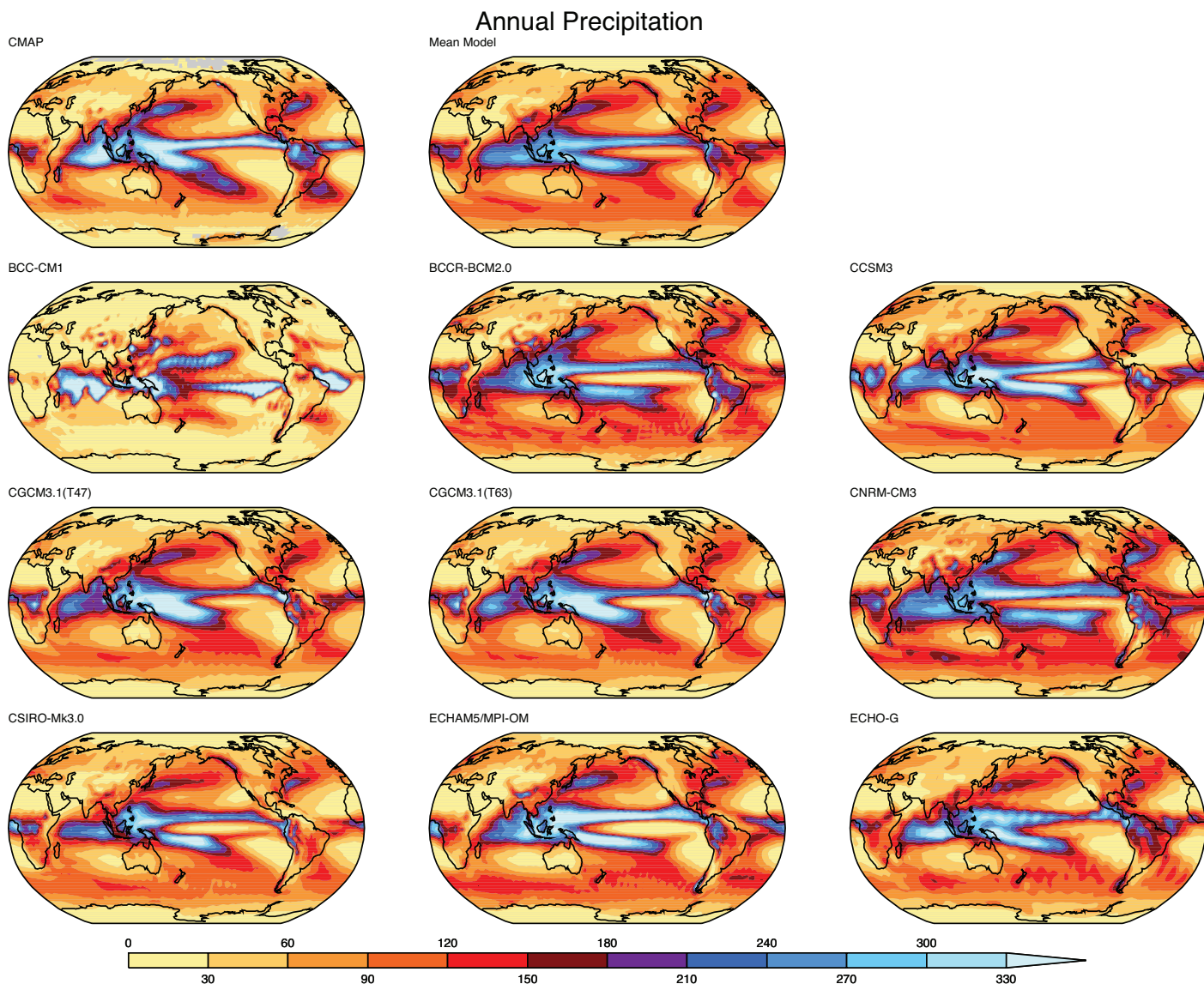


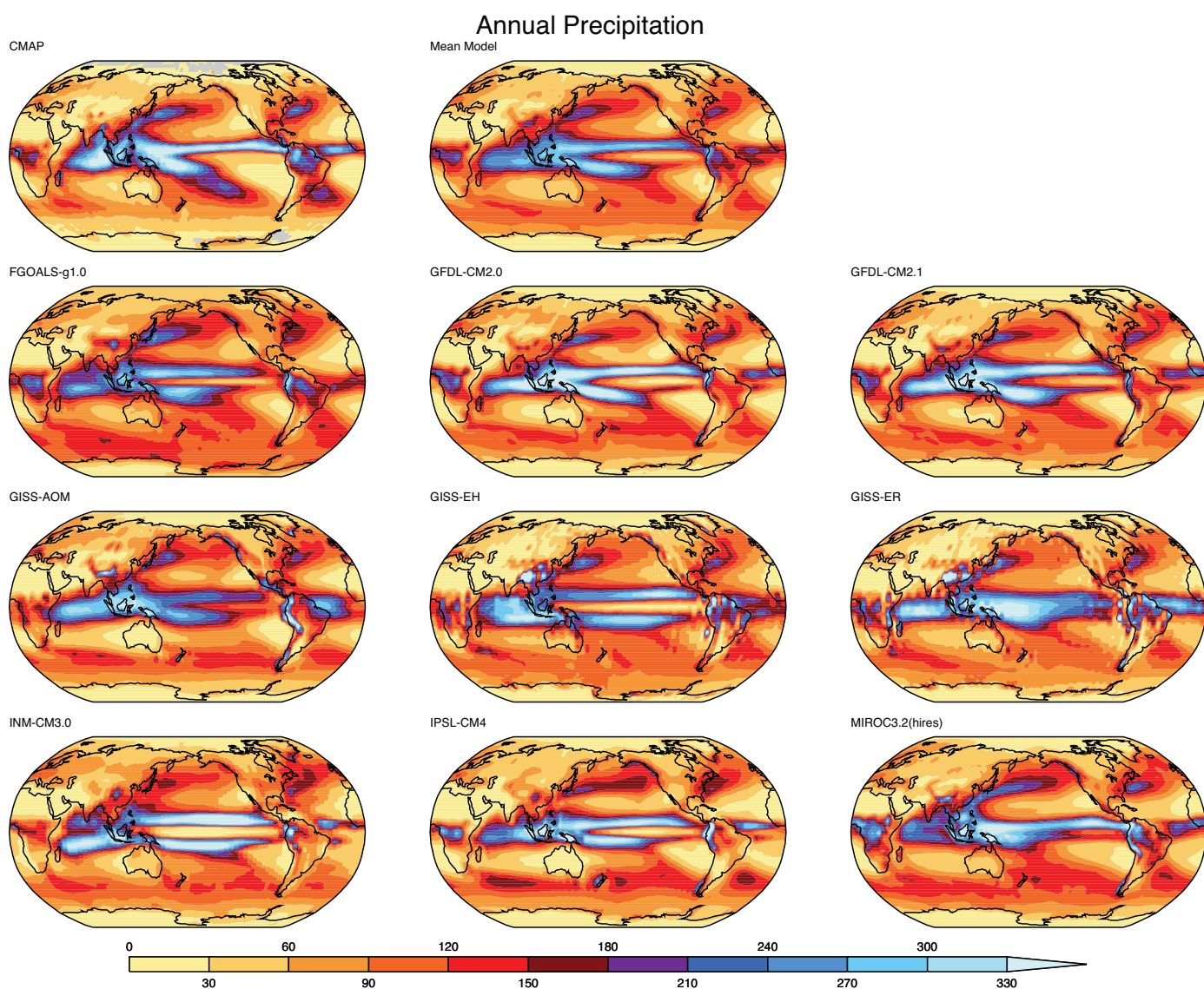


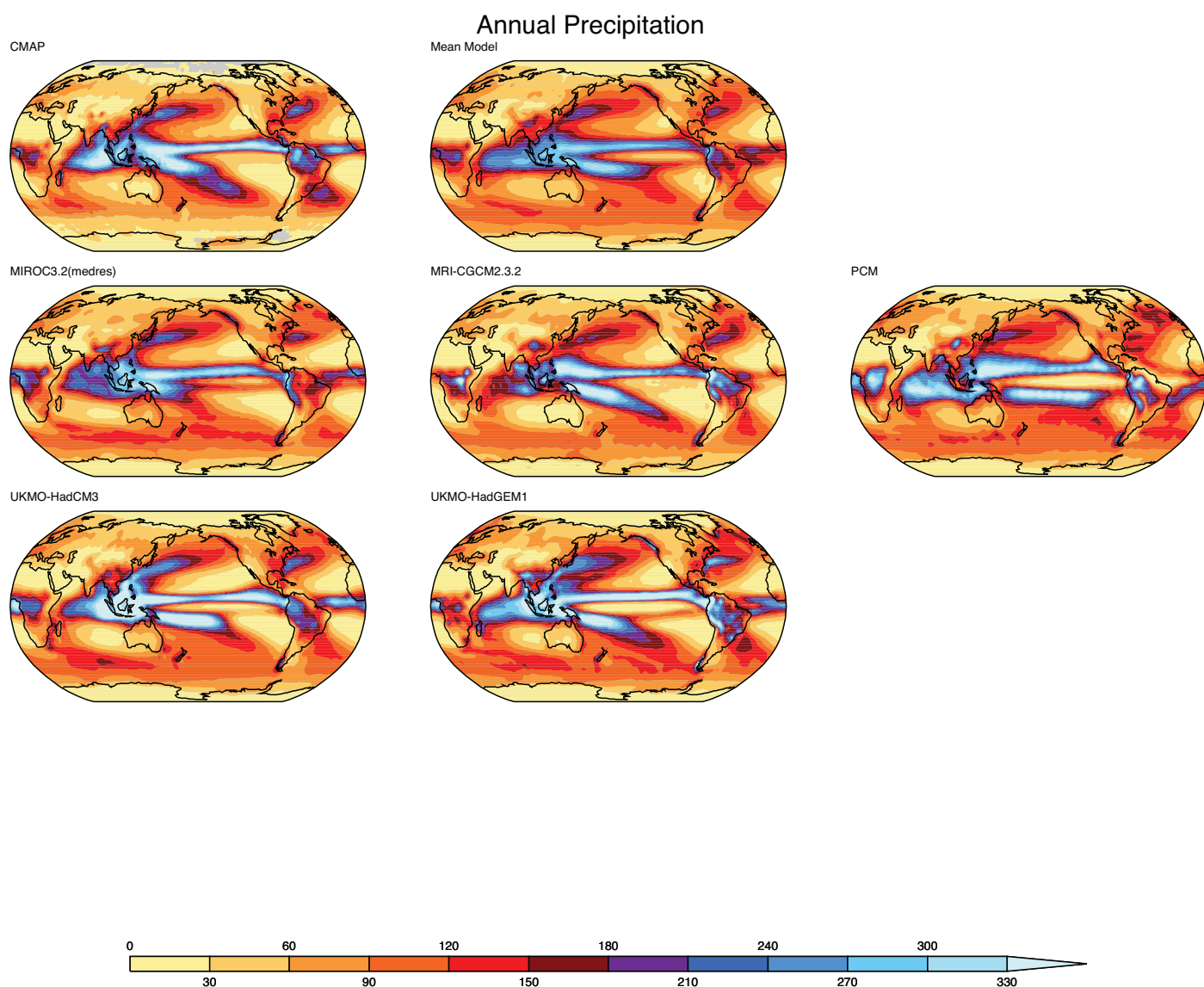
**Figure S8.9: Precipitation:**

Each page of figure S8.9a shows:

- Upper left panel: Observed annual-mean precipitation (cm).
- Upper center panel: Corresponding field averaged over the multi-model ensemble (cm).
- All other panels: Corresponding individual model results (cm).



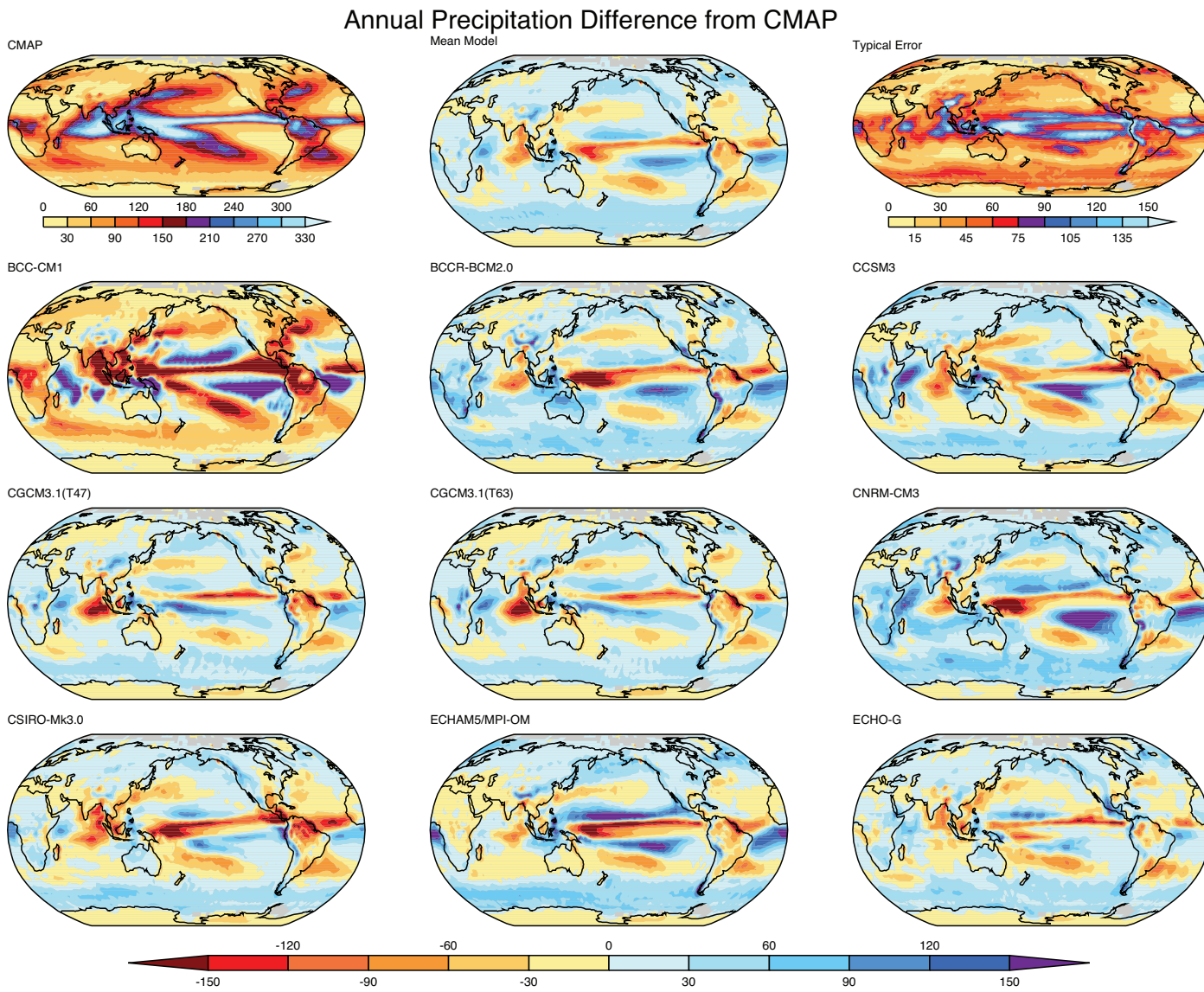


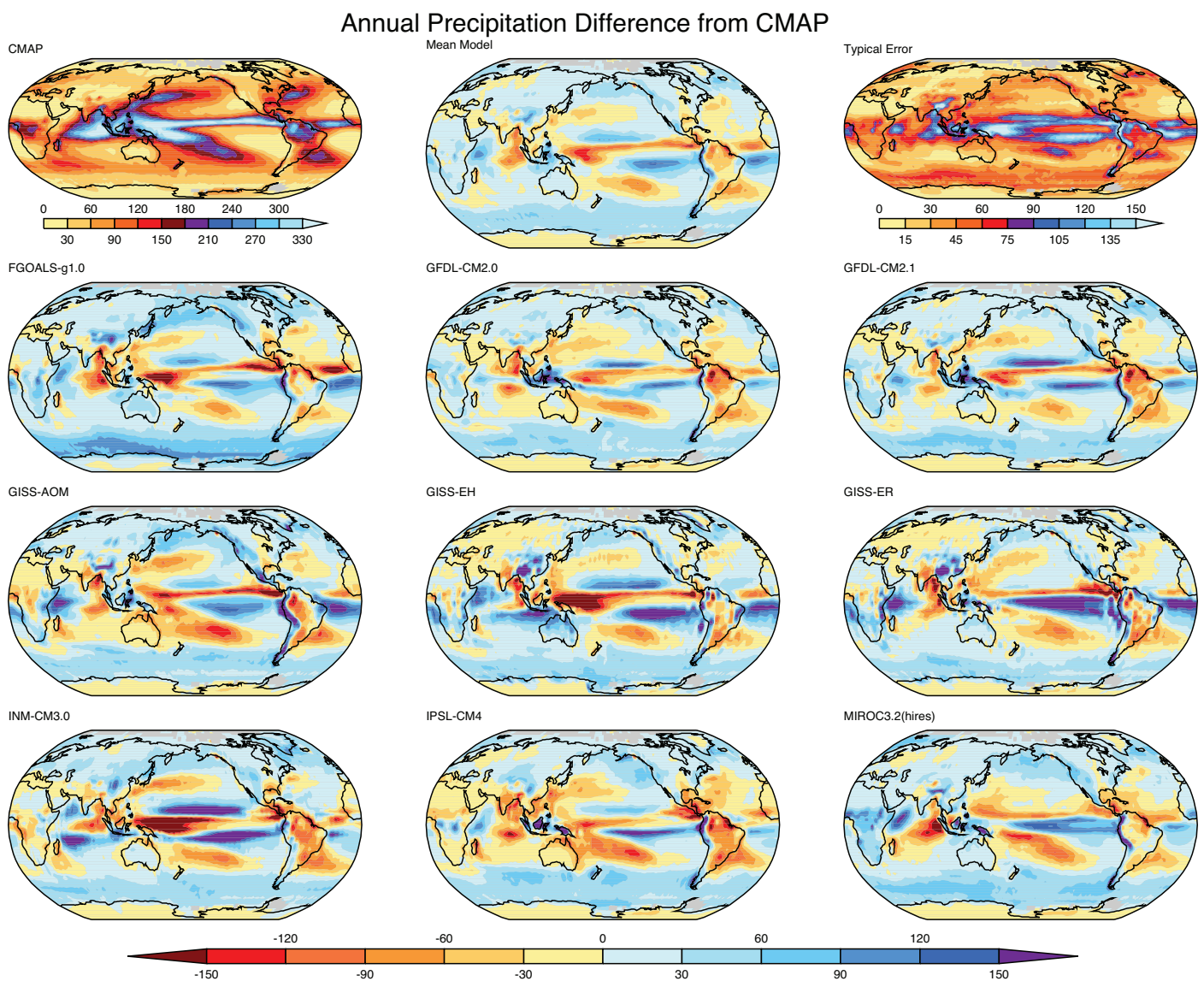


Each page of figure S8.9b shows:

- Upper left panel: Observed annual-mean precipitation climatology (cm).
- Upper center panel: Multi-model mean error (cm), simulated minus observed.
- Upper right panel: Root-mean-square model error (cm), based on all available IPCC model simulations (i.e., square-root of the sum of the squares of individual model errors, divided by the number of models).
- All other panels: Individual model errors (cm), simulated minus observed.

The CMAP (Xie and Arkin, 1997) observation-based climatology for 1980–1999 is shown, and the model results are for the same period of the CMIP3 20th Century simulations. Observations were not available in the grey regions.





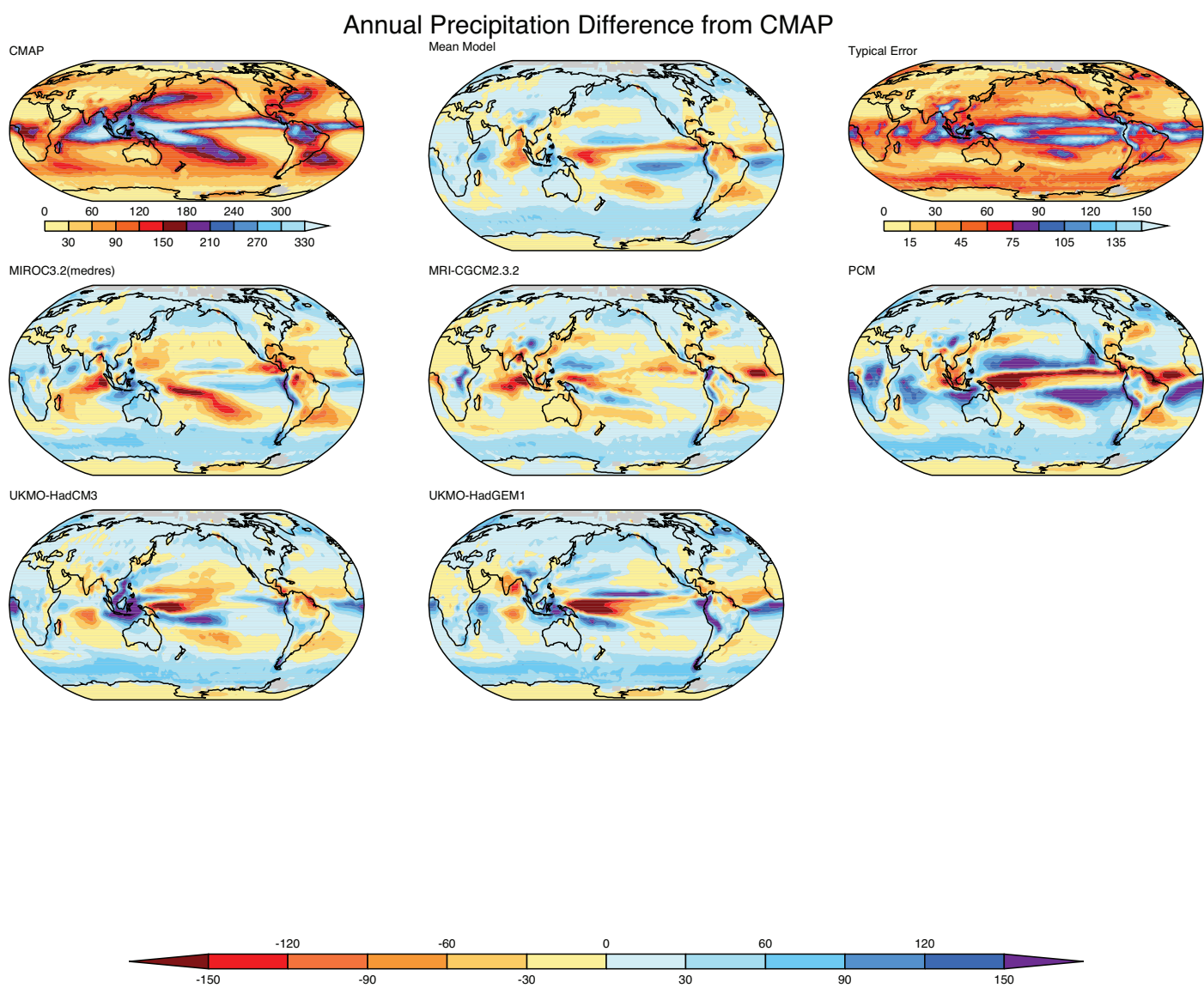
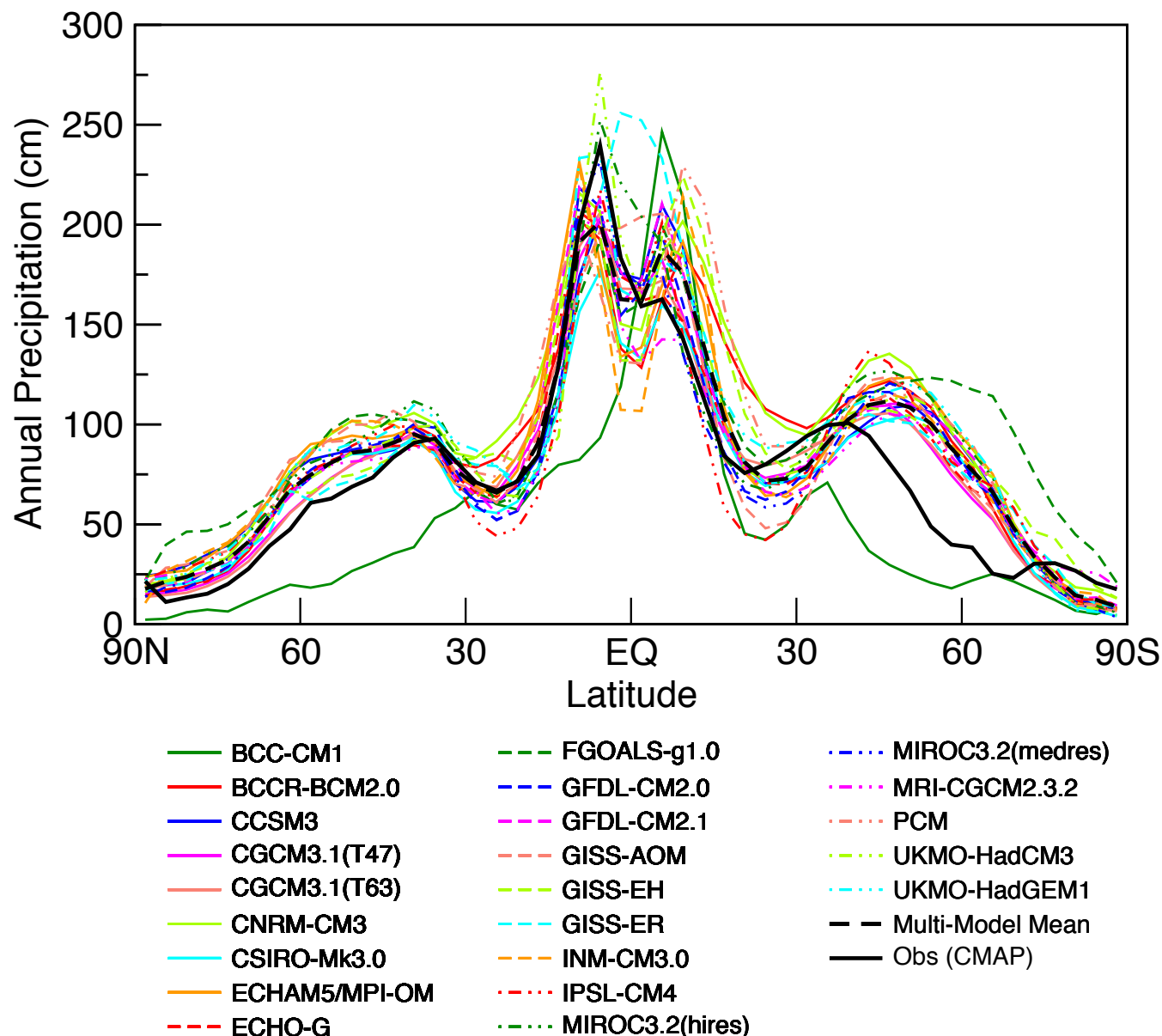


**Figure S8.10: Zonal mean precipitation:**

The first page of figure S8.10 shows:

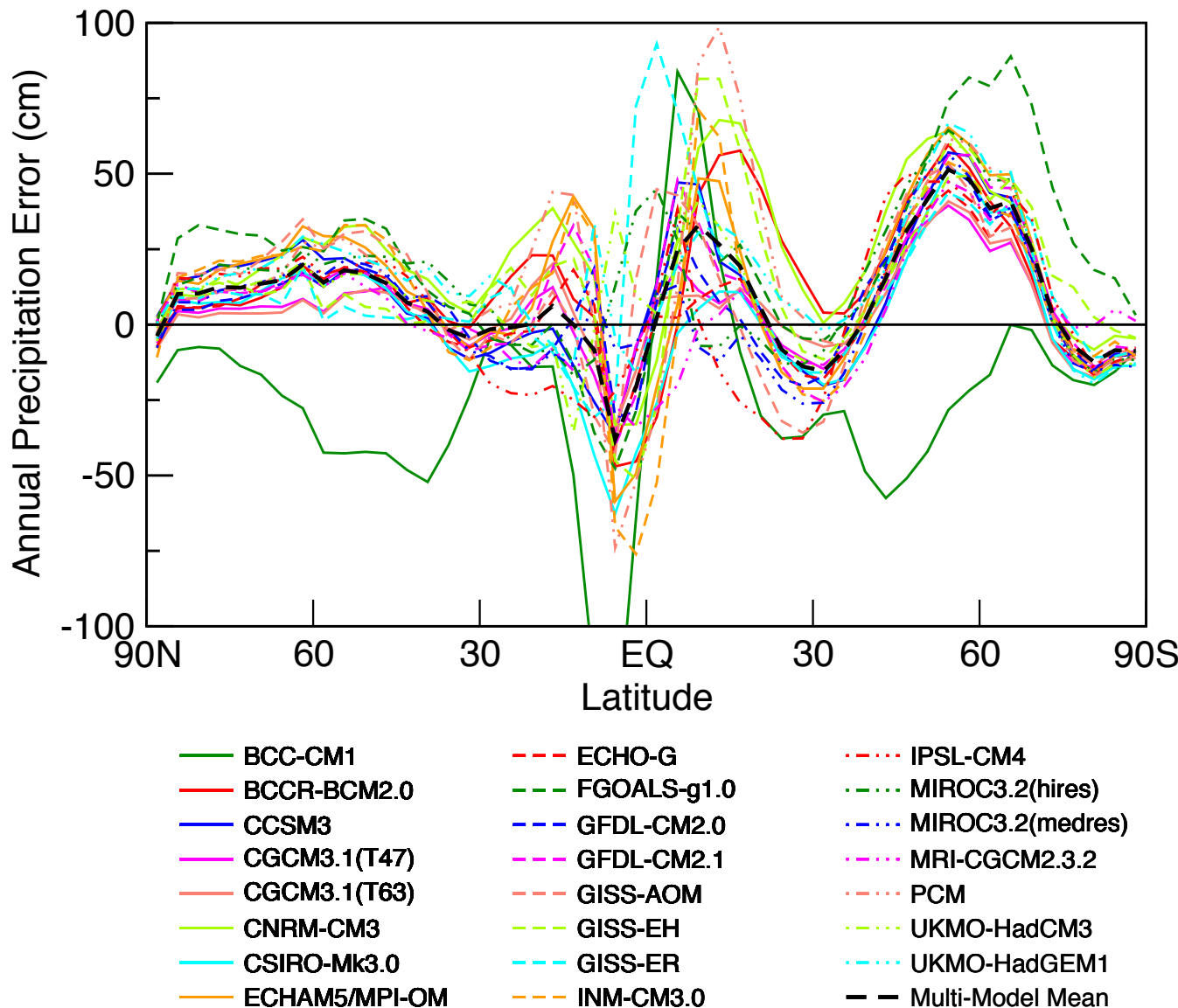
- Observed and simulated annual-mean, zonally-averaged precipitation amount.



The second page figure S8.10 shows:

- Individual model errors in annual-mean zonally-averaged precipitation amount.

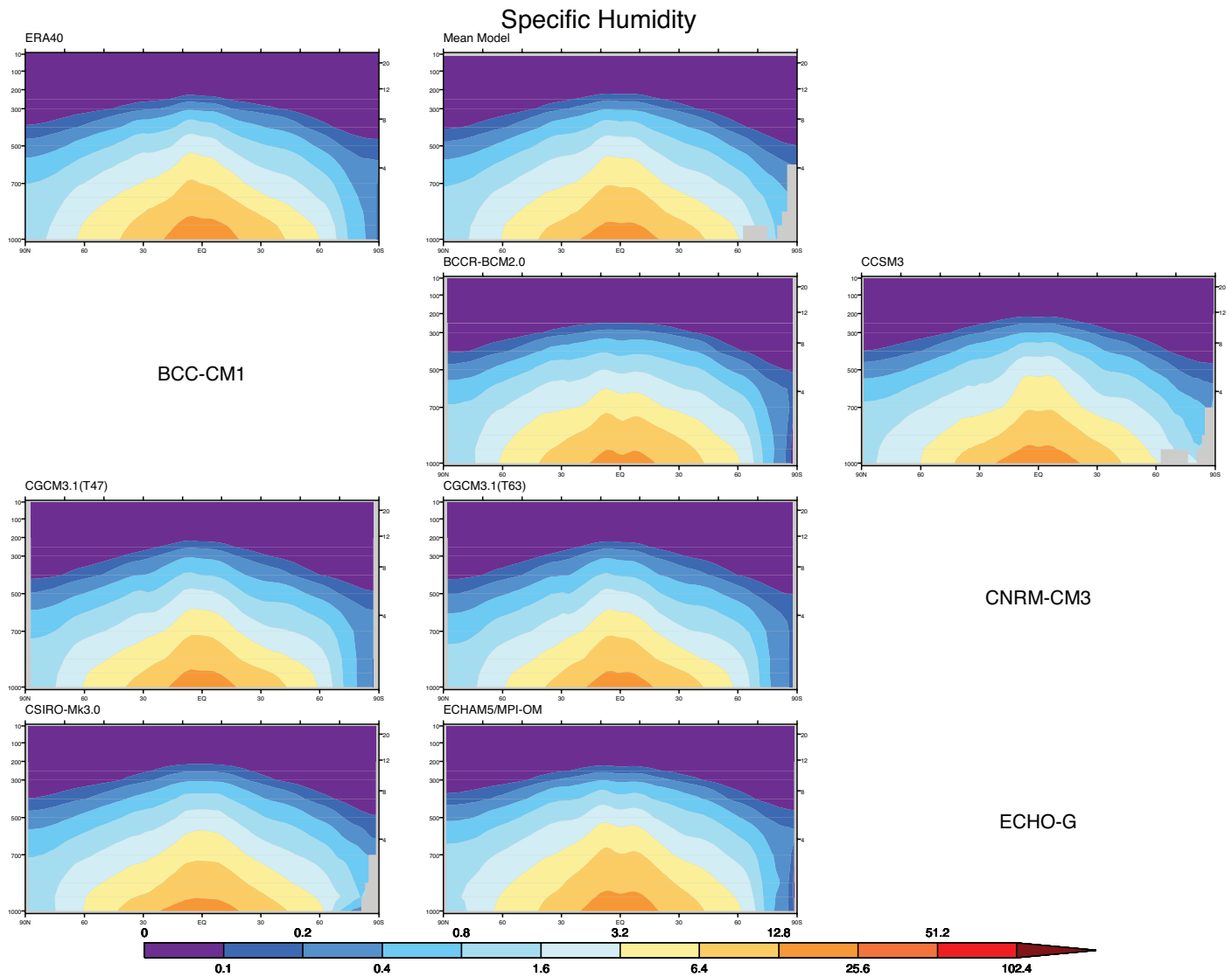
The CMAP (Xie and Arkin, 1997) observation-based climatology for 1980–1999 is shown, and the model results are for the same period of the CMIP3 20th Century simulations. Observations were not available in the grey regions.

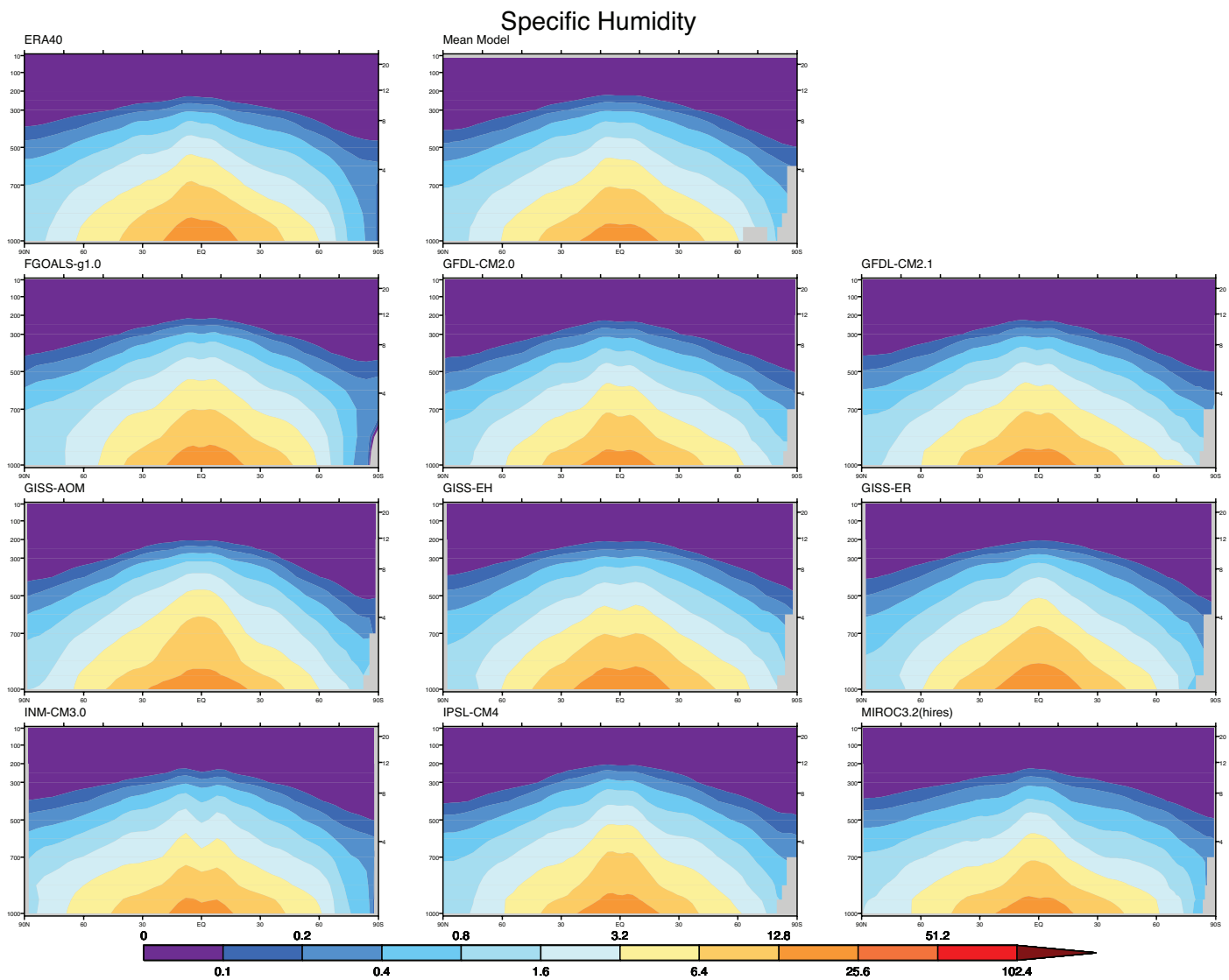


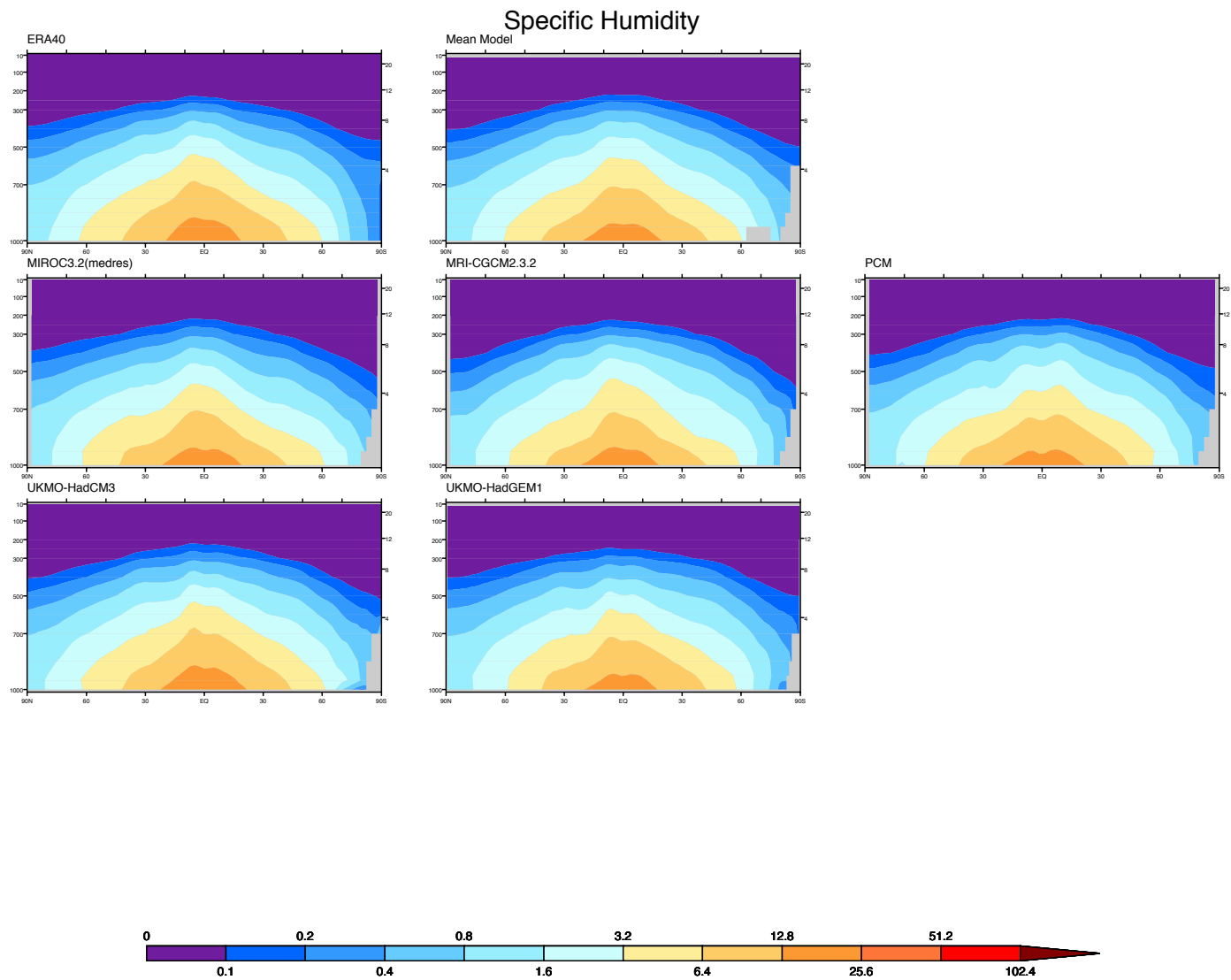
**Figure S8.11: Zonal mean specific humidity cross-sections:**

Each page of figure S8.11a shows:

- Upper left panel: Observed annual mean specific humidity climatology (g/kg), averaged zonally.
- Upper center panel: Corresponding field averaged over the multi-model ensemble (g/kg).
- All other panels: Corresponding individual model results (g/kg).



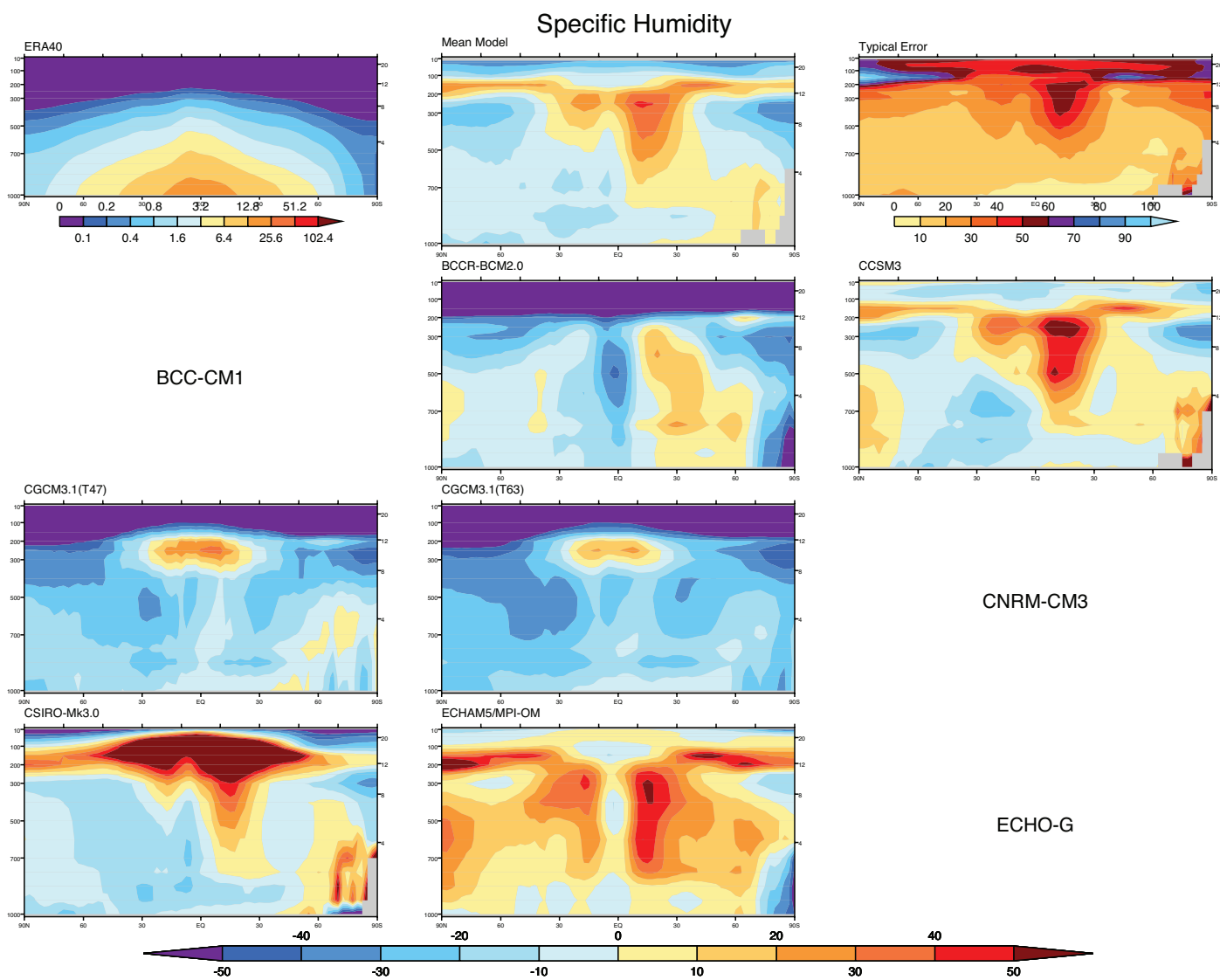


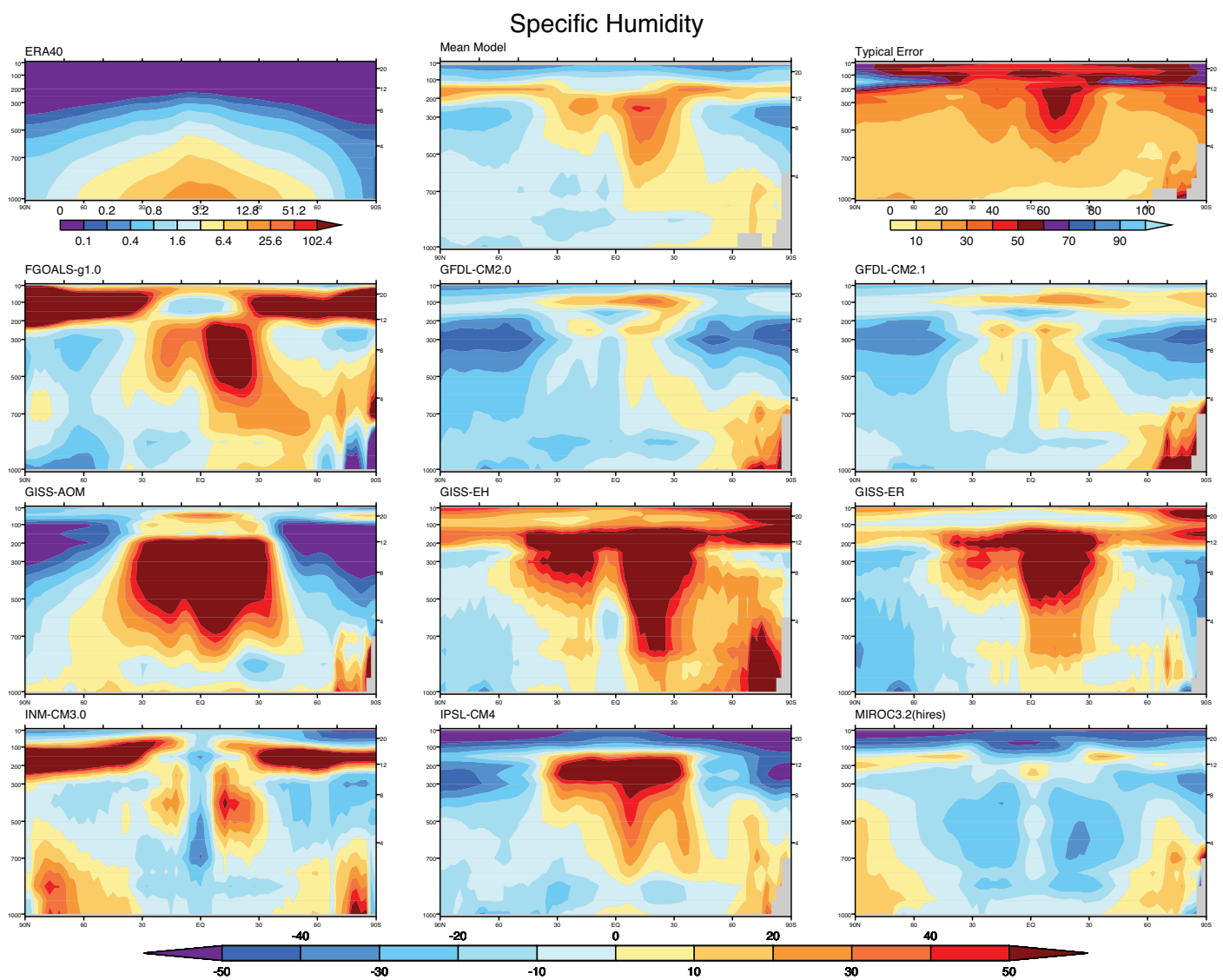


Each page of figure S8.11b shows:

- Upper left panel: Observed annual mean specific humidity climatology (g/kg), averaged zonally.
- Upper center panel: Multi-model mean fractional error, expressed as a percent (i.e., simulated minus observed, divided by observed and multiplied by 100).
- Upper right panel: Root-mean-square model fractional error, expressed as a percent, based on all available IPCC model simulations.
- All other panels: Individual model errors, expressed as a percent (i.e., simulated minus observed, divided by observed and multiplied by 100).

The observational estimate is from the 40-year European Reanalysis (ERA40, Uppala et al., 2005) based on observations over the period 1980-1999. The model results are from the same period of the CMIP3 20th Century simulations.





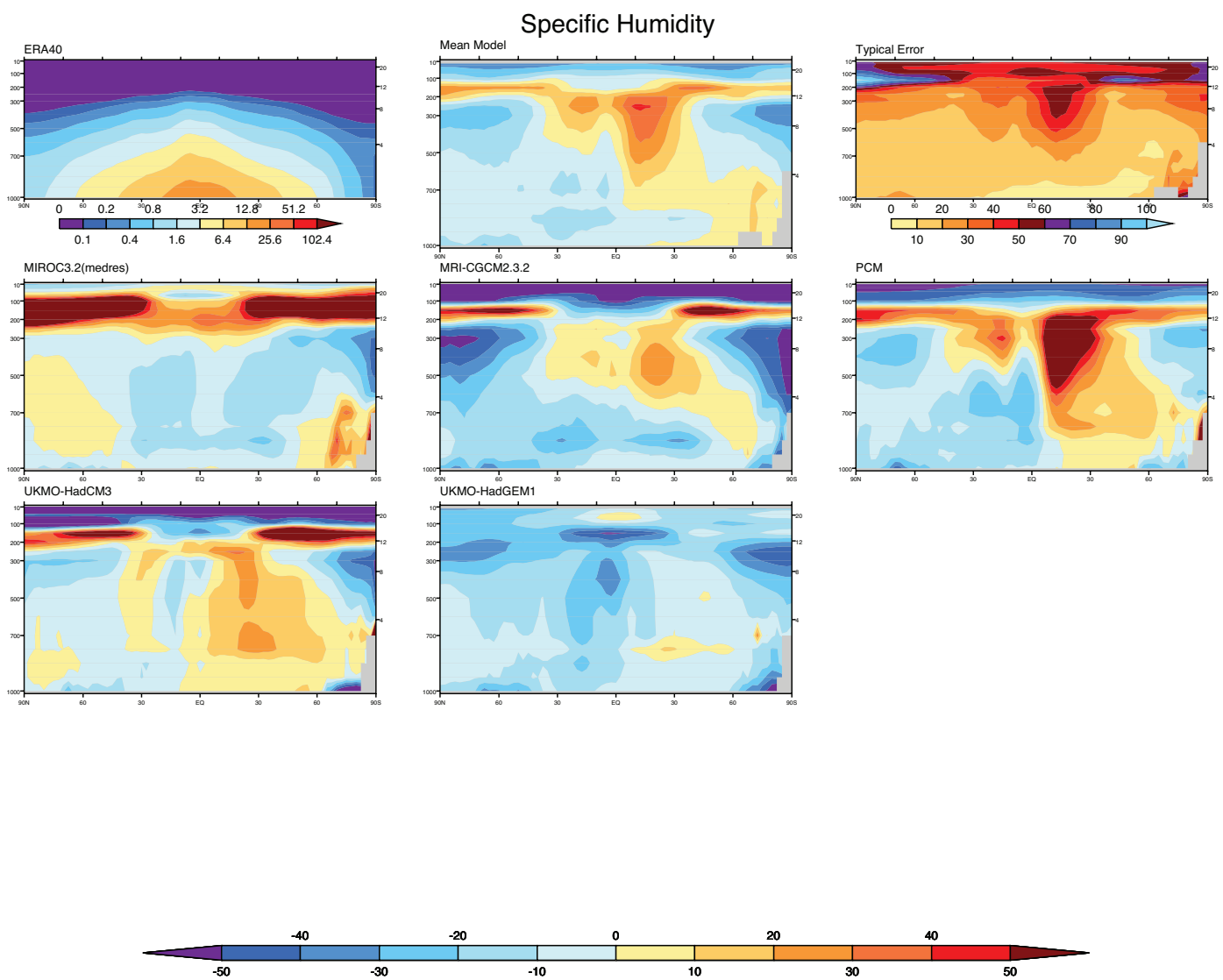
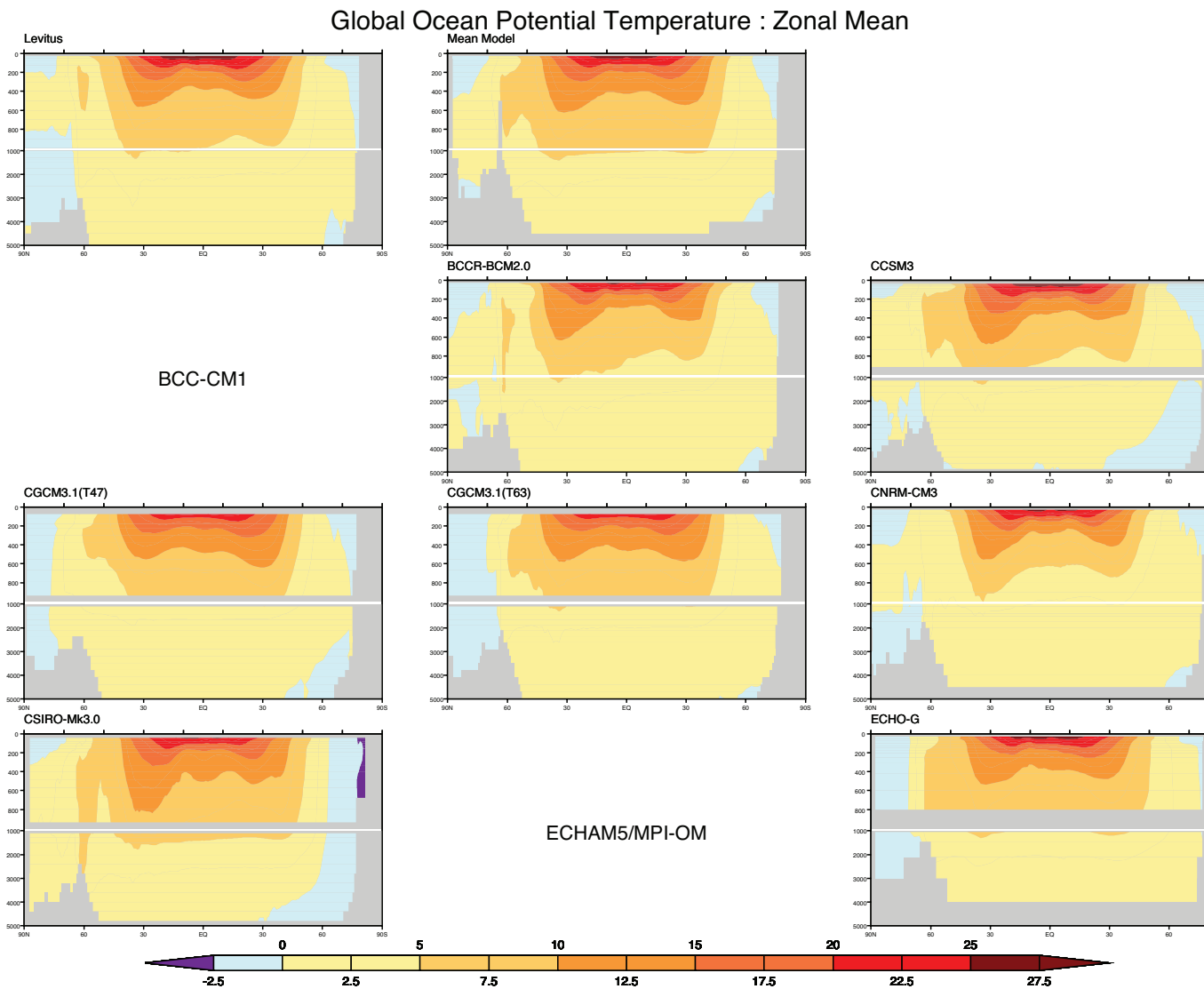


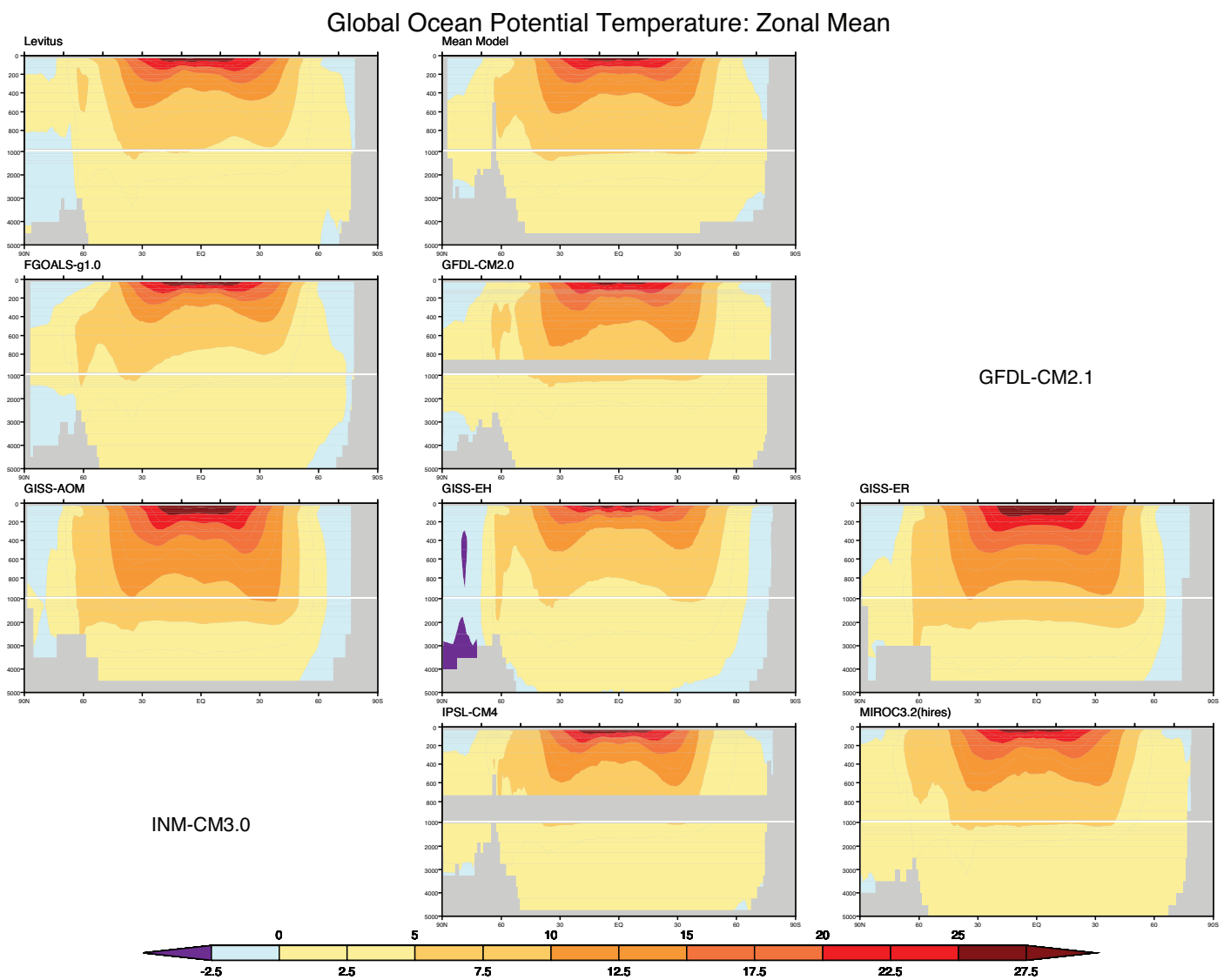
### Figure S8.12: Ocean potential temperature cross-sections:

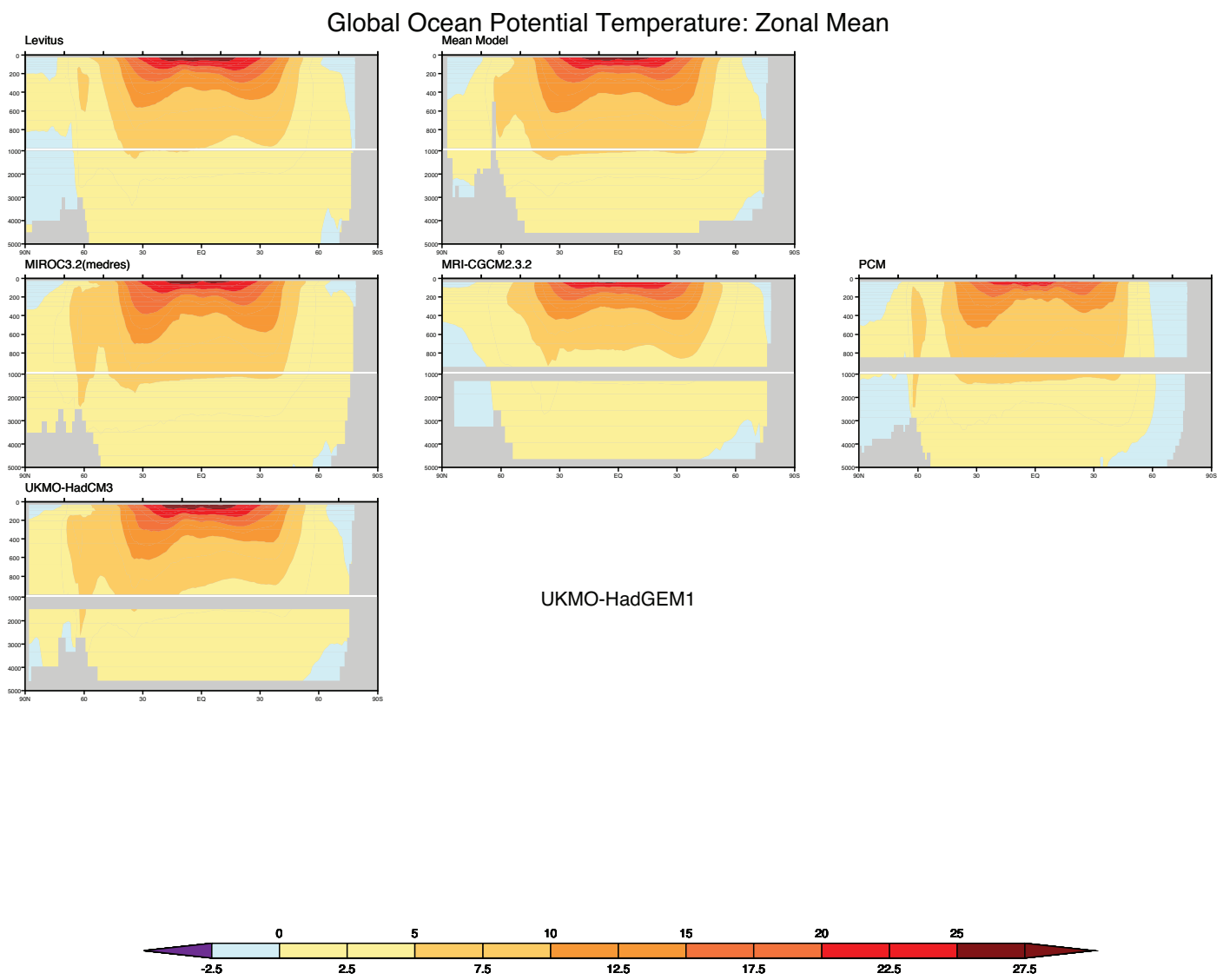
Each page of figure S8.12a shows:

- Upper left panel: Observed annual mean potential temperature climatology ( $^{\circ}\text{C}$ ), averaged zonally over all ocean basins.
- Upper center panel: Corresponding field averaged over the multi-model ensemble ( $^{\circ}\text{C}$ ).
- All other panels: Corresponding individual model results ( $^{\circ}\text{C}$ ).

The observations are from the 2004 World Ocean Atlas (WOA-2004) compiled by Levitus et al. (2005) for the period 1957-1990, and model results are for the same period of the CMIP3 20th Century simulations.



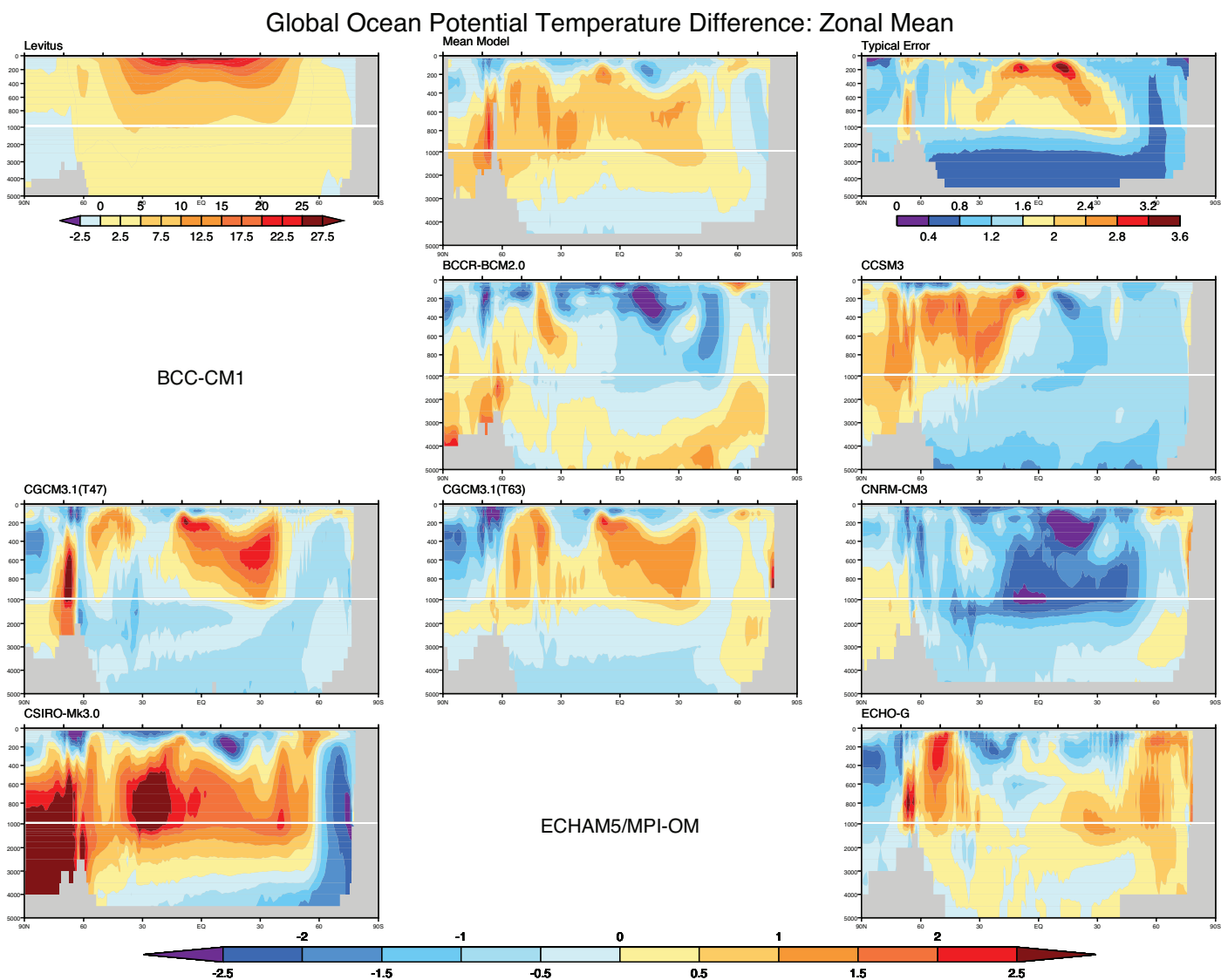


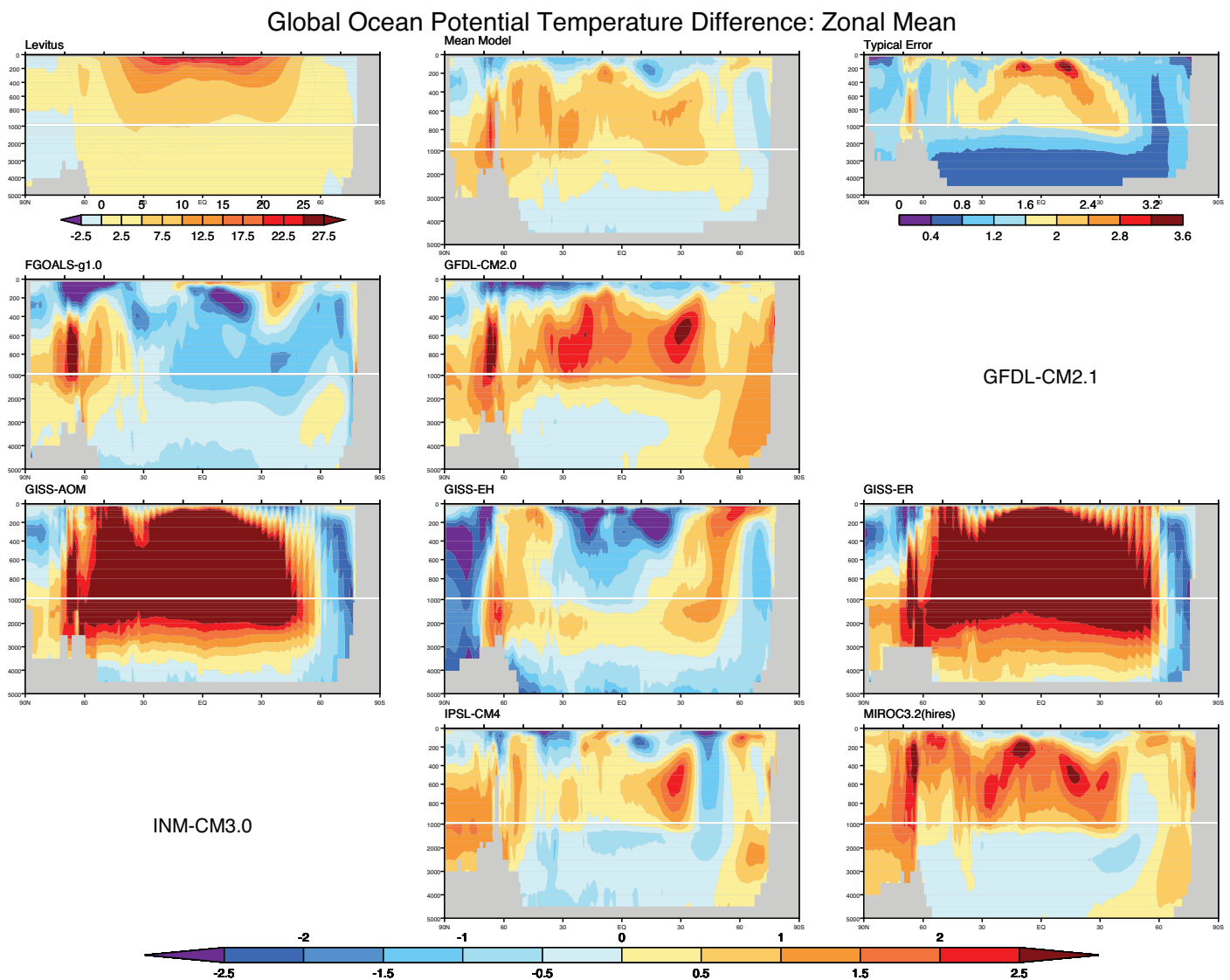


Each page of figure S8.12b shows:

- Upper left panel: Observed annual mean potential temperature climatology ( $^{\circ}\text{C}$ ), averaged zonally over all ocean basins.
- Upper center panel: Multi-model mean error ( $^{\circ}\text{C}$ ), simulated minus observed.
- Upper right panel: Root-mean-square model error ( $^{\circ}\text{C}$ ), based on all available IPCC model simulations (i.e., square-root of the sum of the squares of individual model errors, divided by the number of models).
- All other panels: Individual model errors ( $^{\circ}\text{C}$ ), simulated minus observed.

The observations are from the 2004 World Ocean Atlas (WOA-2004) compiled by Levitus et al. (2005) for the period 1957-1990, and model results are for the same period of the CMIP3 20th Century simulations.





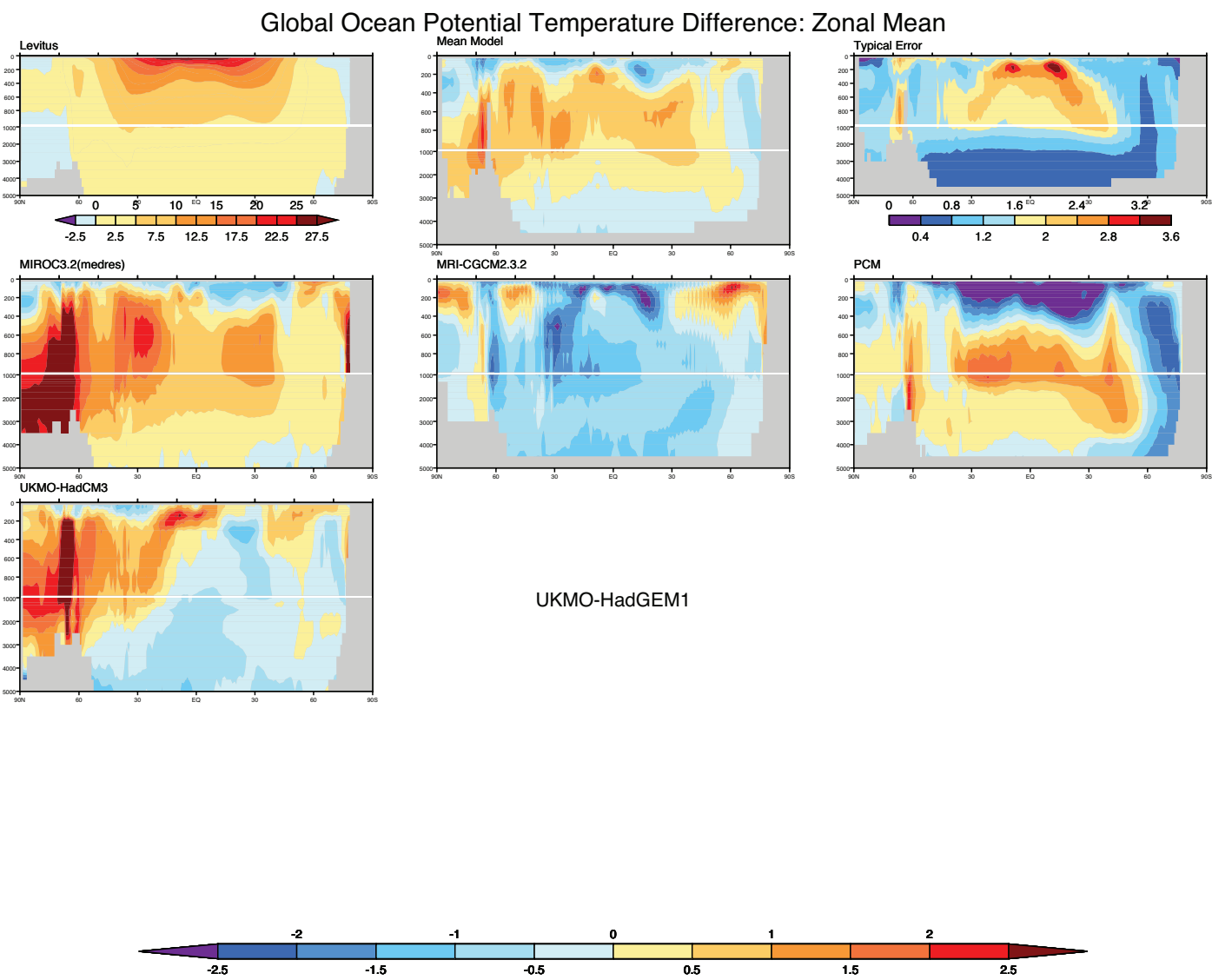
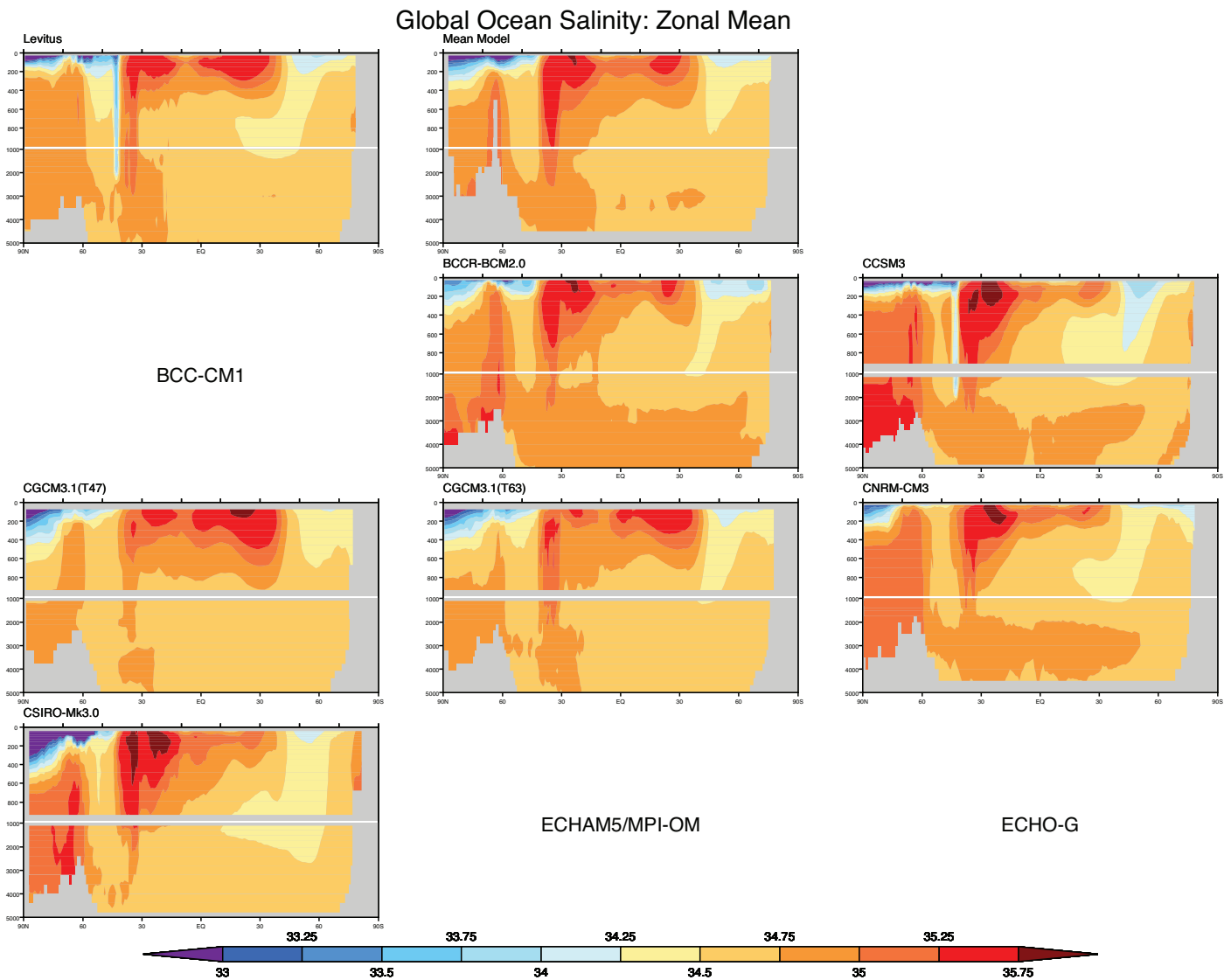


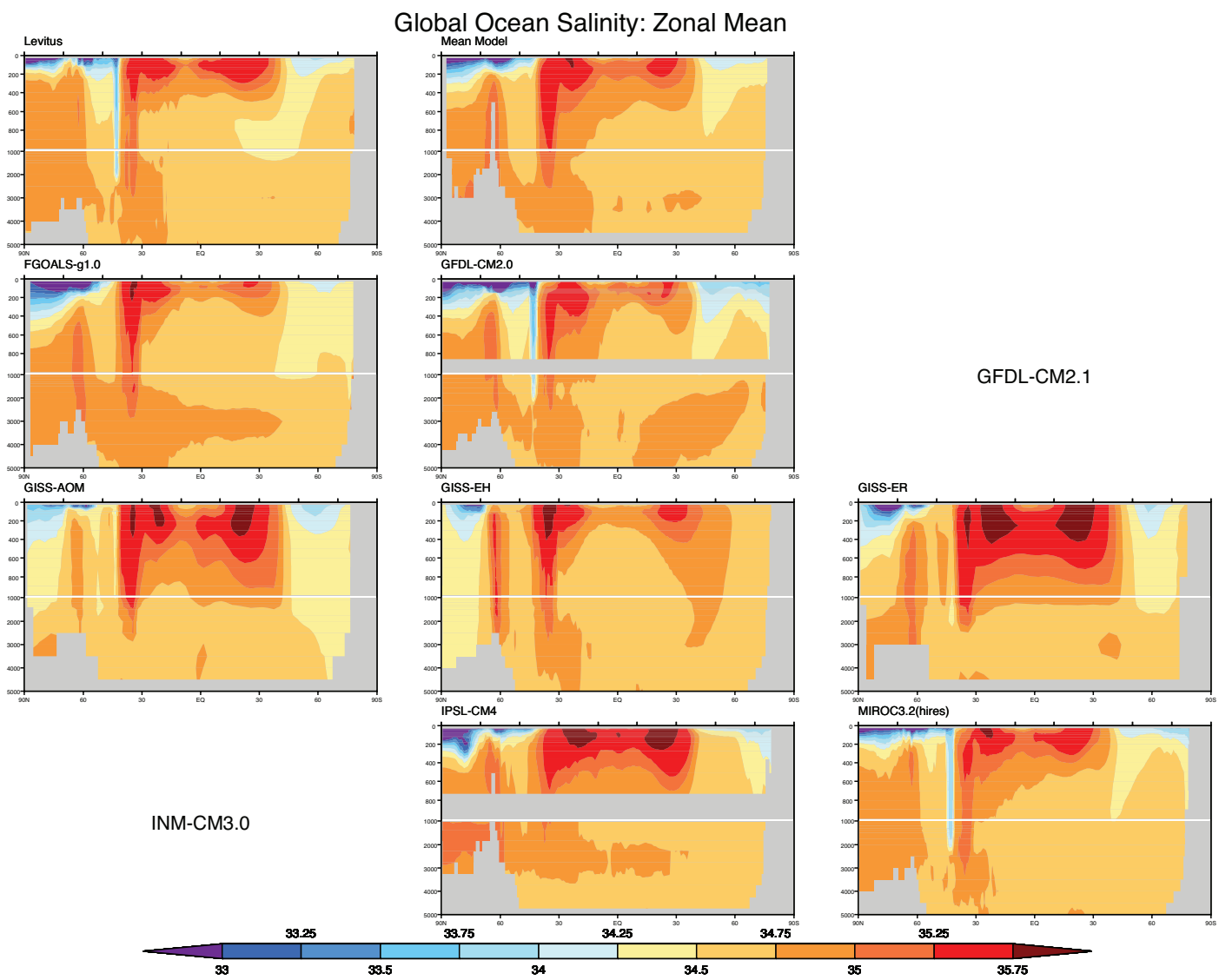
***Figure S8.13: Ocean salinity cross-sections:***

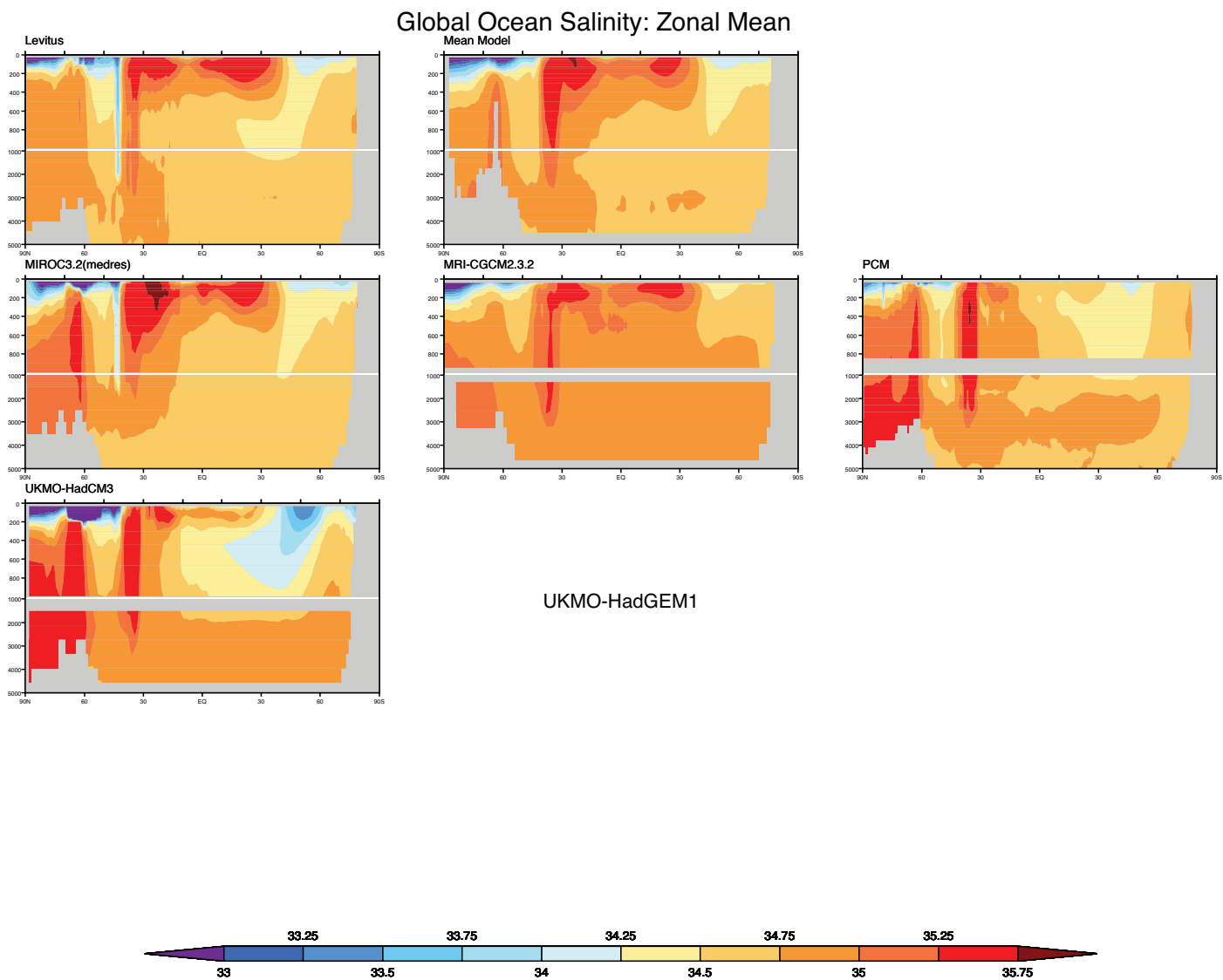
*Each page of figure S8.13a shows:*

- Upper left panel: Observed annual mean salinity (PSU), averaged zonally over all ocean basins.
  - Upper center panel: Corresponding field averaged over the multi-model ensemble (PSU).
  - All other panels: Corresponding individual model results (PSU).

The observations are from the 2004 World Ocean Atlas (WOA-2004) compiled by Levitus et al. (2005) for the period 1957-1990, and model results are for the same period of the CMIP3 20th Century simulations.



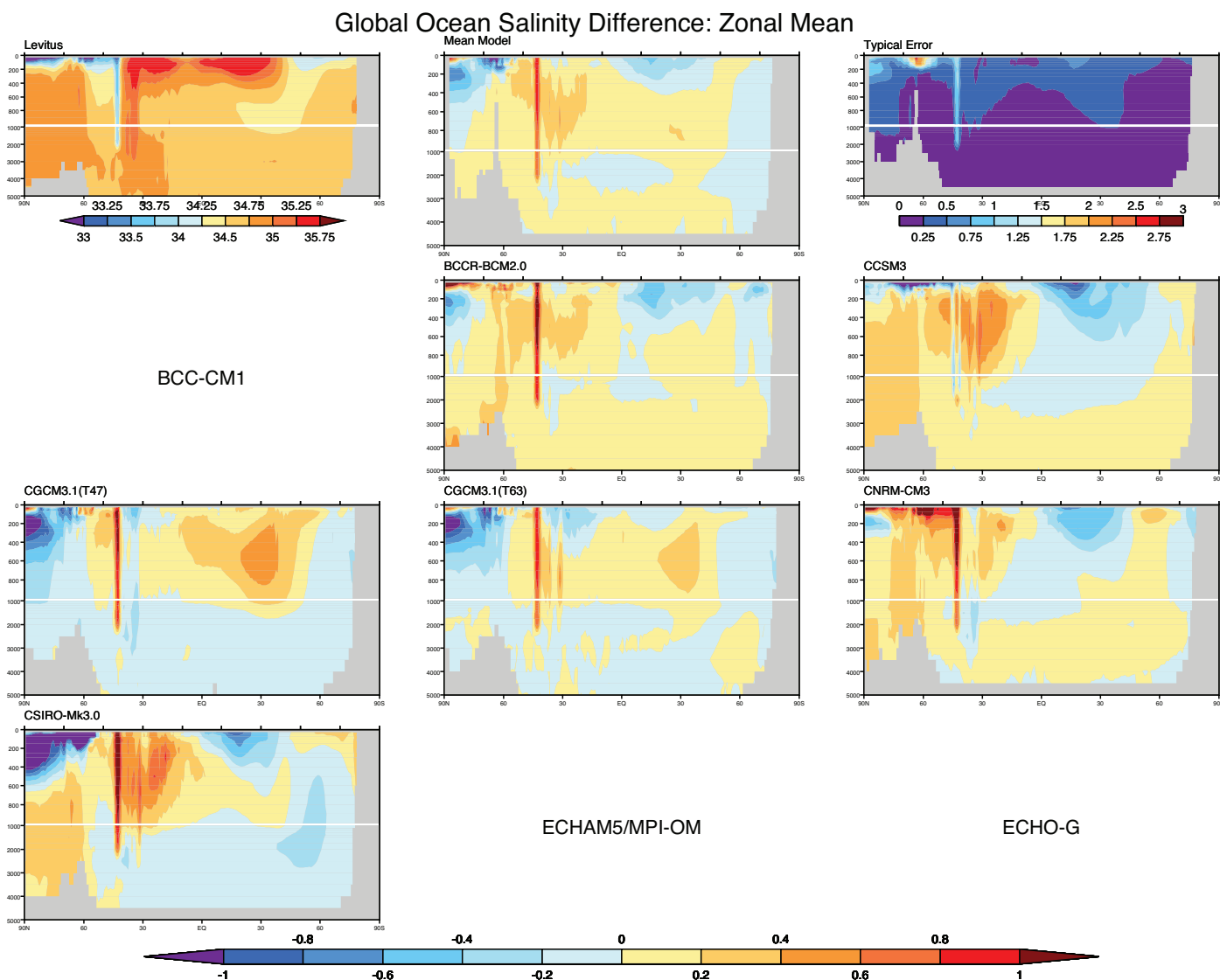


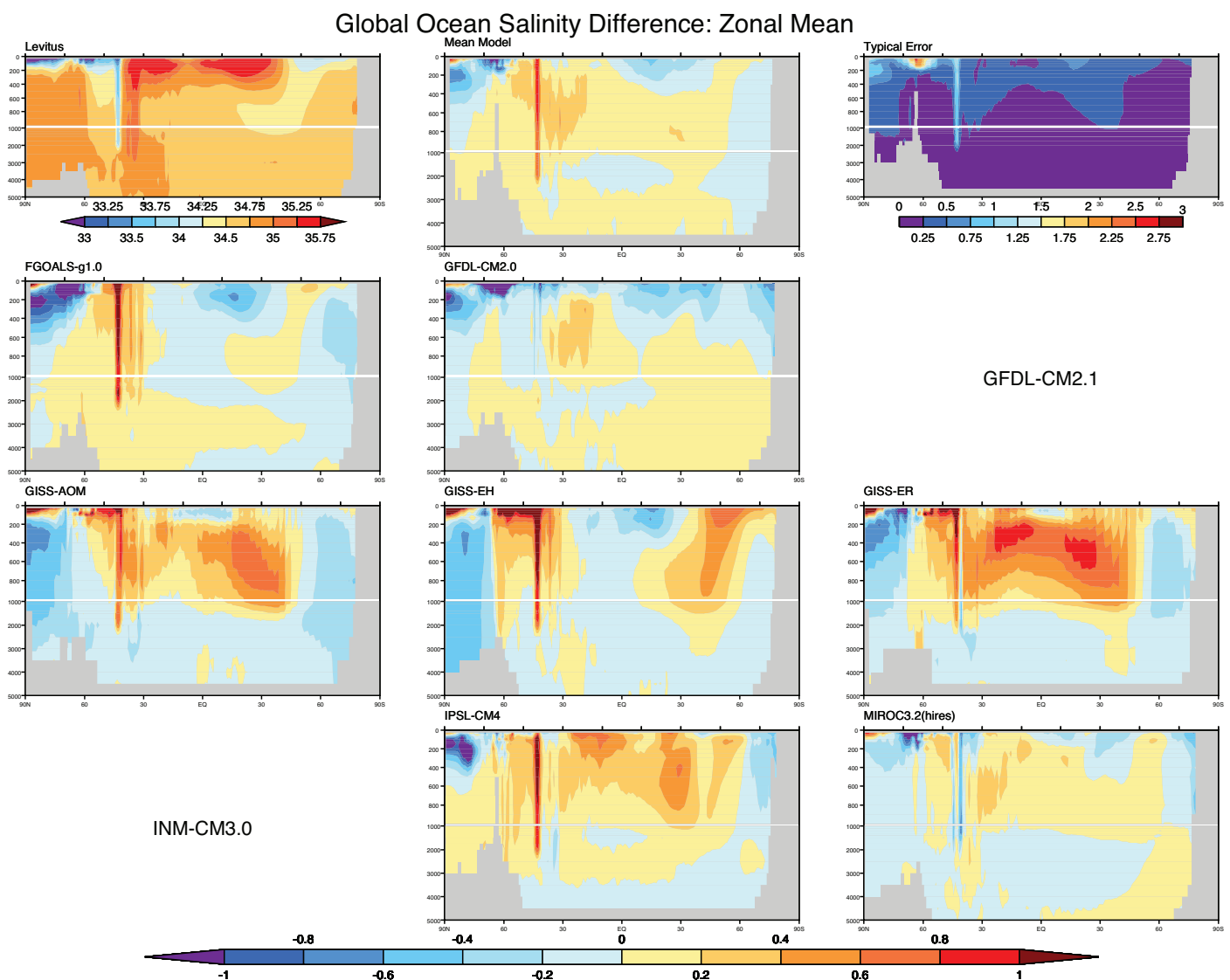


Each page of figure S8.13b shows:

- Upper left panel: Observed annual mean salinity (PSU), averaged zonally over all ocean basins.
- Upper center panel: Multi-model mean error (PSU), simulated minus observed.
- Upper right panel: Root-mean-square model error (PSU), based on all available IPCC model simulations (i.e., square-root of the sum of the squares of individual model errors, divided by the number of models).
- All other panels: Individual model errors (PSU), simulated minus observed.

The observations are from the 2004 World Ocean Atlas (WOA-2004) compiled by Levitus et al. (2005) for the period 1957-1990, and model results are for the same period of the CMIP3 20th Century simulations.





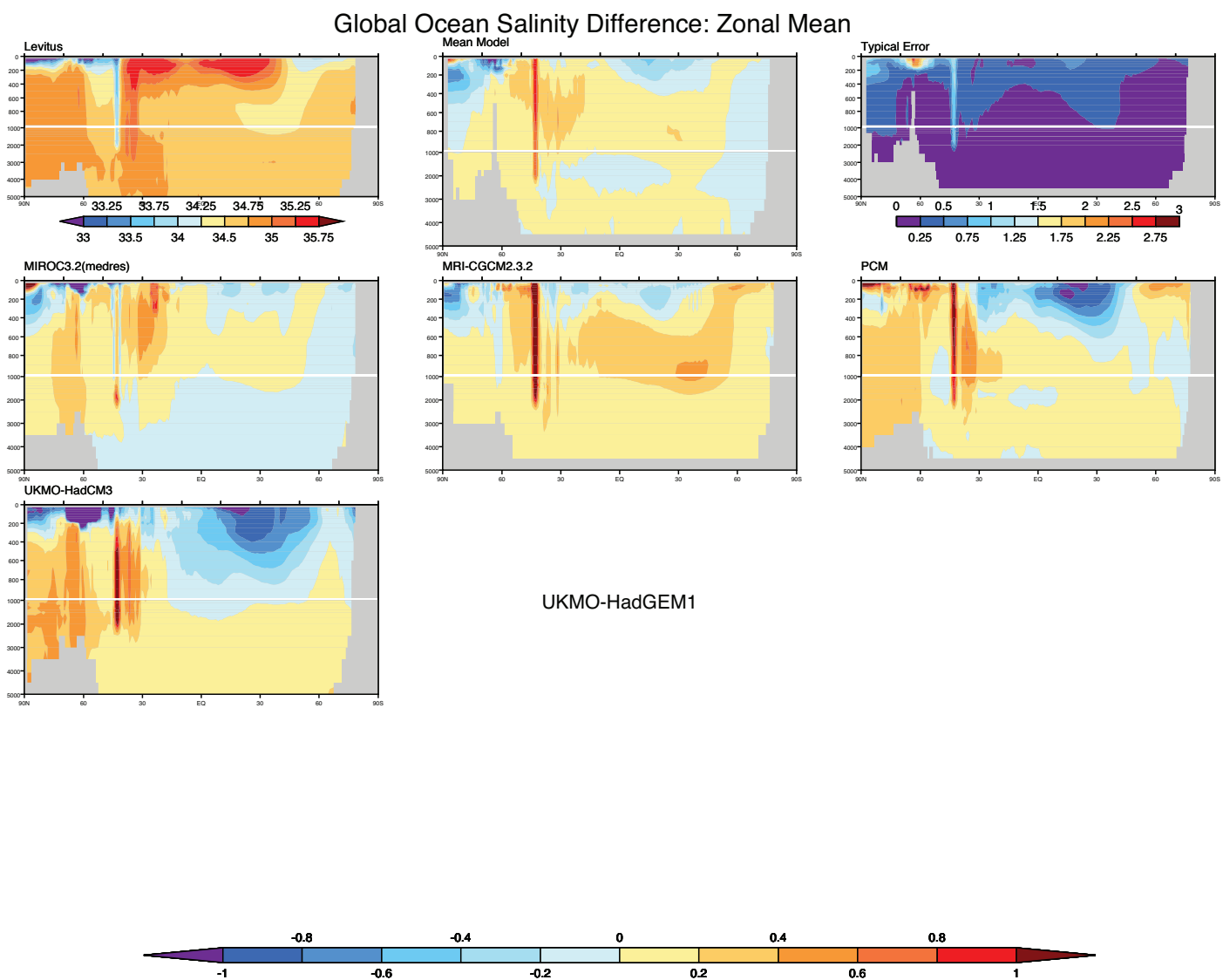
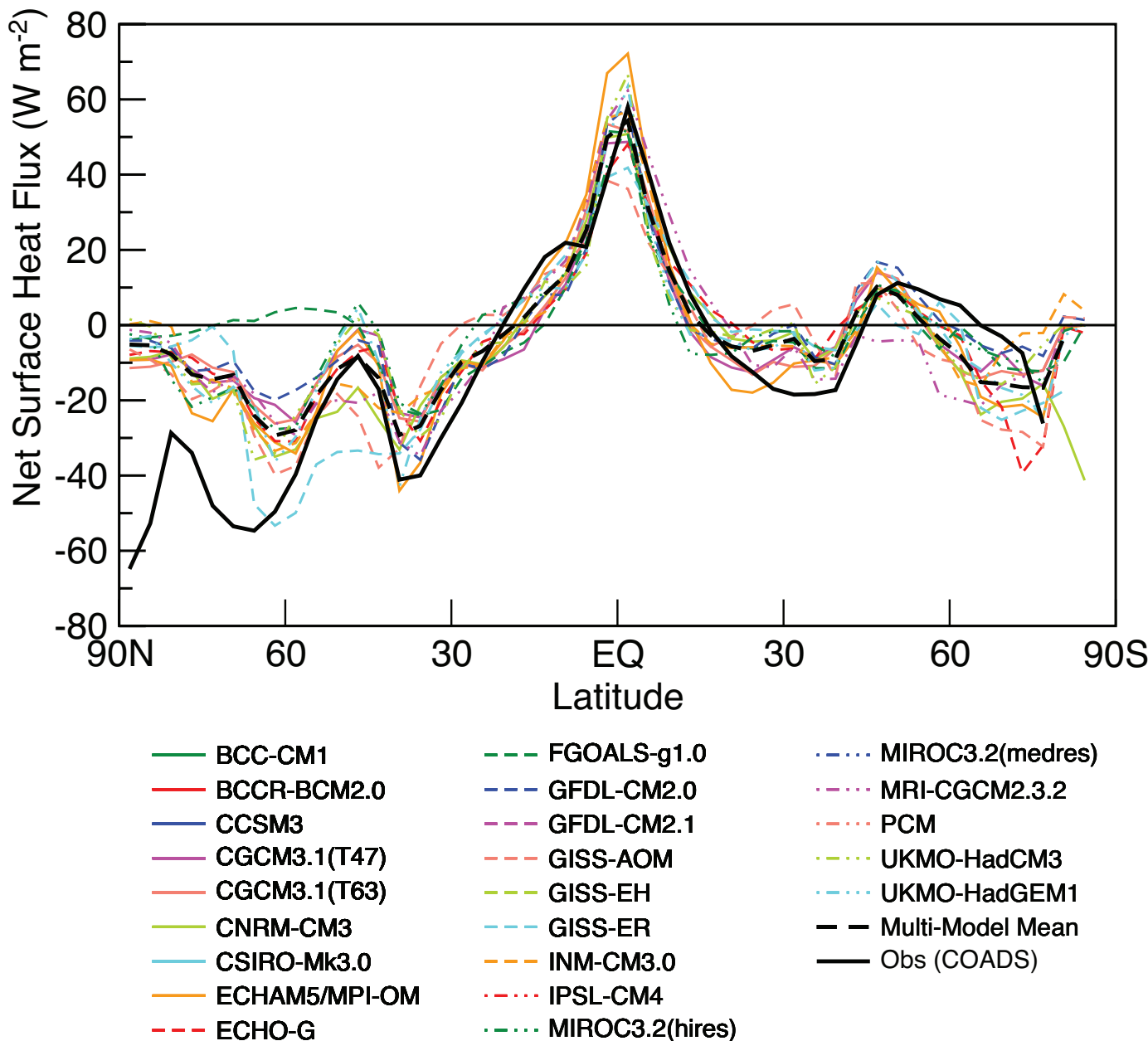


**Figure S8.14: Zonal mean net surface heat flux:**

Figure S8.14 shows:

- Annual mean, zonally averaged, total surface heat flux into the oceans.

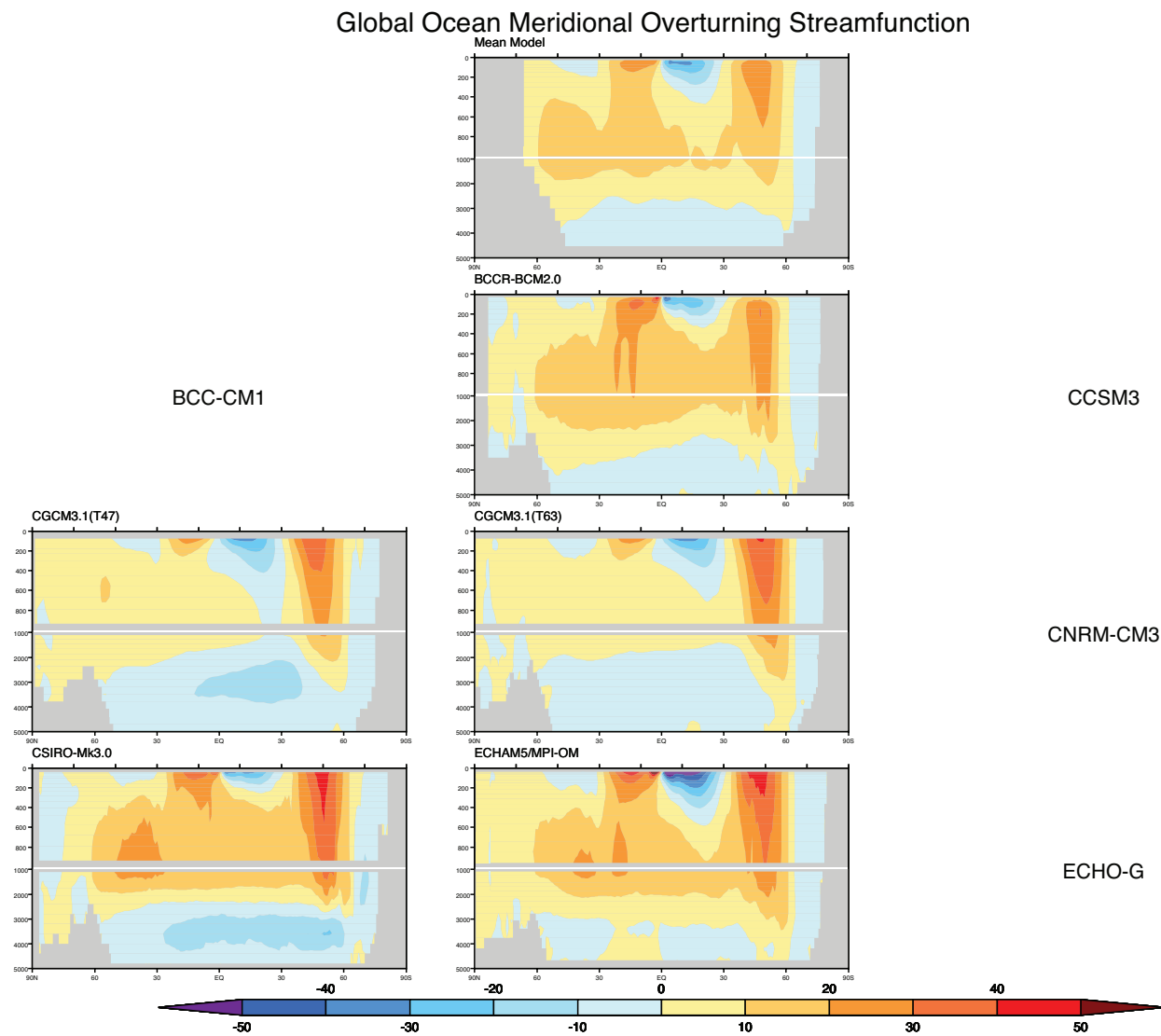
The observational estimates are from da Silva (1994) and are based on COADS observations over the period 1945-1989. The model results are from years 1980-1999 of the CMIP3 20th Century simulations.

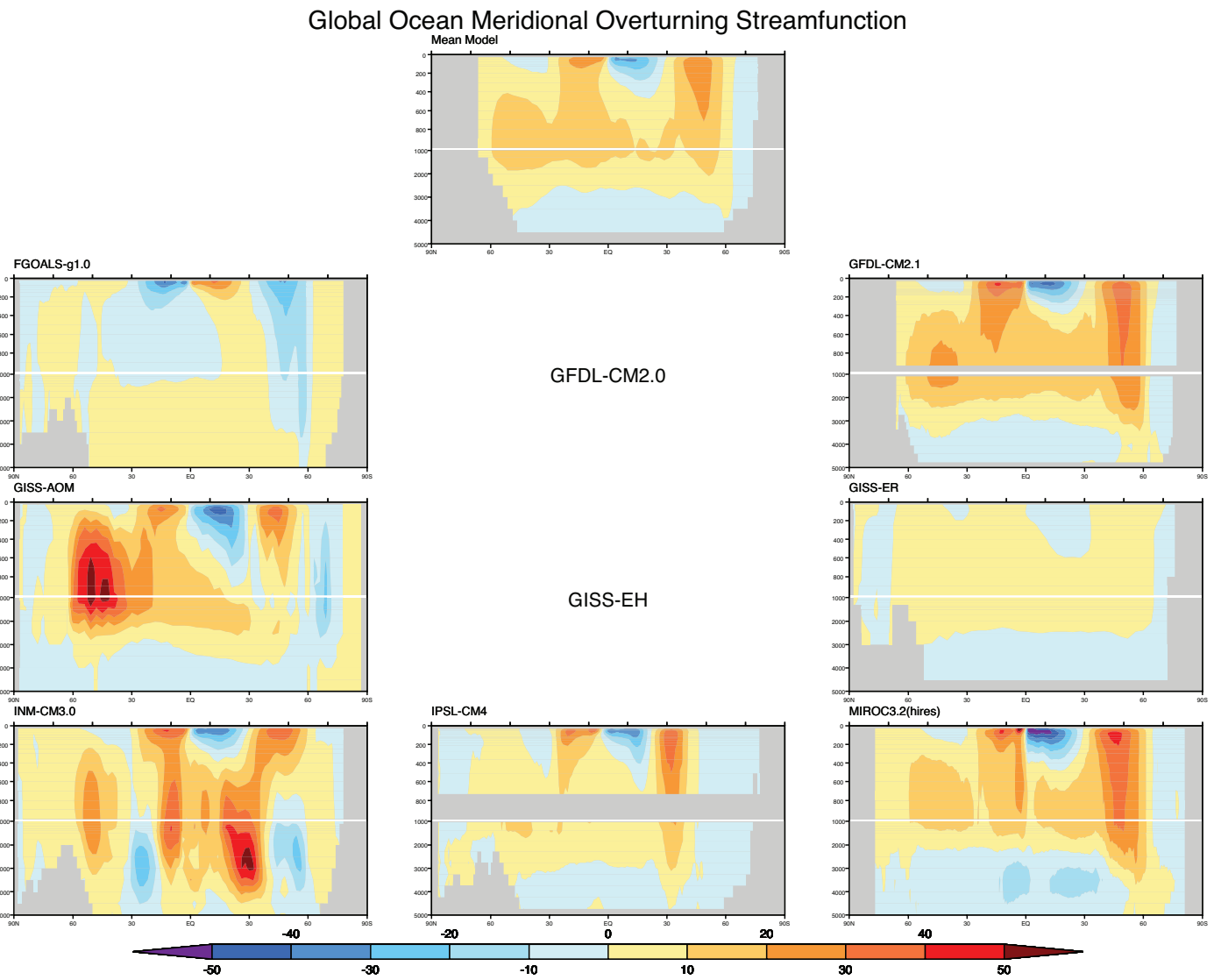


**Figure S8.15: Ocean meridional overturning streamfunction:**

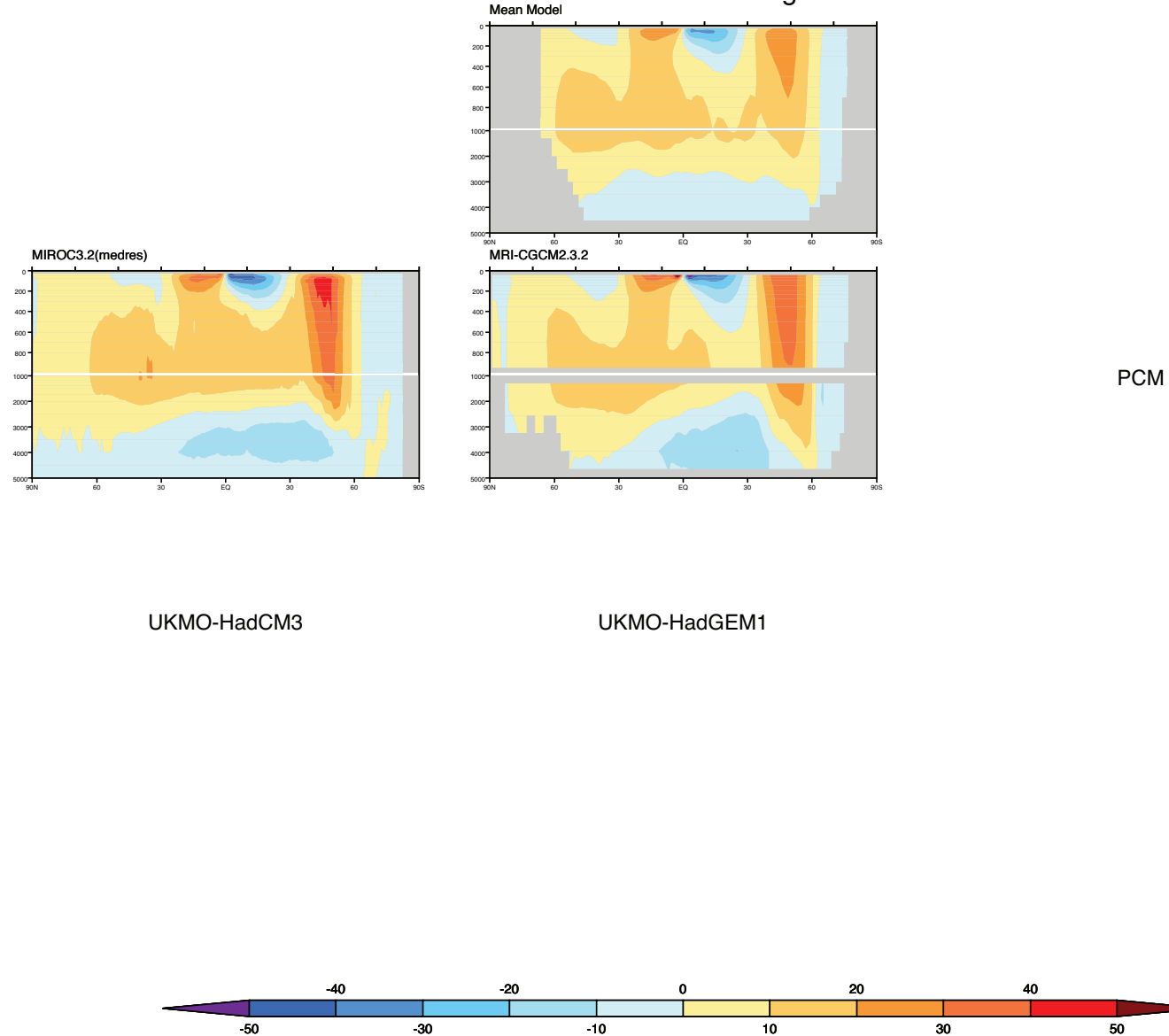
Each page of figure S8.15 shows:

- Upper center panel: Ocean meridional overturning streamfunction, averaged over the multi-model ensemble (Sv).
- All other panels: Corresponding individual model results (Sv).





### Global Ocean Meridional Overturning Streamfunction



**Supplementary Table for Section 8.8****Table S8.1** Parameter values used in a simple climate model (MAGICC) to approximately reproduce results from the AOGCM multi-model dataset at PCMDI.

AOGCM	$F_{2\times}$ (W m <sup>-2</sup> )	$\Delta T_{\text{eff}}$ (°C)	k (cm <sup>2</sup> s <sup>-1</sup> )	RLO
3: CCSM3	3.95	2.37	1.73	1.18
4: CGCM3.1(T47)	3.32	3.02	1.57	1.58
6: CNRM-CM3	3.71	2.45	1.21	1.10
7: CSIRO-Mk3.0	3.47	2.21	2.03	1.33
8: ECHAM5/MPI-OM	4.01	3.86	1.22	1.41
9: ECHO-G	3.71	3.01	2.01	1.65
10: FGOALS-g1.0	3.71	1.97	4.57	1.64
11: GFDL-CM2.0	3.50	2.35	1.42	1.47
12: GFDL-CM2.1	3.50	2.28	2.23	1.58
14: GISS-EH	4.06	3.04	2.35	1.21
15: GISS-ER	4.06	2.57	4.42	1.44
16: INM-CM3.0	3.71	2.28	0.79	1.10
17: IPSL-CM4	3.48	3.83	1.94	1.26
18: MIROC3.2(hires)	3.14	5.87	1.18	1.15
19: MIROC3.2(medres)	3.09	3.93	2.29	1.58
20: MRI-CGCM2.3.2	3.47	2.97	1.22	1.45
21: PCM	3.71	1.88	1.57	1.45
22: UKMO-HadCM3	3.81	3.06	1.01	1.65 <sup>a</sup>
23: UKMO-HadGEM1	3.78	2.63	1.32	1.20

Notes:

$F_{2\times}$ : radiative forcing for doubled CO<sub>2</sub> concentration (with stratospheric adjustment). Where available, values were taken from Forster and Taylor (2006), supplemented with information from the modelling groups. The default value is 3.71 Wm<sup>-2</sup> taken from Myhre et al. (1998).

$\Delta T_{\text{eff}}$ : effective climate sensitivity at the time of doubled CO<sub>2</sub> concentration, as defined in the glossary and discussed in Section 8.8.2.

k: ocean effective vertical diffusivity.

RLO: ratio of the equilibrium temperature changes over land versus ocean.

<sup>a</sup> This value was set from the AOGCM information rather than being tuned in the optimization procedure.